AN INTEGRATED MODELING APPROACH FOR EVALUATION OF PHOSPHORUS LOADING IN RURAL NOVA SCOTIA WATERSHEDS

by

Andrew Charles Sinclair

Submitted in partial fulfilment of the requirements
for the degree of Doctor of Philosophy

at

Dalhousie University
Halifax, Nova Scotia
January 2014

Table of Contents

LIST OF TABLES

LIST OF FIGURES

ABSTRACT

Residential on-site wastewater systems (OWS) are a potential source of phosphorus (P) which can negatively impact surface water quality in rural watersheds. The magnitude of P loading from OWS is typically not monitored, and is further complicated when agricultural land-uses are intermixed with residential dwellings. Watershed-scale computer simulations are commonly used tools for evaluating the impacts of land-use changes on P loading. Existing models simulate OWS P treatment via vertical flow transport in native soils. However, in Nova Scotia (NS) OWS designs rely pre-dominantly on lateral flow and imported sand filter media.

In this thesis, a watershed-scale computer modeling framework for simulating P loads from agriculture and lateral flow OWS designs was developed and tested. The framework consists of the P on-site wastewater simulator (POWSIM), designed specifically for this study, which is used in conjunction with the Soil and Water Assessment Tool (SWAT) model. The POWSIM loading tool has three computational components: (i) OWS disposal field design type selection and treatment media mass calculation; (ii) disposal field P treatment dynamics; and (iii) soil subsurface plume P treatment dynamics. The active P treatment media mass and dynamics equations were developed from numerical modeling (HYDRUS-2D) and lateral flow sand filter (LFSF) OWS disposal field experiments. A 2-part piecewise linear model was found to best represent LFSF P treatment processes.

Testing of the modeling framework in the mixed land-use Thomas Brook Watershed (TBW) in NS demonstrated improved simulation of baseflow total P (TP) loads in both a predominantly residential subcatchment and one dominated by agriculture over the SWAT model without POWSIM. Different residential and agricultural development and beneficial management practice (BMP) scenarios were evaluated in the TBW. Agricultural BMPs were most effective at reducing cumulative TP loads while OWS BMPs were best at mitigating in-stream eutrophication impacts. The 50 year simulation period for the various scenarios found peak OWS TP loading occurring between 25 and 50 years, suggesting that modeling for many decades is required for proper evaluation. This study highlights the importance in identifying specific water quality issues that need to be targeted prior to implementing a BMP strategy.

LIST OF ABBREVIATIONS AND SYMBOLS USED

AAFC	Agriculture and Agri-Food Canada
AIC	Akaike's Information Criterion
AIC_{min}	Minimum Akaike's Information Criterion
Al	Aluminum
α_L	Longitudinal dynamic dispersivity
$area_{hru}$	Area of the hydrologic response unit
b	Linear equation y-intercept
BEEC	Bio-Environmental Engineering Centre
BMP	Beneficial Management Practice
BNQ	Bureau de Normalisation du Quebec
Ca	Calcium
CANSIS	Canadian Soil Information Service
CCME	Canadian Council of the Ministers of the Environment
CEAP	Conservation Effects Assessment Project
C_{eq}	Observed equilibrium solute concentration
CN2	Surface runoff curve number
$conc_{sed,P}$	Phosphorus concentration attached to sediment in the top 10 mm of the first soil layer
D	Saturated depth of effluent leaving disposal field
DEM	Digital Elevation Model
$depth_{surf}$	Depth of soil involved in surface runoff
dh/dx	Slope of soil subsurface plume
D_L	Longitudinal hydrodynamic dispersion coefficient
D_T	Transverse hydrodynamic dispersion coefficient
$\varepsilon_{P:sed}$	Phosphorus enrichment ratio
GIS	Geographic Information System
h	Water pressure head
H	Hydrogen

H_20	Water
HDPE	High-Density Polyethylene
HPO_4^{2-}	Monohydrogen Phosphate
$H_2PO_4^-$	Dihydrogen Phosphate
H_3PO_4	Phosphoric Acid
HRU	Hydrologic Response Unit
Fe	Iron
K	Slope of fitted least squares line
K_L	Langmuir constant
K_s	Saturated hydraulic conductivity
K_d	Adsorption isotherm coefficient
$k_{d,perc}$	Phosphorus percolation coefficient
$k_{d,surf}$	Phosphorus soil partitioning coefficient
LFSF	Lateral Flow Sand Filter
L_{path}	Distance from the on-site wastewater system to water course
m	Linear equation slope
Mg	Magnesium
Mn	Manganese
$minP_{act,surf}$	Amount of phosphorus in the top 10 mm of the first soil layer in the active inorganic phosphorus pool
$minP_{sta,surf}$	Amount of phosphorus in the top 10 mm of the first soil layer in the stable inorganic phosphorus pool
$M_{treatment}$	Mass of sand involved in phosphorus treatment
N	Number of observations
n	effective porosity
N	Nitrogen
NH_4-N	Ammonium
NMP	Nutrient Management Plan
NO_3	Nitrate
NRCS	National Resource Conservation Service
NS	Nova Scotia

NSE	Nash-Sutcliffe Efficiency
O_2	Oxygen
O	Observed value
O_{avg}	Average observed value
Θ_k	Unsaturated volumetric moisture content
Θ_r	Residual volumetric moisture content
$orgP_{frsh,surf}$	Amount of phosphorus in the top 10 mm of the first soil layer in the fresh organic phosphorus pool
$orgP_{hum,surf}$	Amount of phosphorus in the top 10 mm of the first soil layer in the humic organic phosphorus pool
Θ_s	Saturated moisture content
OWS	On-Site Wastewater System
%	Percentage
p	Number of fitted parameters
P	Phosphorus
ρ_b	Soil or filter media bulk density
PBIAS	Percent bias
PHOSKD	Phosphorus soil partitioning coefficient
PO_4^{3-}	Phosphate
P_2O_5	Phosphorus Pentoxide
POWSIM	Phosphorus On-Site Wastewater Simulator
P_{perc}	Amount of soluble phosphorus leaching out of the top 10 mm of the first soil layer
$P_{sol,surf}$	Soluble P in the 10 mm of the first soil layer
PSP	Phosphorus sorption coefficient
P_{STE}	Septic tank effluent phosphorus load
P_{surf}	Soluble P lost via surface runoff
Q_{surf}	Surface runoff on a given day
RMSE	Root Mean Square Error
$RMSE_{Part\ I}$	Root Mean Square Error (Part I)
$RMSE_{Part\ II}$	Root Mean Square Error (Part II)

R_{sp}	Phosphorus adsorption capacity
RSR	Root Mean Square Error to the standard deviation of measured data
RTD	Residence Time Distribution
S	Solute sorbed to filter media
sed	Sediment yield on a given day
$sedP_{surf}$	Amount of phosphorus transported with sediment in surface runoff
S_i	Annual phosphorus load per capita
S_{max}	Maximum adsorption capacity
$S_{max,STE}$	Normalized maximum phosphorus adsorption capacity
S_o	Initial amount sorbed to filter media
SSE	Sum of Squared Errors
SSF	Sloping Sand Filter
σ_T	Standard deviation of soil subsurface plume width
Std.	Standard
STE	Septic Tank Effluent
Stn	Monitoring Station
SUFI-2	Sequential Uncertainty Fitting Version 2
SWAT	Soil and Water Assessment Tool
SWAT2005	Soil and Water Assessment Tool (version 2005)
SWAT2009	Soil and Water Assessment Tool (version 2009)
TBW	Thomas Brook Watershed
TIN	Triangular Irregulated Network
TP	Total Phosphorus
UK	United Kingdom
USDA	United States Department of Agriculture
USEPA	United States Environmental Protection Agency
v_x	Darcy velocity
WARMF	Watershed Analysis Risk Assessment Framework
WEBS	Watershed Evaluation of Beneficial Management Practices
$w_{perc,surf}$	Amount of water percolating downward from the top 10 mm of the first soil layer

W_{sys}	Active width of on-site wastewater system
X_i	Simulated value

ACKNOWLEDGEMENTS

This thesis is the culmination of a long and windy journey as a Ph.D. Candidate at Dalhousie University. I would not have been able to complete this document without the help and support of a cast of many. I want to in particular thank my supervisory committee for providing guidance and direction throughout this process. My supervisors, Drs. Rob Gordon and Rob Jamieson, thank you for providing me with and encouraging me to explore a wide variety of opportunities, including teaching an undergraduate course, presenting my research to a diverse range of audiences around the world, and participating in other research projects that expanded my skill set as an engineer. Rob Jamieson this thesis is a testament to you creating a research group environment that was supportive and never made it feel like a chore to perform research work. Most of all I would not have reached this point without Rob Jamieson's patience as I laboured to develop and test the POWSIM model, and subsequently write about it. Rob Gordon, thank you for helping me always remember both the big picture throughout my Ph.D. and potential end users of my research. Dr. Ali Madani, thank you for providing thorough reviews of all my papers, and always ensuring that I remembered the reader's perspective. Dr. William Hart, I very much appreciate your thoughts and comments over the years, and taking the time to check up on my overall well-being.

Performing great scientific research is seldom a singular effort and I have had the opportunity to work with and develop great friendships with many people throughout this thesis. Within Rob Jamieson's research group I, in particular, acknowledge my fellow Ph.D. Candidate colleagues, Tristan Goulden and Greg Piorkowski, whose participation in many lively pub discussions helped create this document and figure out how to navigate the administrative processes. To my fellow SWAT modeler, Hafiz Ahmad, thank you for being a terrific collaborator in developing the initial Thomas Brook Watershed SWAT model. Rick Scott, you were a great office mate and excellent mentor for all the limnological fieldwork I have participated in over the years. Within the research group I have been fortunate to perform fieldwork with (and sometimes been able to persuade to play intramural sports with the Sedgehammers) an amazing cast of characters including: Leah Boutilier, Evan Bridson-Pateman, Marie-Claire Brisbois,

Katie Campbell, Bruce Curry, Danielle Finlayson, Kevin Garroway, Mark Greenwood, Jenny Hayward, Lee Hynes, Wendy Krkosek, Kira Krumhansl, Michael MacEachern, Kristen MacNeil, Janeen McGuigan, Iain Melvin, Erin Mentink, Colin Ragush, Christina Ridley, Andy VanderZaag, Graham Waugh, and Adam Wile. I want to extend a big thank you as well to Dale Hebb, Beata Lees, Angela Garnett and Katherine Benedict from the Agriculture and Agri-Food Canada (AAFC) research station in Kentville for providing data and information over the years on the Thomas Brook Watershed. I would also like to thank Terry Matheson from the Municipality of East Hants who initially called me out of the wilds of southern Ontario to start this whole endeavour.

My family has been along for the Ph.D. journey whether they like it or not and sometimes there are more 'not like' moments than others. My parents, Sedgewick and Barbara, you raised me into the inquisitive man, who is always striving to better help society and the natural environment, I am today. You also have never told me not to follow a dream and for that you have all my love and appreciation. My siblings, Daniel and Laura, you rock and you know it. Stephanie Gora, you have been with me since almost the beginning of this "process" and have literally been through the worst moments as well. Your patience, encouragement, support, love and hugs throughout these years are acts I will never be able to fully articulate my thankfulness for. Seamus, you are the worst writing partner ever; however, you are a cat and were very good at reminding me about taking a break, so thank you.

I thank the following groups and funds for the generous direct and in-direct financial support for this research project: National Sciences and Research Council (NSERC), Atlantic Rural Centre, Canadian Water Network (CWN), AAFC, Rosetti Scholarship foundation, NSERC Systems Training and Education in Water Assets Research and Development (STEWARD) Create Program, and the Faculty of Graduate Studies (FGS).

CHAPTER 1 INTRODUCTION

Surface water systems in rural watersheds have a diverse range of uses, including human, animal and livestock drinking water, irrigation, recreation and supporting aquatic life. Accelerated eutrophication of aquatic systems can negatively impact water quality by causing reduced biodiversity, loss of aquatic habitat, and blue-green algae (cyanobacteria) blooms that produce toxic microcystins (Carpenter et al., 1998; Chambers et al., 2001). The primary cause of accelerated eutrophication in freshwater systems is increased loading of phosphorus (P) from anthropogenic point and non-point sources (Schindler, 1977; 2006).

Two non-point or diffuse P sources in rural mixed land-use watersheds are agriculture and residential wastewater (Carpenter et al., 1998). Elser and Bennett (2011) and Sharpley et al. (2013) identified that over-application of animal feeds and manures, and chemical fertilizers in agricultural systems can cause increased P loading to surface waters. Storm event and irrigation surface runoff, and subsurface transport via tile drainage systems are the main agricultural field P transport pathways to neighbouring surface waters (Kinley et al., 2007; Sharpley et al., 2001; 2008).

Residential wastewater in rural Nova Scotia (NS), Canada is typically treated using on-site wastewater systems (OWS) (Havard et al., 2008). In the United States, Canada, and in the province of NS the percentage of the population that live in rural areas and would potentially use OWS is 19 (United States Census Bureau, 2012), 19 (Statistics Canada, 2012a) and 45% (Nova Scotia Environment, 2011), respectively. A typical OWS design consists of residential wastewater from a single or cluster of household(s) entering a pre-treatment septic tank that then discharges into a disposal field. The disposal field allows the effluent to percolate through either imported filter media or native soil, with treated water discharging into the surrounding soil profile. Further treatment is provided by the soil before the effluent reaches neighbouring surface water systems, or groundwater, by vertical and lateral flow transport processes. In NS, the majority of OWS designs rely on lateral flow transport in imported filter media, typically sand, because of low permeability soils, shallow bedrock and high water tables (Havard et al., 2008). The two main OWS P transport pathways to surface water systems were identified by the

USEPA (2002) as (i) surface hydraulic failure of the disposal field due to improper drainage or clogging, and (ii) inability of the disposal field and/or surrounding native soil to remove and retain P.

Withers et al. (2009; 2011) identified that OWS P loads are routinely not monitored at the watershed-scale and are often assumed to be relatively small compared to agricultural land-uses. The same studies by Withers et al. investigated the relative contribution of OWS to P concentrations and loads in watersheds in the United Kingdom (UK). Withers et al. (2009) found that farm-yard runoff and septic tank discharges had higher P concentrations and proportions of bioavailable P compared to agricultural field runoff in two small agricultural watersheds. In-stream soluble reactive P concentrations downstream of a group of OWS were found to be elevated and the highest concentrations occurred during baseflow conditions in a small residential watershed studied by Withers et al. (2011). Several studies have also estimated the percent contribution from OWS to the total P load in a watershed to be 4 to 55 (Lombardo, 2006), 14 (Dudley and May, 2007) and 10% (Withers et al., 2012). In general, the magnitude of the P loading from OWSs and its relative contribution to the total P load in a watershed is poorly understood.

Watershed managers address eutrophication associated water quality issues by implementing strategies that employ beneficial management practices (BMPs) to reduce P loading from non-point source surface runoff or shallow groundwater flow (Chambers et al., 2012). Conducting continuously monitored bio-physical studies of implemented BMPs, individually or in various combinations within a watershed, to develop management strategies is expensive, difficult and not time efficient. A commonly used tool in watershed management for evaluating the temporal and spatial environmental impacts of BMP implementation is the hydrological-water quality computer simulation model. A number of watershed-scale models have been used to evaluate the efficacy of a wide-variety of agricultural land-use BMPs; the Soil and Water Assessment Tool (SWAT) being one of the most popular models (Gassman et al., 2007). Both the US Department of Agriculture Conservation Effects Assessment Project (CEAP) and Agriculture and Agri-Food Canada (AAFC) Watershed Evaluation of Beneficial Management Practices (WEBs) BMP research programs utilized the SWAT model to evaluate agricultural BMPs (AAFC, 2013; USDA NRCS, 2013). The SWAT model has

been successfully tested and validated in NS, and used to evaluate agricultural BMPs for reducing nitrate and sediment loading in the rural, mixed land-use Thomas Brook Watershed (TBW) (Ahmad et al., 2011; Amon-Armah et al., 2013).

In general, there has been significantly less research into OWS BMPs, compared to agricultural BMPs. Currently, only the Watershed Analysis Risk Management Framework (WARMF) and SWAT models have specific algorithms to simulate OWS P treatment at the watershed-scale (Weintraub et al., 2002; Jeong et al., 2011). Both models simulate P treatment in OWS disposal fields as occurring via vertical transport in native soils. The P load from an OWS in both models is input into the soil layer and removed using a linear sorption isotherm. A maximum sorption capacity is used to cap off the linear isotherm when the soil layer is P saturated. The SWAT model (version 2009) does not simulate P transport in the soil profile via lateral flow, while WARMF simulates lateral flow when the soil layer water content reaches or exceeds field capacity. The NS OWS disposal field designs rely on lateral flow processes in imported sand filter media, which would not be adequately represented in the existing watershed-scale P treatment algorithms. There is a need to develop and test a watershed-scale modeling approach to simulate P loads from lateral flow dominated OWS designs to develop appropriate and effective BMP strategies in watersheds with both agricultural and residential land-uses.

The main research goal of this thesis is to develop and test a watershed-scale computer modeling framework for simulating P loads from agricultural land-uses and lateral flow OWS designs. To achieve this main research theme the thesis is divided into the following research objectives:

i) Produce a method to estimate the mass of filter media involved in active P treatment in a lateral flow dominated OWS disposal field (Chapter 2);

ii) Evaluate different temporal removal models to simulate long-term P treatment processes in lateral flow dominated OWS disposal field designs and select the most appropriate for use in a watershed modeling framework (Chapter 2);

iii) Develop and test the P on-site wastewater simulator (POWSIM) model in conjunction with the SWAT model in a small mixed land-use watershed in

relation to its ability to simulate P loading from agricultural land-uses and residential OWS (Chapter 3); and

iv) Evaluate and compare different residential OWS and agricultural land-use BMP implementation strategies using the modeling framework in a small mixed land-use watershed to reduce cumulative sediment and P loads and accelerated eutrophication rates (Chapter 4).

The literature review for this study, in particular the description of the main P treatment mechanisms in OWSs and how they are represented in existing watershed models, is contained within the 'Introduction' sections of Chapters 2, 3 and 4.

Chapter 2 presents the development and evaluation of the P treatment algorithms that will be utilized in the POWSIM loading tool. The development of a methodology is presented for estimating the active P treatment sand mass in the lateral flow sand filter (LFSF) type of OWS disposal field. Linear and non-linear P temporal removal models are developed and evaluated, using the estimated active P treatment sand masses, for LFSFs that differ in design by slope, sand grain-size, and filter-length. Utilizing the active P treatment sand mass will allow the normalization of the temporal removal models for comparison amongst the different LFSF designs and model adaptation to simulate other lateral flow dominated disposal field designs. The developed temporal removal models are compared against observed P treatment data to select the models with the best statistical fit for each LFSF design.

The development and evaluation of the POWSIM model in conjunction with the SWAT model is presented in Chapter 3. The design of the POWSIM computational components, algorithms and input parameters are described. The modeling framework is multi-site calibrated and tested in the TBW, NS by comparing against observed hydrologic flow, sediment and phosphorus data using model performance evaluators. A comparison of the modeling framework against the calibrated SWAT model without POWSIM is conducted. Watershed-scale sensitivity analyses on the POWSIM input parameters for two different OWS operating time periods are performed.

Chapter 4 reports the use of the modeling framework to simulate agricultural and residential development and BMP scenarios in the TBW for 50 yr time periods. The scenarios are assessed and compared against each other using cumulative pollutant loads

for the simulation period and changes in the trophic status frequency distribution. The best ranked individual agricultural and residential BMPs are combined together sequentially to evaluate potential environmental impacts. The socio-political factors that potentially would influence BMP implementation are also discussed.

The main conclusions and novel contributions of this thesis, and recommendations for future research avenues are provided in Chapter 5.

CHAPTER 2 MODELING PHOSPHORUS TREATMENT CAPACITIES OF ON-SITE WASTEWATER LATERAL FLOW SAND FILTERS

Portions of this chapter have been published in the **Journal of Environmental Engineering** and are being produced in this thesis with permission from the publisher, the **American Society of Civil Engineers**.

Sinclair, A., R. Jamieson, R.J. Gordon, A. Madani, and W. Hart. 2013. Modeling phosphorus treatment capacities of on-site wastewater lateral flow sand filters. J. Environ. Eng. (in press).

2.1 Introduction

Accelerated eutrophication of aquatic systems can cause blue-green algae (cyanobacteria) blooms that produce microcystins, which are toxic to humans and livestock. Other negative impacts of accelerated eutrophication include reduced biodiversity and loss of aquatic habitat (Chambers et al., 2001). Increased loading of phosphorus (P) is the primary cause of accelerated eutrophication in most freshwater systems (Schindler, 1977). Residential wastewater has been identified as a potential P source in watersheds (Carpenter et al., 1998). Wilhelm et al. (1994) identified toilet wastes, dishwashing soaps, and other household cleaning products as the major contributors of P in residential wastewater.

In watersheds with sparse human populations, the on-site wastewater system (OWS) is typically used to treat residential wastewater. The percentage of the populations of the United States, Canada, and the Canadian province of Nova Scotia who live in rural areas and would potentially use OWSs are 19 (United States Census Bureau, 2012), 19 (Statistics Canada, 2012a), and 45% (Nova Scotia Environment, 2011), respectively. Lombardo (2006) observed that OWSs potentially contributed from 4 to 55% of the total P loads in six North American lakes. A typical OWS design includes a pre-treatment septic tank that receives wastewater from an individual residence or cluster of residences. The septic tank effluent (STE) then enters a disposal field where it percolates through native soil or imported filter media that either discharges to a surface water system or the surrounding soil profile. Phosphorus can be transported to surface water bodies from

OWSs mainly from: (i) surface hydraulic failure of the disposal field and (ii) inability of the disposal field and/or the surrounding native soil to remove and retain P (USEPA, 2002).

One OWS disposal field technology is a lateral flow sand filter (LFSF), also referred to as the sloping sand filter (SSF). The LFSF has been used as a replacement option for hydraulically failed disposal fields (Check et al., 1994; Havard et al., 2008). Although they have shown promise, long-term P removal efficiency has been identified as an issue. Check et al. (1994) found that lab-scale LFSFs initially removed P, but after 6-months of loading, increased P effluent concentrations were observed. Havard et al. (2008) studied six field-scale LFSFs that varied in slope and sand grain-size and found acceptable P treatment, with an average LFSF effluent total phosphorus (TP) concentration of 0.92 mg P L^{-1}, but noted that the study period (1 yr) was insufficient to properly evaluate P treatment. Wilson et al. (2011) investigated P treatment in the same LFSFs established by Havard et al. (2008) for the monitoring period of September 2004 to December 2008 with increased STE loading from January 2007 to December 2008. The TP effluent concentrations were found to have increased in all LFSFs, even before the increase in hydraulic loading (Wilson et al., 2011). Both Check et al. (1994) and Wilson et al. (2011) found a reduction in P treatment capabilities with continuous STE loading. There is an identified need to determine when the outlet P loads from LFSFs, and similar types of disposal fields, will potentially become an environmental issue, particularly at the field- and watershed-scales.

2.1.1 Phosphorus Treatment in On-Site Wastewater Systems

The majority of P in STE is in the inorganic form of soluble orthophosphates (PO_4^{3-}, HPO_4^{2-}, $H_2PO_4^-$, H_3PO_4) and typically constitutes 85% of the TP (McCray et al., 2005). Soluble orthophosphates are a plant available form of P, and if present in aquatic environments, contribute to algal growth. The two main orthophosphate treatment processes that occur within a disposal field, including the LFSF, are sorption and precipitation, which are often inter-related (Robertson, 2008; McCray et al., 2009).

Sorption involves attachment of orthophosphates to filter media particles primarily through binding to positively charged metal-oxide or clay minerals at near-

neutral pH ranges (Brady and Weil, 2008). Sorption will also occur, to a lesser extent, on calcium carbonate surfaces, and by weak partitioning into organic carbon (Harman et al., 1996). The amount of P that can be removed by sorption processes is limited by the number of available sorption sites within the filter media and is dependent on pH and redox conditions (Parkhurst et al., 2003; McCray et al., 2009). The pH controls the amount of H^+ protons available at the surface of the media, with higher H^+ concentrations (lower pH) creating more potential sorption sites (McCray et al., 2009). The redox conditions represent the amount of oxygen present for oxidation reactions, such as the conversion of ammonium (NH_4-N) to nitrate (NO_3) through the process of oxidation (Equation 2.1).

$$NH_4^+ + 2O_2 \rightarrow NO_3^- + 2H^+ + H_2O \quad (2.1)$$

The process in equation 2.1 produces H^+ protons as part of the reaction, which in conjunction with other oxidation reactions of STE constituents (e.g. organic N) increases the availability of orthophosphate sorption sites (Robertson, 2012). The metal-oxide minerals that have the highest capacity for P sorption contain iron (Fe), aluminium (Al) and manganese (Mn) (Brady and Weil, 2008). A general assumption about the P sorption process is that it is a two phase reaction. The first phase is the previously described sorption process, which is rapid, reversible and reaches a maximum sorption capacity. The second is viewed as a kinetic, irreversible process caused by either molecular diffusion into pores in the media particles, slow crystallization into metal-phosphate minerals, or precipitation reactions with metal-oxides creating irreversibly sorbed P (Robertson, 2008; McCray et al., 2009). A recent study disputes the existence of this two phase process in certain soils. Robertson (2008) did not observe any of the three kinetic, irreversible secondary sorption processes occurring in an OWS constructed in noncalcareous soil and operated for 16 yrs, suggesting that most of the sorbed P in the disposal field and native soils was in reversible form. The study also hypothesized that these reactions may still be occurring, but at slower rates than could be observed in the 16 yr monitoring period.

The precipitation process involves soluble orthophosphates reacting with mineral cations and is controlled by pH, redox conditions, flow rate, hydraulic saturation, orthophosphate concentration, and void space for precipitate formation (McCray et al., 2009). The same mineral cations that are part of sorption are involved in precipitation reactions, and include Ca (hydroxyapatite [$Ca_5(PO_4)_3OH$], fluorapatite [$Ca_{10}(PO_4)_6F_2$]), Fe (strengite [$FePO_4 \cdot 2H_2O$], vivianite [$Fe_3(PO_4)_2 \cdot 8H_2O$]), Al (variscite [$AlPO_4 \cdot 2H_2O$]), Mn ($MnHPO_4$) and magnesium (Mg) (struvite [$MgNH_4PO_4$]) (Robertson et al., 1998; Nelson and Parsons, 2007; Robertson, 2008; McCray et al., 2009). The pH within the filter governs the types of precipitation reactions that can occur with Ca-P precipitates forming in basic conditions and metal-oxide precipitates forming in acidic conditions (McGechan and Lewis, 2002). The types of precipitates that form also depend on the extent of Ca^{2+} present (calcareous or noncalcareous soil), and the STE effluent mineral concentrations (Zanini et al., 1998; Robertson, 2008).

Robertson et al. (1998), Zanini et al. (1998), Zurawasky et al. (2004) and Robertson (2003, 2008, 2012) studied P retention in OWS subsurface plumes in both calcareous and noncalcareous soils, and identified the dominant P removal mechanism as rapidly occurring (<4 d) precipitation. The redox condition was identified as the dominant control mechanism for precipitation. The operating time periods for the OWS studied ranged from 9 to 44 yrs.

Zanini et al. (1998) found the highest Fe and Al concentrations within 5 to 30 cm of the disposal field distribution system in four OWS with either calcareous or noncalcareous soils. All sites in the study identified the redox condition as undergoing oxidation, which increased the oxidation rate of STE ammonium in the plume, and a subsequent release of H^+ that decreased the pH to acidic conditions. The acid generated in the calcareous soils was hypothesized to increase the concentration of Fe^{2+} or Fe^{3+} through mineral dissolution and promote formation of strengite and vivianite. In the noncalcareous soils it was suggested that there was increased availability of the Al mineral gibbsite ($AlOH_3 \cdot H_2O$) for dissolution in the lower pH environment and subsequently precipitation out of solution as variscite. A study by Robertson (2012) of P retention in an OWS site that operated for 20 yrs using Al and Fe enriched, noncalcareous filter sand media, found that strengite and variscite compounds formed within the filter

bed. The STE effluent was also identified as a source of Al and Fe for precipitation reactions. Oxidation of the filter environment caused acidic conditions (pH ~6) to occur and increased dissolved Al and Fe concentrations available for precipitation reactions. The majority of the P load the OWS sand filter received for the 20 yr operating period was retained within the filter bed. The longevity of the OWS disposal field and soil profile to remove and retain P depends on whether the dominant source of the cations for precipitation is either the wastewater or the filter media, with the filter media theoretically being exhausted as a source first (Zanini et al., 1998).

A study by Robertson et al. (1998) of 10 OWS and the distribution of P in their subsurface plumes in both calcareous and noncalcareous soils found that the highest orthophosphate concentrations (~5 mg P L^{-1}) were present in two OWS in calcareous soils at neutral pH, while the lowest phosphate concentrations (0.1 to 1 mg P L^{-1}) were observed in reducing plumes at near-neutral pH (6.6 to 7.2). The calcareous soil plumes had supersaturated hydroxyapatite concentrations demonstrating that the Ca-P precipitate compound was predominantly in dissolved form and available for lateral flow transport. These results are similar to another study by Robertson (2003) who investigated three noncalcareous and one calcareous OWS sites and found that the oxidized noncalcareous sites caused acidic pH conditions that increased dissolved Al concentrations and Al-P precipitate formation. The calcareous site had near-neutral pH with oxidation causing increased concentrations of dissolved Ca^{2+} in the subsurface plume and average orthophosphate concentrations of 4.8 mg P L^{-1} compared to <0.1 mg P L^{-1} in the three noncalcareous plumes. Robertson (2008) investigated P mobility in an OWS plume in calcareous soil and found that the plume was also supersaturated with hydroxyapatite (Ca-P), and other possible Ca-P precipitate compounds suggesting that Ca precipitation is not effective for long-term attenuation of P. The compound $MnHPO_4$ also had supersaturated conditions. The only P compound that was precipitated out of solution in the plume was strengite; however there were low dissolved Fe concentrations in the plume (<0.1 mg P L^{-1}). These studies examining OWS in calcareous soils identify that these soil types are potentially not effective at long-term P retention via precipitation reactions.

A study by Zurawasky et al. (2004) examined the stability of precipitation formed P compounds in subsurface plumes using column tests for three OWS representing both calcareous and noncalcareous soils. The stability of Fe^{3+} precipitate compounds were found to be susceptible to changes in the redox condition with a reducing environment causing increased dissolved P concentrations. However, two of the OWS sites used in the study had operated for 23 and 44 yrs, and did not experience a change in redox conditions towards creating a reducing environment. It was hypothesized by the authors that increases in the level of plume hydraulic saturation would create reducing conditions (e.g. switch from seasonal to year-round OWS use).

The P sorption and precipitation processes that occur within OWS disposal fields are important to understand before they can be appropriately represented by algorithms in computer models. In particular, the finite number of sorption sites impacts the P removal rate by reducing P removal with time as the sites are filled. The use of long-term OWS disposal field P treatment study results, when precipitation reactions are the primary removal mechanism, for the development of OWS P treatment algorithms would increase model confidence in representing OWS P loads at the watershed-scale.

2.1.2 Existing On-Site Wastewater System Computer Models

Computer modeling is often used to evaluate the potential P loads from OWS, particularly at the watershed-scale (McCray et al., 2005). In many jurisdictions, lakeshore development capacity models using empirical P loading coefficients to represent OWS inputs are commonly used for planning purposes (Robertson, 2003; Brylinsky, 2004). Only the Watershed Analysis Risk Management Framework (WARMF) and Soil and Water Assessment Tool (version 2009 [SWAT2009]) watershed-scale models have specific OWS biomat and hydraulic failure algorithms that simulate OWS P fate and transport (Weintraub et al., 2002; Jeong et al., 2011). The biomat is a biologically active layer that forms at the filter media-infiltration trench interface that has a lower hydraulic conductivity then the filter media (Radcliffe and West, 2009). Both models are relatively simplistic in how they simulate OWS P fate and transport using the biozone algorithm developed by Siegrist et al. (2005). Phosphorus treatment is not simulated directly using the biozone algorithm, but the soil layer that is directly underneath. Both WARMF and

SWAT2009 simulate P removal using a linear sorption isotherm and a maximum sorption capacity for the soil layers. Jeong et al. (2011) identified that the P routines in SWAT2009 need to be improved for simulating OWS P fate and transport, particularly for subsurface flow.

McCray et al. (2009) reviewed a number of field-scale models, based on the advection-dispersion equation, that could be or have been used to simulate P treatment processes in individual disposal fields, including HYDRUS (Hanson et al., 2006), LEACHN (Hutson and Wagenet, 1992), CW2D (Langergraber and Šimůnek, 2005), and a multi-component transport model (Spiteri et al., 2007). These models use linear and/or non-linear isotherms to simulate the P sorption and precipitation processes, with the non-linear isotherms typically being Freundlich or Langmuir (McCray et al., 2009). The HYDRUS model has been used extensively to simulate saturated and unsaturated flow conditions in disposal fields, particularly related to biomat formation (Bumgarner and McCray, 2007; Beal et al., 2008; Radcliffe and West, 2009). However, only the multi-component P and nitrogen transport model developed by Spiteri et al. (2007) has been specifically used to simulate the P treatment process in an OWS disposal field.

2.1.3 Research Objectives

The field-scale models reviewed by McCray et al. (2009) all require a number of input parameters that may not be available at the watershed-scale. Some are computationally intensive making them inappropriate to interface directly with SWAT and WARMF. There is a need to develop improved OWS P fate and transport algorithms for watershed-scale models that balance model complexity and functionality. The objectives of this study are to: i) develop an approach for estimating the mass of sand in LFSFs actively involved in P treatment; and ii) develop and evaluate linear and non-linear temporal removal models using the estimated active P treatment LFSF sand masses to simulate cumulative P sorption and precipitation removal in LFSFs.

2.2 Materials and Methods

2.2.1 Lateral Flow Sand Filter Monitoring Program

The LFSF study site was located at the Bio-Environmental Engineering Centre (BEEC) in Truro, Nova Scotia, Canada and consisted of six LFSFs (LFSF1-6) installed in 2004 and two shorter length LFSFs (LFSF7-8) installed in 2007. All eight LFSFs were constructed according to the *Nova Scotia Environment On-site Sewage Disposal Technical Guidelines* (Nova Scotia Environment, 2009) and received effluent through a flow splitter from a septic tank fed wastewater from the Village of Bible Hill. Filters 1-3, 7, and 8 were constructed on a 5% slope and filters 4-6 were built on a 30% slope to represent the high and low slope limits. Three different imported sands of varying particle size were used as filter media; they were classified (Table 2.1) as fine (LFSF1, 4), medium (LFSF2, 5, 7, 8) and coarse (LFSF3, 6). The LFSFs 1-6 constructed at 1:10 scale were 8 m long, 1.5 m wide and consisted of a 2.5 m long gravel distribution trench at the head, which was then followed by a 5.5 m long sand toe. Filters 7 and 8 were constructed with a shorter sand toe length of 3 m for a total filter length of 5.5 m. Filter effluent from all eight filters was collected individually and directed into a heated sampling hut before flowing through a P-trap fixture and into a calibrated tipping bucket for flow measurement. A Campbell Scientific CR510 data logger (CSI, Logan, UT) recorded flow every 10 minutes.

Table 2.1 Fixed, initial and calibrated filter media and biomat hydraulic and advection-dispersion parameters for the BEEC LFSFs.

Parameter	Units	Gravel*	Fine Sand† (LFSF1,4)	Medium Sand† (LFSF2,5,7,8)	Coarse Sand† (LFSF3,6)	Horizontal Biomat‡	Vertical Biomat‡
Hydraulic (Fixed values)							
Residual water content, Θ_r	$cm^3\ cm^{-3}$	0.056	0.026	0.027	0.023	0.09	0.07
Saturated water content, Θ_s	$cm^3\ cm^{-3}$	0.15	0.375	0.365	0.373	0.3	0.35
Fitted parameter, α	cm^{-1}	0.145	0.145	0.145	0.145	0.005	0.006
Fitted parameter, n	-	1.92	2.68	2.68	2.68	2.68	2.68
Saturated hydraulic conductivity, K_s	$cm\ d^{-1}$	1.44E6	2186	6328	11534	1.5	2.16
Pore-connectivity, l	-	0.5	0.5	0.5	0.5	0.5	0.5
Fitted parameter, Θ_m	$cm^3\ cm^{-3}$	0.15	0.375	0.365	0.373	0.3	0.35
Fitted parameter, Θ_a	$cm^3\ cm^{-3}$	0.05	0.026	0.027	0.023	0.09	0.07
Water content for K_k, Θ_k	$cm^3\ cm^{-3}$	0.15	0.075	0.109	0.075	0.3	0.35
Unsaturated hydraulic conductivity, K_k	$cm\ d^{-1}$	1.44E6	0.411	16.070	6.48	1.5	2.16
Advection-Dispersion [Calibrated Values]							
Media bulk density, ρ_b	$g\ cm^{-3}$	1.4 [1.3]	1.4 [1.3]	1.4 [1.3]	1.4 [1.3]	1.35 [1.25]	1.35 [1.25]
Longitudinal dispersivity, D_L§	cm	20 [5]	20 [5]	20 [5]	20 [5]	20 [5]	20 [5]
Transverse dispersivity, D_T‖	cm	2 [0.5]	2 [0.5]	2 [0.5]	2 [0.5]	2 [0.5]	2 [0.5]
Diffusion coefficient, D_w#	$cm^2\ d^{-1}$	0.40608	0.40608	0.40608	0.40608	0.40608	0.40608
Adsorption isotherm coefficient, K_d•	$cm^3\ g^{-1}$	0.2 [0]	0.2 [0.05]	0.2 [0]	0.2 [0]	0.3 [0]	0.3 [0]
Biomat Thickness	cm	-	3 [0]	3 [0]	3 [0]	-	-

Note: * Literature: Langergraber and Šimůnek (2005).

† Measured: K_s – ASTM method D2434-68 (2006), Θ_r, Θ_s, Θ_k – ASTM D6836-02 method (2008), K_k - Marshall (1958)-Millington and Quirk (1959) Method (MMQ), Literature: Other – HYDRUS-2D Rosetta Database (Carsel and Parrish, 1988).

‡ Literature: Beach and McCray (2003).

§ Measured: Average D_L value calculated from mean RTDs for observed rhodamine tracer studies.

‖ Literature: Assumed 10:1 longitudinal to transverse dispersivity ratio (Pang et al., 2000).

Literature: Sabatini (2000).

• Initial value adapted from Richardson et al. (2004).

Flow and TP data collected from November 2004 to October 2011 (7 yrs) for LFSF1-6 and October 2007 to October 2011 for LFSFs 7 and 8 were used in this study. Filters 1-6 each received approximately 100 L d^{-1} of effluent from a septic tank with a 2 to 4 d residence time, starting in September 2004. As the LFSFs were built at 1:10 scale the 100 L d^{-1} loading rate was used as it matched the NS OWS technical guideline design loading rate of 1000 L d^{-1} for a 3 bedroom home with low flow fixtures (Nova Scotia Environment, 2009). In January 2007 the effluent loading was increased to 175 L d^{-1} to assess treatment performance at a higher loading rate (Wilson et al., 2011). Filters 7 and 8 each received approximately 100 L d^{-1} of STE starting in August 2007 and effluent quality monitoring started in October 2007. Influent STE and effluent from each filter were sampled on a monthly basis using ISCO 6712 auto-samplers (ISCO Inc., Lincoln, NE) to collect composite samples over a 24-hr period. The samples were analysed for TP (Std. Method 4500-P [1999 revision], ascorbic acid method), and for a suite of other water quality parameters not reported in this study, at the Nova Scotia Agricultural College Environmental Research Laboratory. The eight LFSFs and their monitoring programs for this study have previously been described by Havard et al. (2008) and Wilson et al. (2011).

2.2.2 Active Phosphorus Treatment LFSF Sand Mass

Two-dimensional water flow and solute transport were simulated in the eight LFSFs to estimate the mass of sand actively involved in active P treatment. The HYDRUS-2D (version 1.11) model was chosen as it has been used in a number of other studies to simulate unsaturated flow in OWS disposal fields with biomats (Bumgarner and McCray, 2007; Beal et al., 2008; Radcliffe and West, 2009). Radcliffe and West (2009) used HYDRUS-2D to determine steady state hydraulic loading rates for 12 soil textural classes that were overlain with a biomat and ponded wastewater that had a constant 5 cm of vertical head. Distribution trench sidewall flow above the biomat zone was adequately modeled using HYDRUS-2D for extreme hydraulic loading events (30 cm ponded wastewater) by Beal et al. (2008).

The spatially related output of HYDRUS-2D allows for estimation of the volume of sand involved in P treatment. The model uses a Galerkin-type linear finite element

model to numerically solve the Richards Equation and the advection-dispersion equation to simulate water flow and solute transport, respectively (Šimůnek et al., 2006). The use of a finite element mesh allows for calculation of the filter media area where solute is transported by unsaturated flow processes and would be actively involved in P treatment. Unsaturated hydraulic properties of the LFSF materials were predicted in HYDRUS-2D using the modified van Genuchten analytical model (Vogel and Cislerova, 1988). This was chosen because unsaturated hydraulic conductivities predicted by water tension measurements were available for the three filter sands for low fractions of saturation (0.2 to 0.3). The modified van Genuchten equation reverts to the original van Genuchten equation if the unsaturated input parameters are not known (Šimůnek et al., 2006).

Phosphorus transport was not simulated using HYDRUS-2D as the projected model run times for simulating 8 yrs of continuous STE loading were considered unreasonable at 15 to 77 d. The results of three rhodamine WT tracer studies conducted by Wilson et al. (2011) within each LFSF were used to verify that HYDRUS-2D adequately simulated water and solute transport processes by comparing observed and simulated tracer residence time distributions (RTDs). The three studies were conducted in June 2007, July 2008 and October 2008. Each involved injection of 10 mL of rhodamine WT dye (20% by weight) into each filter. Each of the tracer studies had the same daily STE loading rate throughout the monitoring time period (LFSF1-6 175 L d^{-1}; LFSF7-8 100 L d^{-1}). ISCO autosamplers were used to sample each filter outlet at 4 to 6 h intervals. The rhodamine WT concentrations were measured using a DR 5000 UV-Vis spectrophotometer (HACH, Loveland, CO) with a wavelength of 580 nm. The Fogler (1992) RTD method was used to analyse the tracer study results. Wilson et al. (2011) discusses the rhodamine WT tracer experiment methodology in more detail.

Figure 2.1 shows the setup of the LFSF4 HYDRUS-2D model with the filter material distribution, boundary conditions, and location of the continuous daily hydraulic loading rate. The HYDRUS-2D model requires water retention and unsaturated hydraulic conductivity inputs for each of the filter materials. The fine, medium, and coarse sands had their saturated hydraulic conductivities (K_s) determined using the constant hydrostatic water head method D2434-68 (ASTM, 2006). The D6836-02 Standard Test Method C (ASTM, 2008) with a pressure plate apparatus was used to develop the

moisture retention curve for each sand type. Both the saturated hydraulic conductivity and moisture retention tests were conducted at the Nova Scotia Agricultural College Soils Laboratory. The residual (Θ_r) and saturated (Θ_s) volumetric moisture contents were determined from the moisture retention curves. The Marshall (1958) and Millington and Quirk (1959) method was used to determine unsaturated hydraulic conductivities (K_k) for volumetric moisture contents (Θ_k) close to the Θ_r values using the saturated hydraulic conductivity and soil moisture retention curve results. Other HYDRUS-2D hydraulic input parameters for the three sands were assumed to be the default values developed by Carsel and Parrish (1988). No site specific hydraulic properties were available for the gravel and biomat layers. The input parameters for the gravel layer were adapted from Langergarber and Šimůnek (2005). Initial biomat input parameters were adapted from Beach and McCray (2003) for their model scenario of a biomat overlying a coarse sand material (K_s = 2000 cm d^{-1}) with a hydraulic loading rate of 3.5 cm d^{-1}. Table 2.1 presents the input hydraulic parameters for the HYDRUS-2D model.

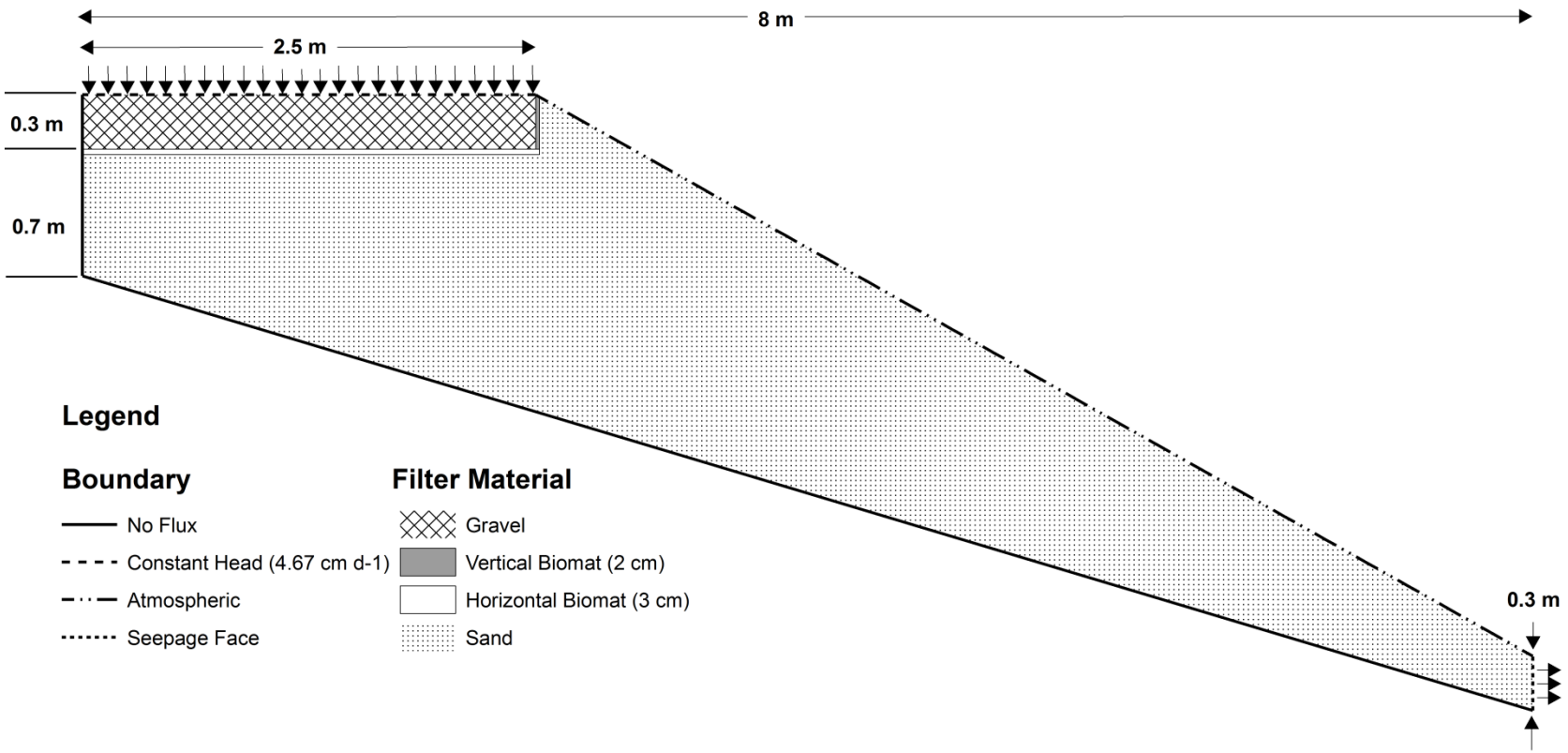

Figure 2.1 Cross-sectional view of LFSF4 as input into the HYDRUS-2D model showing filter media dimensions and boundary conditions.

A trial and error method, adapted from Radcliffe and West (2009), was used to setup the finite-element mesh size for the different LFSF layers that minimized water and tracer mass balance error (<5%) for all time steps, resulting in a 2.5 cm mesh for the sand and gravel layers and a 1 cm mesh for the horizontal and vertical biomats. A smaller mesh size was chosen for the 0.5 to 3 cm thick biomat layers to ensure flow was adequately modeled. The HYDRUS-2D model for each LFSF was run in two stages to simulate the rhodamine WT tracer studies. The first stage involved development of a steady-state flow condition within each simulated filter by simulating 25 d of STE loading with an initial water pressure head (h = -1000 cm). The 25 d simulation period was chosen using a trial and error process where the difference between the inflow and outflow rates was less than 2%. The initial water content of each LFSF for the second model run stage was set at the 25 d water content from the first stage. The second model run stage involved the introduction of a 10 s solute pulse into the gravel distribution trench that was equivalent to 2 g rhodamine WT for all eight filters. Again a trial and error method was applied to develop the simulation time period with the constraints that it be longer than any of the rhodamine WT tracer studies and a minimal percent change (<1%) in total sand area exposed to rhodamine WT over a 5 d time period. A 30 d simulation period was chosen for the second model run stage as the area of total sand exposed to rhodamine WT differed by 0.6% between 25 and 30 d. The initial input advection and dispersion parameters to set-up the solute transport component of HYDRUS-2D are presented in Table 2.1.

The RTD of modeled solute tracer at the down gradient seepage face for each LFSF HYDRUS-2D model was calculated using the Fogler (1992) RTD method, and then compared against the observed RTDs for the Summer 2007, Summer 2008, and Fall 2008 tracer studies. Calibration of the HYDRUS-2D models was accomplished by manually changing the values of the biomat hydraulic parameters and rhodamine WT advection-dispersion input parameters (Table 2.1), and biomat thicknesses (0, 0.5, 1, 2, and 3 cm). Root mean square error (RMSE), agreement between simulated and observed mean residence times, and graphical methods were used to assess model performance (Gooseff et al., 2003).

The LFSF HYDRUS-2D models were calibrated in groups according to sand grain-size and STE loading rate (LFSF1, 4; LFSF2, 5; LFSF3, 6; LFSF7, 8). Biomat formation in the LFSFs with the same sand grain-size and STE loading rate was assumed to be the same as all eight filters have the same gravel distribution layer dimensions and slope at the sand-gravel interface (Figure 2.1). Initially the inverse solution option in the HYDRUS-2D model was used to calibrate the solute transport input parameters. The inverse solution model did not allow convergence of observed and simulated data, so manual calibration was performed. Beggs et al. (2011) had a similar issue with fitting an inverse solution to bromide tracer study results in HYDRUS-2D.

After HYDRUS-2D model calibration, the mass of sand involved in active P treatment for each LFSF was evaluated by two methods; the first involved calculating the area of sand exposed to the tracer solute in the stage two model run. A point shapefile was first created in ArcGIS 9.3 (ESRI, Redlands, CA) using the spatially related finite element mesh and day 30 internal rhodamine WT concentration ASCII HYDRUS-2D output files for each LFSF. Initially a triangular irregulated network (TIN) was created from the point shapefile. A contour line was then created from the TIN to define the active P treatment area's edge. A solute concentration of 1 μg L^{-1} was used to define the contour line as it has previously been reported by Richardson et al. (2004) as a fluorometer method detection limit in a wastewater environment. The active P treatment area was calculated from a polygon created by merging the contour line and a polygon outline of the sand media layer. The LFSF design width of 1.5 m and an assumed sand density of $1.3x10^3$ kg m^{-3} were then multiplied by the active P treatment area to calculate the mass of sand involved in active P treatment. A second analysis was also conducted to verify the active treatment area, where the area of sand possessing water contents at or above the field capacity water content (100 cm tension) was delineated (USDA, 2013). The same ArcGIS procedure used to delineate the solute interaction area was used on the day 30 water content ASCII HYDRUS-2D output file. The level of agreement between the results of the two methods for calculating the mass of sand involved in active P treatment was then evaluated.

2.2.3 Phosphorus Temporal Removal Models

2.2.3.1 Phosphorus Sorption Capacity Experiment

The P sorption capacities of the three sands used in the BEEC LFSFs were determined experimentally using a method adapted from Cucarella and Renman (2009). The experiment created individual batches of three 50 mL centrifuge tubes, each filled with 50 mL of distilled water, approximately 2.5 g of sand and then spiked with KH_2PO_4 to obtain the appropriate initial P concentration. The initial P concentrations for each sand were 0, 0.25, 0.5, 1, 5, 7.5, 10, 20, 50, 100, and 200 mg P L^{-1}. All batch experiments were conducted in triplicate and for each initial P concentration a set of centrifuge tubes with no sand added were run as standards. Another three centrifuge tubes were filled with distilled water and run as the blank. The prepared centrifuge tubes were sealed and then placed horizontally on a reciprocal shaker table (100 rpm) and shaken for 24 h at room temperature. The tubes were centrifuged at 2400 rpm for 10 min and then the supernatant was filtered through 1.5-µm Whatman 934-AH filters. The filtered supernatant was diluted to the appropriate concentration range and then analysed for TP using the molybdenum blue-ascorbic acid method (Murphy and Riley, 1962) with a mean detection limit of 1 µg L^{-1}. Sand samples were also analysed for P_2O_5, Ca, Fe and Mg at the Nova Scotia Department of Agriculture Laboratory.

The results of the P sorption experiment were then analysed by fitting the observed data to the Langmuir adsorption isotherm that is expressed as:

$$S = \frac{S_{\max} K_L C_{eq}}{1 + K_L C_{eq}} \tag{2.2}$$

where S is the observed amount of solute sorbed to the filter media, C_{eq} is the observed equilibrium P concentration in solution, S_{max} is the maximum P adsorption capacity, and K_L is the Langmuir constant. Each S value was adjusted by adding the initial amount of P sorbed to the sand (S_o). The S_o was determined by plotting observed C_{eq} against S data for C_{eq} values ≤10 mg P L^{-1} and fitting the following least squares equation (Rao and Davidson, 1979):

$$S = KC_{eq} - S_o \tag{2.3}$$

where K is the slope of the fitted least squares line and S_o is the y-intercept. To calculate the S_{max} and K_L values from the observed data a linearized Langmuir equation was used:

$$\frac{C_{eq}}{S} = \frac{S}{K_L} + \frac{1}{S_{\max} K_L} \tag{2.4}$$

2.2.3.2 Phosphorus Treatment Capacity Analysis

Observed P input and output load data for each BEEC LFSF were analysed to assess changes in P treatment performance over the 2004 to 2011 monitoring period. The observed data analysis involved comparison of average TP influent and effluent loads, and calculating percent TP reduction for the time periods 2004-06, 2007-08 and 2009-11 for each LFSF to correspond with the Havard et al. (2008) and Wilson et al. (2011) study periods.

The cumulative P removal by sorption and precipitation for each LFSF was then modeled by fitting linear and non-linear temporal removal models to the observed datasets and evaluating the model performance. The P temporal removal models were developed and evaluated to examine their ability to predict long-term (7+ yrs) P treatment. Predicting long-term P loads from LFSFs using a P temporal removal model would be a useful tool for watershed managers that have residential OWS as a potential P source in their watershed. As the observed influent and effluent P loading data was in the form of TP it was assumed that 100% of the TP was in the form of soluble orthophosphates, and affected by sorption and precipitation processes. The influent and effluent TP loads were normalized (kg TP kg^{-1} active P treatment sand) using the active P treatment sand masses estimated using the HYDRUS-2D model for each of the eight LFSFs. This normalization process allowed P temporal removal models with the same sand grain size and filter length, but differing slopes to be directly compared against each other and also average models to be developed for these same filters. The observed cumulative influent TP load (kg P kg^{-1} active P treatment sand) was used as the independent input variable and the temporal removal models were developed on a monthly time step. As shown in Table 2.2 the temporal removal model equations tested were linear, Langmuir, Freundlich and 2-part piecewise linear. Other temporal removal models were evaluated that involved the Langmuir isotherms developed from the results

of the batch P sorption tests in the previous section added to either a linear, Freundlich or 2-part piecewise linear temporal removal model (Table 2.2). The linear, Langmuir and Freundlich temporal removal models are commonly used to simulate P treatment processes in a subsurface environment (McCray et al., 2005). These temporal removal models, as well as the others used in this present study, are based on several assumptions and exhibit different limitations in how well they describe the two P treatment processes: sorption and precipitation. The linear equation is the most simplistic model with two fitted parameter variables: slope or linear distribution coefficient (*m*) and y-intercept (*b*) (Table 2.2). The *b* variable represents the initial amount of P that is sorbed and/or precipitated in the filter media. McCray et al. (2005) identified the main limitation of the linear equation is that it does not limit the amount of P that can be removed by sorption and precipitation. Sorption is physically limited by the number of sorption sites, which the linear equation cannot directly take into account. The SWAT2009 biozone algorithm uses the linear equation, but indirectly takes into account the maximum P sorption capacity by stopping P removal when the linear equation equals the maximum sorption capacity (Jeong et al., 2011).

Table 2.2 Optimized input parameters for each individual phosphorus temporal removal model for each lateral flow sand filter.

Temporal Removal Model	Equation*	Fitted Parameter	LFSF 1	LFSF 2	LFSF 3	LFSF 4	LFSF 5	LFSF 6	LFSF 7	LFSF 8
Langmuir	$y = (S_{\max} K_L x)/(1 + K_L x)$	S_{max}	507	381	200	331	306	159	63	60
		K_L (10^{-3})	2.50	3.49	7.07	4.23	4.58	9.10	16.01	16.25
Freundlich	$y = K_F x^{(1/n)}$	$1/n$	0.76	0.71	0.60	0.70	0.70	0.60	0.61	0.65
		K_F	3.00	3.64	4.92	3.73	3.62	4.57	2.50	2.11
Linear	$y = mx + b$	m	0.75	0.66	0.48	0.69	0.69	0.49	0.37	0.39
		b	13.72	16.39	17.92	14.76	13.72	14.50	7.94	6.51
2-Part Piecewise Linear	$y = \begin{cases} m_1 x + b_1, y < S_{\max} \\ m_2 x + b_2, y \geq S_{\max} \end{cases}$	m_1	0.94	0.91	0.74	0.92	0.89	0.75	0.37	0.39
		b_1	0.41	-0.47	-1.12	-0.16	1.13	-0.25	7.94	6.51
		m_2	0.52	0.34	0.14	0.37	0.27	0.10	-	-
		b_2	65.0	91.4	89.2	77.2	89.9	78.0	-	-
Langmuir + Linear†	$y = Langmuir + mx + b$	m	0.58	0.50	0.46	0.51	0.51	0.46	0.15	0.17
		b	3.33	12.99	17.73	5.85	11.39	14.38	7.28	5.95
Langmuir + Freundlich†	$y = Langmuir + K_F x^{(1/n)}$	$1/n$	0.84	0.69	0.59	0.76	0.67	0.58	0.42	0.46
		K_F	1.40	3.01	4.92	1.95	3.12	4.57	2.94	2.37
Langmuir + 2-Part Piecewise Linear†	$y = Langmuir + \begin{cases} m_1 x + b_1, y < S_{\max} \\ m_2 x + b_2, y \geq S_{\max} \end{cases}$	m_1	0.47	0.68	0.71	0.55	0.69	0.70	0.15	0.17
		b_1	1.57	-0.63	-1.13	-1.89	0.18	0.59	7.28	5.95
		m_2	0.40	0.19	0.12	0.27	0.13	0.07	-	-
		b_2	44.3	83.9	88.5	53.3	80.3	78.4	-	-

Note: * y = P sorbed and precipitated (kg TP); x = normalized influent P load (kg TP kg^{-1} active treatment sand).
† Langmuir = P sorption experiment isotherm for appropriate sand grain-size.

The Freundlich equation is relatively complicated with two empirical constants (K_F, $1/n$). This equation is typically constructed by fitting to an observed dataset (McCray et al., 2005). The $1/n$ value regulates the P removal rate as the cumulative influent P load increases. If $1/n<1$ then the P removal rate is reduced as the cumulative influent P load increases, and can approach a maximum limit, such as a maximum P sorption capacity. The P removal rate increases as the total P influent load increases, if $1/n>1$. This presents a physically unrealistic scenario as most OWS experience a decrease in P removal rate with continuous P loading (McCray et al., 2009; Wilson et al., 2011). The Freundlich equation does not quite reach an end point for total P removal when $1/n<1$, which makes it inappropriate for representing finite sorption processes; however, precipitation processes can be continuous depending on the mineral content in the STE, which could be potentially represented by the Freundlich equation (Zanini et al., 1998). This equation would be very useful for representing long-term P treatment in OWS disposal fields.

The Langmuir equation is specifically designed to stop P treatment when the maximum P sorption capacity is reached. It is typically used for batch maximum P sorption capacity experiments, such as the one in this present study. It utilizes an adsorption constant (K_L) and S_{max} as its fitted parameters. McCray et al. (2005) identified that there are many literature sources for maximum P sorption capacities of different filter media, but fewer for soils. As the Langmuir equation stops P removal, once it reaches its maximum sorption capacity, it cannot represent continuous P treatment via precipitation processes.

The 2-part piecewise linear equation has been used by Nair et al. (2004) to calculate sorbed P based on the degree of P saturation in soils. As the name implies there are two linear equations in a 2-part piecewise linear equation and a decision variable is required to switch from equation I to II; for this study the S_{max} value calculated from the P sorption test experiments was used (Table 2.2). The S_{max} value was used because it describes where the P sorption process stops and treatment would then be dominated by precipitation, and S_{max} values have been determined for a variety of soil classes and OWS filter media (Cucarella and Renman, 2009). Linear equation I potentially will represent when both sorption and precipitation processes are occurring and linear equation II would

represent after the sorption sites have been depleted and precipitation is the dominant treatment process.

The Langmuir+Linear, Langmuir+Freundlich and Langmuir+2-Part Piecewise Linear temporal removal models are the most complex equations investigated in this study. They represent the sorption process by using the batch experiment Langmuir sorption isotherms, developed in this present study in association with another equation (linear, Freundlich, 2-part piecewise linear), that represents the precipitation process. As the P temporal removal models are supposed to represent both sorption and precipitation processes, using the equation that is most commonly used to represent sorption, Langmuir, in conjunction with another equation to represent precipitation processes (linear, Freundlich, and 2-part piecewise linear) would potentially be the best at representing both processes at the same time, instead of trying to represent both processes with one equation. This approach has the most uncertainty of the equations investigated as there are three to six fitted parameters that have to be determined. However, it models both sorption and precipitation using two separate equations that may theoretically better fit the overall treatment process.

To allow comparison of temporal removal models and develop average models for LFSFs with the same sand grain-size and filter lengths the influent TP loads were normalized. Normalization involved dividing the influent TP load for each filter by the mass of sand actively involved in active P treatment that was determined from the calibrated HYDRUS-2D model results. The fitted parameters for each temporal removal model were optimized by minimizing a weighted RMSE objective function using the Solver function in Microsoft Excel. The temporal removal models that combined batch P sorption Langmuir and either linear, Freundlich or 2-part piecewise equations did not have the Langmuir equation optimized using the objective function.

One of the objectives of using P temporal removal models was to predict long-term (>10 year) cumulative P effluent loads to surface water systems. To ensure that the fitted P temporal removal models did not preferentially fit the earlier portion of the observed dataset and potentially over- or under-predict the long-term P treatment, the observed data were split into two parts. A weighted RMSE was then calculated for model

optimization with preferential weighting for the latter part of the observed dataset using the following equation:

$$RMSE_{optimal} = RMSE_{Part\ I} + 2 * RMSE_{Part\ II} \tag{2.4}$$

where $RMSE_{Part\ I}$ represents the first part of the observed dataset and $RMSE_{Part\ II}$ is the second part of the observed dataset. The last 20 individual months of observed TP treatment data were used as the Part II dataset for each LFSF.

The performance of the P temporal removal models for each LFSF Part I and II dataset was evaluated using the Nash-Sutcliffe Efficiency (NSE) (Nash and Sutcliffe, 1970), RMSE, and graphical techniques. The models were directly compared against each other using the F-test method (99% confidence interval; P>0.01) in Excel outlined by Bolster and Hornberger (2007) and the corrected Akaike's Information Criterion (AIC) (Burnham and Anderson, 2002) to determine if models with a greater number of fitted parameters were significantly better than models with fewer fitted parameters. The AIC was calculated by:

$$AIC = N \ln\left(\frac{SSE}{N}\right) + 2(p+1) + \frac{2(p+1)(p+2)}{N-p-2} \tag{2.5}$$

where N is the number of observations, SSE is the sum of squared errors and p is the number of fitted parameters for the model. The model with the lowest AIC value is then compared against the other models by calculating the probability it is the correct model (Bolster and Hornberger, 2007):

$$P_i = \frac{\exp\left(0.5 * \left(AIC_i - AIC_{\min}\right)\right)}{1 + \exp\left(0.5 * \left(AIC_i - AIC_{\min}\right)\right)} \tag{2.6}$$

where AIC_i is the AIC value for the model being compared and AIC_{min} is the lowest AIC value. The lowest the probability value can be is 0.5 when AIC_i and AIC_{min} are equal.

Wilson et al. (2011) found that performance was similar in the BEEC site LFSFs with the same sand grain-size and filter length, but different slopes. Therefore, average P temporal removal models were developed by selecting the best model type, based on model performance, for the two filters with the same sand grain-size and filter length and then averaging their fitted input parameters. The same P temporal removal model

performance analysis as for the individual LFSFs was performed on the results of these best average models.

2.3 Results and Discussion

2.3.1 Active Phosphorus Treatment LFSF Sand Mass

The calibrated HYDRUS-2D LFSF models produced a satisfactory level of agreement between the observed and simulated tracer mean residence times, as shown in Table 2.3. The average difference between the simulated and observed mean residence times was ±0.76 d. However, all of the HYDRUS-2D models had RMSE values above 1 mg L^{-1}, and models for all of the 8 m long LFSFs (1-6) tended to over-predict the maximum peak rhodamine WT concentrations (Table 2.3). The calibrated advection-dispersion input parameters, as shown in Table 2.1, for all eight models were generally set to reduce the mean residence time of the rhodamine WT tracer. The calibrated simulated and observed RTDs for the coarse and medium sand LFSFs had vertical and horizontal biomat thicknesses set to 0 cm and adsorption isotherm coefficient (K_d) values of 0 cm^3 g^{-1}. The calibrated fine sand LFSFs 1 and 4 had a K_d value of 0.05 cm^3 g^{-1} for the sand layer and vertical and horizontal biomat thicknesses of 0 cm.

Table 2.3 Model performance results for HYDRUS-2D simulations of rhodamine WT tracer in the lateral flow sand filters.

LFSF	Observed Data	RMSE (mg L^{-1})	Mean Residence Time (d)		Observed vs. Simulated Mean Residence Time (d)	Peak Rhodamine WT Concentration (mg L^{-1})	
			Observed	Simulated		Observed	Simulated
1	Summer	1.04	5.79	5.91	-0.12	1.16	3.06
	Summer	0.98	7.78	6.00	1.78	0.66	
	Fall 2008	0.83	8.39	6.01	2.38	0.61	
4	Summer	1.31	4.23	4.64	-0.41	1.21	3.84
	Summer	1.39	4.74	4.76	-0.02	0.87	
	Fall 2008	1.43	5.02	4.76	0.26	0.95	
2	Summer	2.08	2.13	3.38	-1.25	5.35	6.19
	Summer	1.96	3.19	3.35	-0.16	1.99	
	Fall 2008	2.93	2.73	3.37	-0.64	3.15	
5	Summer	1.54	2.78	3.17	-0.39	3.02	6.0
	Summer	2.06	3.73	3.11	0.62	1.16	
	Fall 2008	1.76	4.74	3.26	1.48	1.65	
7	Summer	3.69	3.0	4.12	-1.12	5.69	4.27
	Fall 2008	2.62	2.33	4.04	-1.71	8.32	
8	Summer	2.72	3.82	4.28	-0.46	8.64	4.27
	Fall 2008	2.63	3.43	4.04	-0.61	8.58	
3	Summer	2.77	4.43	2.73	1.7	2.11	7.93
	Summer	2.49	2.80	2.71	0.09	4.80	
	Fall 2008	2.35	2.33	2.69	-0.36	5.87	
6	Summer	1.56	2.01	2.70	-0.69	6.36	6.51
	Summer	1.38	2.68	2.61	0.07	3.96	
	Fall 2008	2.48	2.32	2.66	-0.34	4.88	

Three possible reasons for the over-prediction of the maximum rhodamine WT concentrations and RMSE values above 1 mg L^{-1} would be uncertainty in solute sorption behaviour, preferential flow and non-ideal transport processes. Rhodamine WT is known to undergo sorption to sand particles when used as a tracer (Richardson et al., 2004). Wilson et al. (2011) selected this non-conservative tracer as their primary study objective was to compare relative residence times in the eight LFSFs and it was assumed rhodamine WT sorption would equally affect the RTD for each filter. The observed RTD data for the three tracer studies had mass-in to mass-out ratios from 0.21 to 0.95, suggesting that sorption of rhodamine WT is occurring within the LFSFs (Wilson et al., 2011). The LFSFs are only 1.5 m wide and have an HDPE liner, and therefore this could potentially allow sidewall preferential flow to occur between the liner and filter media. Sidewall flow has been observed to occur in soil lysimeter experiments (Corwin, 2000). Fingered preferential flow at the interface between the LFSF gravel and sand media layers could also have occurred. The non-ideal transport processes that may not be being modeled by HYDRUS-2D include rate-limited sorption, and diffusion in and out of lower-permeability domains within the sand filter media. These processes would reduce the peak concentration leaving the filter by lengthening the travel time for a certain percentage of the tracer particles, but should not be significant enough to change when the centre of tracer mass leaves the filter. These non-ideal transport processes may be the most realistic in explaining why the HYDRUS-2D models had a good match for mean RTDs and over-predicted peak concentrations.

The calibrated HYDRUS-2D simulations with no vertical and horizontal biomats and solute K_d values of either 0.05 or 0 cm^3 g^{-1} represent a scenario that typically would not be expected to develop within an OWS disposal field. Different biomat and sorption input parameter scenarios were modeled in HYDRUS-2D for the eight filters to assess the effect of these parameters on the predicted active P treatment areas. Figure 2.2 shows the modeled active P treatment areas for LFSF1 calculated using the tracer solute area method for three different biomat and sorption scenarios. The LFSF1 HYDRUS-2D model with a 3 cm thick horizontal and vertical biomat with a sand and biomat K_d value of 0.2 cm^3 g^{-1} had an active P treatment area that was 4.9% smaller than the calibrated LFSF1 model with no biomat and a K_d value of 0.05 cm^3 g^{-1}. The percentage difference

in active treatment areas between the calibrated and biomat/sorption scenarios was also approximately 5% for the coarser grained sand and steeper sloped filters (results not shown). In addition, the area of the filter possessing water contents greater than or equal to field capacity did not change for the different scenarios. The presence of a biomat and a solute undergoing sorption in the LFSF HYDRUS-2D has little impact on the predicted active area involved in P treatment.

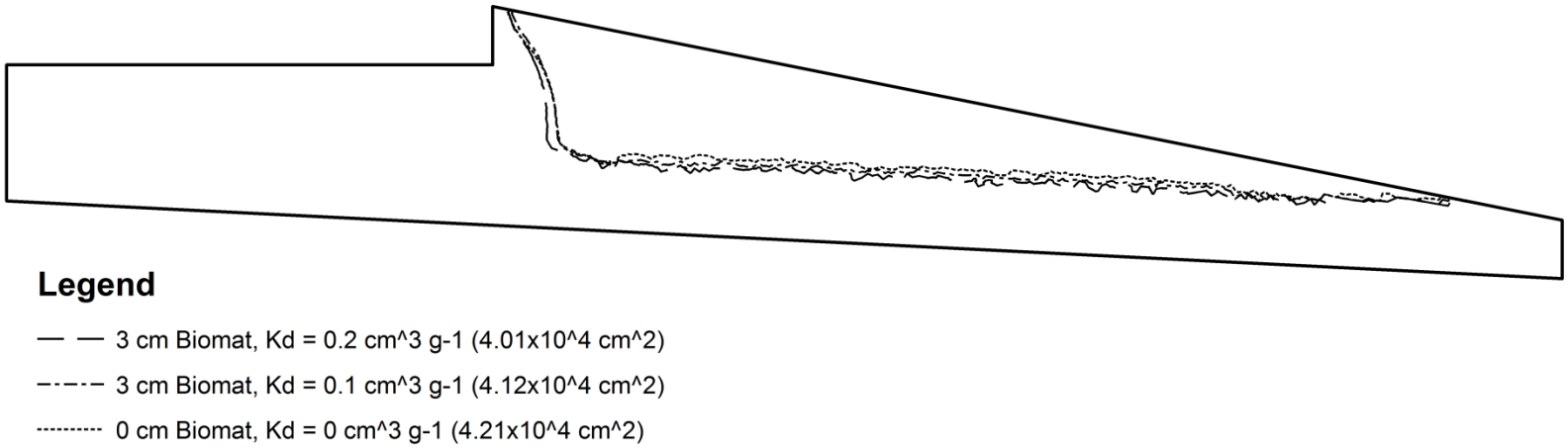

Figure 2.2 HYDRUS-2D modeled rhodamine WT flow areas for different biomat and sorption scenarios in LFSF1.

Havard et al. (2008) previously reported that flow within the LFSFs is dominated by unsaturated flow processes. In the present study free water was not observed in piezometers installed within the sand and gravel layers in the eight LFSFs during the 2004 to 2011 monitoring period. Figure 2.3 shows contours in LFSF1 representing different soil moisture tensions at 30 d for the HYDRUS-2D model run stage two. The other LFSF HYDRUS-2D models had similar water content conditions simulated within their filter media. A soil moisture tension of 0 cm represents saturated conditions and none of the LFSF HYDRUS-2D models had saturated conditions in either the gravel or sand layers. Both the simulated and observed LFSF moisture contents are unsaturated suggesting that tension-saturated flow predominates.

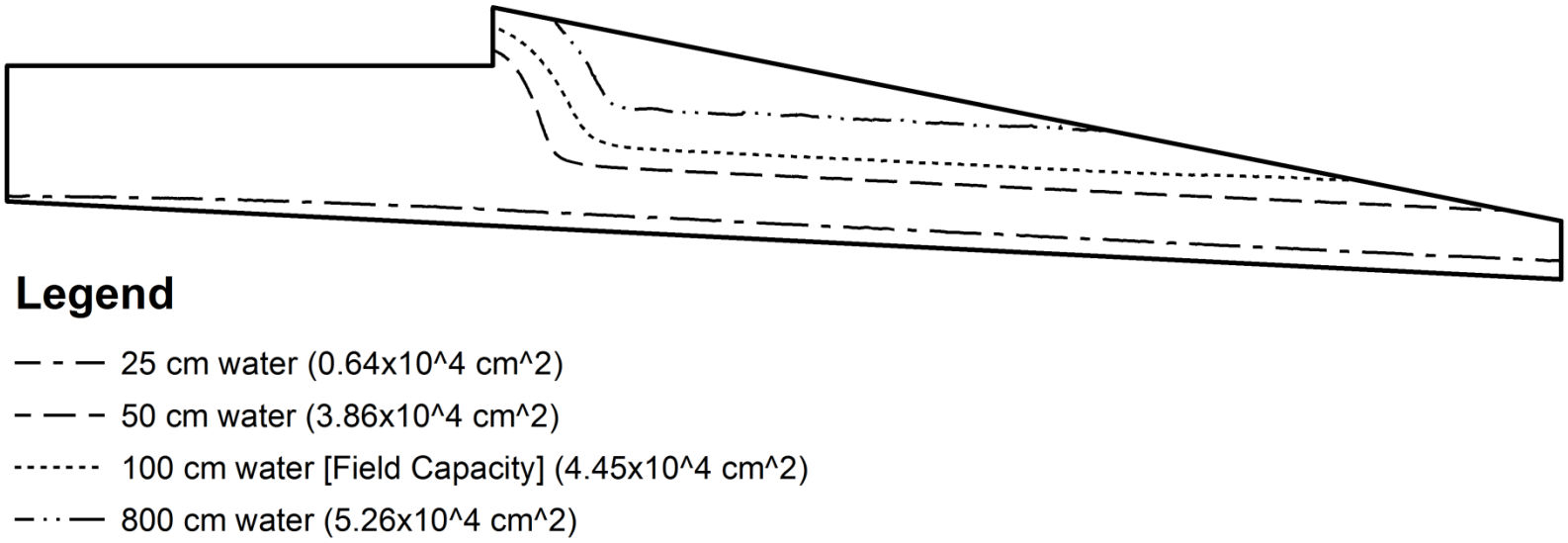

Figure 2.3 HYDRUS-2D modeled water content distributions in LFSF1.

Although preferential flow is potentially occurring within the LFSFs the relatively low impact of the solute sorption and biomat input parameters on determination of active P treatment area, satisfactory agreement between the observed and simulated mean residence times, and observed and simulated unsaturated soil moisture contents in the sand layers suggest that the calibrated HYDRUS-2D model results are acceptable for predicting the mass of sand involved in active P treatment. Table 2.4 shows the predicted mass of sand involved in active P treatment for each LFSF using either solute transport or moisture levels (field capacity) as indicators. In general, there was good agreement between the two methods, however, using field capacity as the indicator produced active P treatment masses that ranged from 0 to 16% larger (average 6%) than those predicted using solute transport as the indicator. As mentioned earlier it was found that the predicted area exposed to 1 μg L^{-1} or more of solute increased slightly in total area by 0.6% from 25 to 30 d. Moisture level distributions within the filter, however, remained stable during the simulation period, indicating the establishment of steady state conditions. Therefore, the active treatment area, delineated as the area with water tension greater than 100 cm, was used for P temporal removal model development. Although, it should be noted that differences between these two approaches for estimating active treatment area are small (Table 2.4, Figures 2.2 and 2.3).

Table 2.4 **Predicted active phosphorus treatment sand mass for each lateral flow sand filter using solute transport (Rhodamine WT) and water content (field capacity) as indicators.**

Filter	Rhodamine WT: Active P Treatment Mass of Sand (10^3 kg)	Rhodamine WT: Percentage of Sand Media Involved in Active P Treatment (%)	Field Capacity: Active P Treatment Mass of Sand (10^3 kg)	Field Capacity: Percentage of Sand Media Involved in Active P Treatment (%)
1	8.2	72	8.6	76
2	7.9	69	8.5	75
3	7.9	70	9.7	85
4	9.4	58	10.1	62
5	10.9	67	10.9	67
6	11.1	69	12.5	77
7/8	6.4	76	6.6	80

An estimated active P treatment sand mass in other types of OWS disposal fields (e.g. contour trench, mound) or LFSFs with different design slopes and filter-lengths based on the HYDRUS-2D LFSF model results would be a useful input parameter for field- and watershed-scale models. One method for estimating the active P treatment sand mass in other LFSFs with different design slopes than those in this study would be linear interpolation based on sand-type and slope. The shorter LFSF7 and 8 had the highest percentage active P treatment sand masses (80%), but with the shorter sand toe length were approximately 2000 kg smaller in sand mass than the 8 m long filters. The HYDRUS-2D predicted active P treatment sand mass was recalculated for LFSF2 by shortening its filter length to 5.5 m, which produced an estimated percent active sand mass of 82% relatively close in value to the 80% for LFSFs 7 and 8, even with the higher hydraulic loading rate for LFSF2. Satisfactory estimations of the active P treatment sand mass for LFSFs with the same distribution trench dimensions and sand grain-size, but different sand toe lengths could then be done by further area analysis of the 8 m long LFSF HYDRUS-2D model results. This would reduce the amount of field-scale model runs required for estimating disposal field inputs in a watershed-scale model.

Another important output from the HYDRUS-2D simulations is the height of the effluent plume at the LFSF outlet boundary. The effluent outlet height will be useful as an input into other models simulating the transport of contaminants, such as P, in the surrounding native soil profile to determine the dimensions of the flow pathway and the soil mass involved in active treatment. All of the LFSF HYDRUS-2D model results had P effluent heights at the outlet boundary equal to the design boundary height of 0.3 m.

2.3.2 Lateral Flow Sand Filter Phosphorus Treatment

2.3.2.1 Phosphorus Sorption Capacity Experiments

The fitted Langmuir equation parameters for each of the three sand types from the batch P sorption experiments are shown in Table 2.5. The S_{max} values ranged from 131.6 mg P kg^{-1} sand for medium grain-size to 46.3 mg P kg^{-1} sand for coarse grain-size. Cucarella and Renman (2009) developed a classification table of S_{max} values for various OWS filter media. The medium LFSF sand would be classified according to this table as

low (100 – 600 mg P kg^{-1} sand) and the fine and coarse sands would be considered very low (<100 mg P kg^{-1} sand).

Table 2.5 Sand mineral analysis and P sorption capacity experiment results based on equilibrium P concentrations and influent P loads.

Parameter	Fine Sand (LFSF1,4)	Medium Sand (LFSF2,5,7,8)	Coarse Sand (LFSF3,6)
P_2O_5 as P (mg kg^{-1})	11.3	18.7	1.1
Ca (mg kg^{-1})	54.5	66.5	19.5
Fe (mg kg^{-1})	68	106	23
Al (mg kg^{-1})	526	634	24.29
	Equilibrium P Concentration (C_{eq})		
S_o (mg kg P kg^{-1} sand)	0.254	0.296	0
Linear R^2	0.736	0.80	0.36
S_{max} (mg P kg^{-1} sand)	73.5	131.6	46.3
K_L (L mg^{-1} P)	0.189	0.048	0.015
	Influent P Load		
Linear R^2	0.734	0.79	0.36
S_{max} (mg P kg^{-1} sand)	74.7	134.5	46.8
K_L (kg sand mg^{-1} P)	7.61×10^{-3}	1.96×10^{-3}	7.46×10^{-4}

Langmuir isotherms were also fitted to the batch sorption experiment results using normalized P influent loads (kg P) in place of C_{eq} to develop the combination P sorption and precipitation temporal removal models in the next section. As shown in Table 2.5 the R^2 and fitted S_{max} values from these linearized Langmuir equations are approximately the same as the values for the C_{eq} based linearized Langmuir equation for all three sand types.

2.3.2.2 Observed phosphorus treatment

The average P treatment performance of the eight LFSFs for the monitoring period January 2009 to October 2011 was compared against the average treatment performance for the studies completed by Havard et al. (2008) and Wilson et al. (2011) as shown in Table 2.6. Although the monitoring periods compared are for different monitoring period lengths and loading rates the average influent P loads to each filter are close in value for all three periods. The percent TP reduction for the 2009-11 monitoring

period declined in value for all eight LFSFs compared to the 2007-08 monitoring period. As sorption is one of the main P treatment processes in the LFSFs it is expected that there would be a significant decline in TP removal as P sorption sites are filled over time. This is shown in the 58% average reduction in TP removal for the six 8 m long LFSFs from the 2004-06 and 2009-11 monitoring periods. The coarse sand LFSFs 3 and 6 consistently had the worst TP treatment performance of the six 8 m long LFSFs. The percent TP reduction for LFSFs 3 and 6 for the 2009-11 study period were 11% and 8% respectively, demonstrating these filters provided little P removal. The shorter 5.5 m long LFSFs (7 and 8) both provided average TP reductions of above 80% during the 2007-08 monitoring period, while for the 2009-11 study period the average percent TP reductions dropped to 35%. The smaller amount of sand media available for P sorption and precipitation in the 5.5 m long LFSFs has potentially caused the steeper decline in percent TP reduction than what has been observed in the 8 m long medium sand LFSFs 2 and 5.

Table 2.6 Comparison of average TP influent and effluent loads and percent removal for three monitoring periods in the lateral flow sand filters.

Parameter	Study Period	LFSF 1	LFSF 2	LFSF 3	LFSF 4	LFSF 5	LFSF 6	LFSF 7	LFSF 8
Approx. STE Hydraulic Load (10^3 L)	2004-06	80.4	79.8	79.5	79.7	80.2	79.6	-	-
	2007-08	122.5	121.8	123.7	121.6	122.5	123.7	48.8	42.4
	2009-11	169.8	173.4	175.9	175.9	176.6	176.8	100.8	90.7
Average Influent TP load (kg P)	2004-06	0.57	0.57	0.56	0.57	0.57	0.57	-	-
	2007-08	0.58	0.57	0.58	0.57	0.58	0.58	0.23	0.20
	2009-11	0.57	0.59	0.59	0.59	0.60	0.60	0.34	0.31
Average Effluent TP load (kg P)	2004-06	0.04	0.08	0.16	0.05	0.06	0.15	-	-
	2007-08	0.16	0.18	0.32	0.18	0.18	0.31	0.05	0.04
	2009-11	0.32	0.40	0.53	0.40	0.41	0.55	0.22	0.20
Percent TP Reduction (%)	2004-06	93	86	72	92	90	73	-	-
	2007-08	72	68	45	68	68	47	79	81
	2009-11	44	32	11	32	32	8	35	35

Note: 2004-06 and 2007-08 loading periods adapted from Havard et al. (2008) and Wilson et al. (2011)

Wilson et al. (2011) compared the LFSF effluent TP concentrations against the Bureau de Normalisation du Quebec (BNQ) guidelines for P treatment and found all eight LFSFs exceeded the minimum requirement of 1 mg TP L^{-1} for the 2007-08 monitoring period (BNQ, 2009). The average TP effluent concentrations of each LFSF for the 2009-11 study period have all increased to well above the BNQ P treatment requirement (Table 2.6). Overall, the three sands used in the BEEC LFSFs were not effective media for long-term P treatment.

2.3.2.3 Phosphorus Temporal Removal Models

The optimized P temporal removal model input parameters for each individual LFSF are shown in Table 2.2. All of the 8 m long LFSF Part I datasets had acceptable P temporal removal model results for the 7 model types with good NSE (>0.88) and low RMSE (≤0.16 kg) values (Table 2.7). The selection of the best P temporal removal model was accomplished by examining model performance for the Part II datasets. The AIC results for the 8 m long LFSF Part II datasets typically indicated that the 2-part piecewise linear or Langmuir + 2-part piecewise linear equations were the best models; the F-test P value showed that there was no significant difference between the two models. The 2-part piecewise linear P temporal removal model with fewer fitted input parameters would therefore be the most appropriate choice for modeling purposes. As shown in Figure 2.4 the use of the S_{max} value as the decision variable for the 2-part piecewise linear P temporal removal models shows a reasonable fit for the fine and medium 8 m long LFSFs. The 2-part piecewise linear P temporal removal models for LFSFs 3 and 6 show initial over-predictions of the observed data when the S_{max} decision variable is first activated.

Table 2.7 Phosphorus temporal removal model performance results for the Part I and II observed datasets for each lateral flow sand filter (Highlighted results have the best performance for each dataset).

Model	Parameter	LFSF1		LFSF2		LFSF3		LFSF4		LFSF5		LFSF6		LFSF7		LFSF8	
		I	II	I	II	I	II	I	II	I	II	I	II	I	II	I	II
Langmuir (2 input parameters)	NSE	**0.99**	**0.86**	**0.99**	**0.65**	**0.96**	-0.3	**0.99**	**0.80**	**0.99**	**0.72**	**0.96**	-1.8	**1.00**	**0.97**	**1.00**	**0.95**
	RMSE (kg)	0.04	0.01	0.06	0.02	0.10	0.01	0.06	0.01	0.06	0.02	0.10	0.02	0.00	0.00	0.00	0.00
	AIC P	1.00	**0.50**	1.00	1.00	1.00	1.00	1.00	0.98	1.00	1.00	1.00	1.00	**0.50**	**0.66**	**0.50**	1.00
	F-test	**0.13**	**0.35**	0.00	0.01	0.02	0.00	0.00	**0.03**	0.00	0.00	0.00	0.00	-	-	-	-
Freundlich (2 input parameters)	NSE	**0.99**	**0.60**	**0.97**	-0.1	**0.92**	-3.7	**0.97**	0.25	**0.97**	0.06	**0.92**	-7.8	**0.98**	**0.97**	**0.99**	**0.98**
	RMSE (kg)	0.07	0.03	0.08	0.03	0.13	0.03	0.09	0.03	0.09	0.03	0.13	0.03	0.01	0.00	0.00	0.00
	AIC P	1.00	1.00	1.00	1.00	1.00	1.00	1.00	1.00	1.00	1.00	1.00	1.00	1.00	**0.50**	1.00	**0.50**
	F-test	0.00	0.01	0.00	0.00	0.00	0.00	0.00	0.00	0.00	0.00	0.00	0.00	-	-	-	-
Linear (2 input parameters)	NSE	**0.97**	0.00	**0.95**	-1.7	**0.88**	-11	**0.95**	-1.0	**0.95**	-1.4	**0.88**	-21	**0.86**	**0.89**	**0.90**	**0.96**
	RMSE (kg)	0.09	0.04	0.11	0.04	0.16	0.04	0.13	0.04	0.12	0.05	0.16	0.04	0.02	0.01	0.01	0.00
	AIC P	1.00	1.00	1.00	1.00	1.00	1.00	1.00	1.00	1.00	1.00	1.00	1.00	1.00	1.00	1.00	1.00
	F-test	0.00	0.00	0.00	0.00	0.00	0.00	0.00	0.00	0.00	0.00	0.00	0.00	-	-	-	-
2-Part Piecewise Linear (4 input parameters)	NSE	**1.00**	**0.84**	**1.00**	**0.87**	**0.97**	**0.87**	**1.00**	**0.90**	**1.00**	**0.99**	**0.99**	**0.91**	**0.86**	**0.89**	**0.90**	**0.96**
	RMSE (kg)	0.04	0.02	0.08	0.01	0.08	0.00	0.04	0.01	0.02	0.00	0.04	0.00	0.02	0.01	0.01	0.00
	AIC P	1.00	0.99	**0.50**	**0.77**	**0.50**	**0.50**	0.93	**0.50**	0.96	**0.50**	**0.50**	**0.85**	1.00	1.00	1.00	1.00
	F-test	-	**0.06**	**1.00**	**0.03**	**0.86**	**0.89**	**0.04**	**0.11**	**0.03**	**0.86**	**0.22**	**0.03**	0.00	**0.03**	0.00	**0.09**
Langmuir + Linear (4 input parameters)	NSE	**0.99**	0.41	**0.96**	-1.1	**0.88**	-11	**0.97**	-0.2	**0.96**	-1	**0.88**	-20	**0.89**	**0.92**	**0.91**	**0.97**
	RMSE (kg)	0.06	0.03	0.10	0.04	0.16	0.04	0.09	0.03	0.11	0.04	0.16	0.04	0.02	0.01	0.01	0
	AIC P	1.00	1.00	1.00	1.00	1.00	1.00	1.00	1.00	1.00	1.00	1.00	1.00	1.00	1.00	1.00	1.00
	F-test	-	0.00	0.00	0.00	0.00	0.00	0.00	0.00	0.00	0.00	0.00	0.00	0.00	**0.05**	0.00	**0.14**
Langmuir+ Freundlich (4 input parameters)	NSE	**0.99**	**0.70**	**0.98**	0.03	**0.92**	-3.8	**0.98**	0.47	**0.98**	0.12	**0.92**	-8.0	**0.97**	**0.96**	**0.98**	**0.98**
	RMSE (kg)	0.06	0.02	0.08	0.03	0.13	0.03	0.08	0.02	0.09	0.03	0.13	0.03	0.01	0.00	0.01	0.00
	AIC P	1.00	1.00	1.00	1.00	1.00	1.00	1.00	1.00	1.00	1.00	1.00	1.00	1.00	1.00	1.00	0.97
	F-test	-	0.00	0.00	0.00	0.00	0.00	0.00	0.00	0.00	0.00	0.00	0.00	0.00	**0.22**	**0.03**	**0.97**
Langmuir + 2-Part Piecewise Linear (6 input parameters)	NSE	**1.00**	**0.90**	**1.00**	**0.93**	**0.97**	**0.87**	**1.00**	**0.93**	**1.00**	**0.99**	**0.99**	**0.95**	**0.89**	**0.92**	**0.91**	**0.97**
	RMSE (kg)	0.03	0.01	0.03	0.01	0.08	0.00	0.03	0.01	0.02	0.00	0.04	0.00	0.02	0.01	0.01	0.00
	AIC P	**0.50**	0.99	**0.92**	**0.50**	**0.89**	0.98	**0.50**	**0.72**	**0.50**	0.98	0.99	**0.50**	1.00	1.00	1.00	1.00
	F-test	0.01	-	-	-	-	-	-	-	-	-	-	-	0.00	**0.10**	0.01	**0.25**

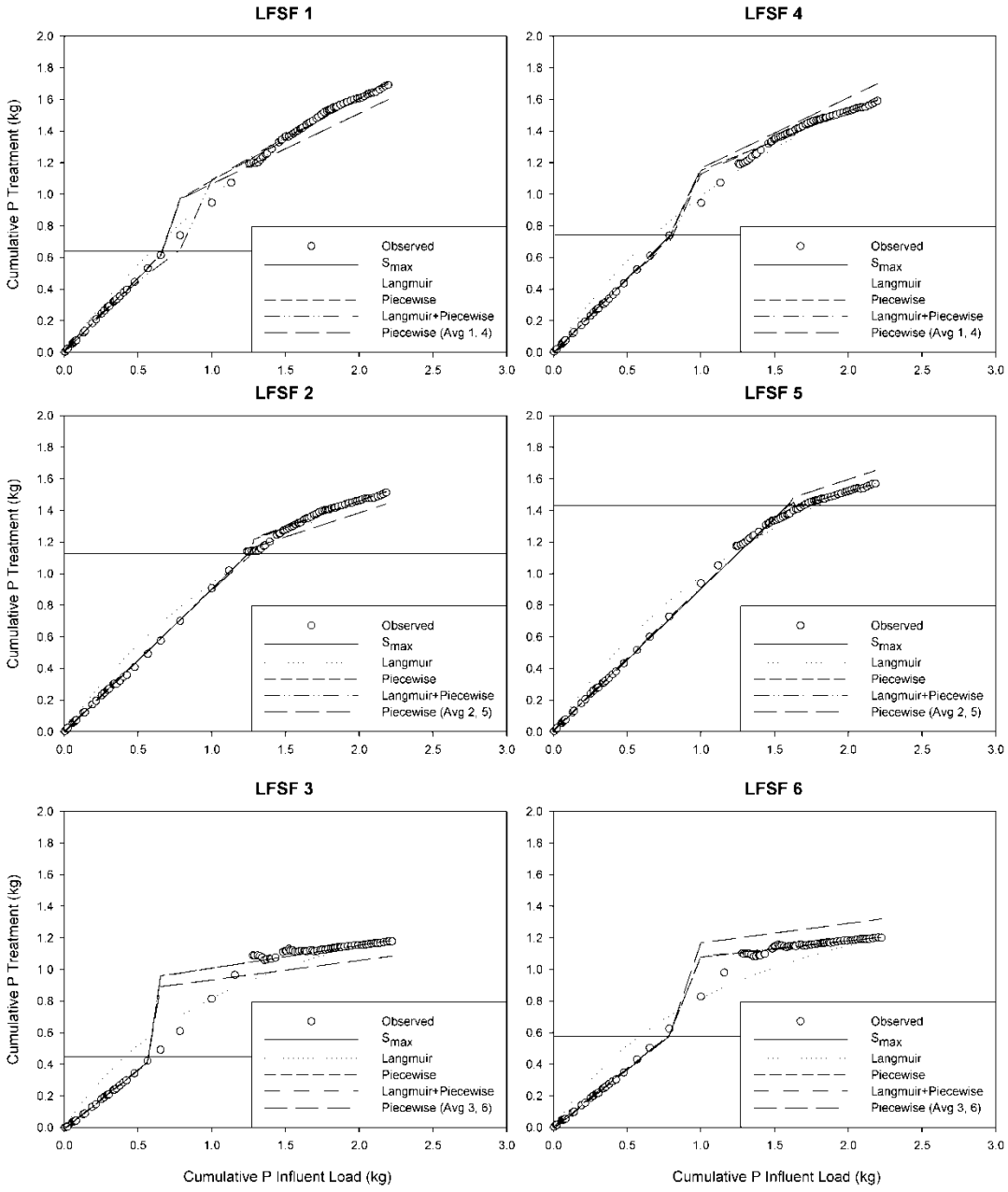

Figure 2.4 Cumulative observed and selected temporal removal modeled phosphorus treatment for each 8 m long lateral flow sand filter.

The best P temporal removal models for LFSFs 7 and 8 were Langmuir, Freundlich, 2-part piecewise linear, Langmuir + Linear, Langmuir + Freundlich, and Langmuir + 2-part piecewise equations based on the AIC probability values and F-test results for both the Part I and II datasets (Table 2.7). The Freundlich and Langmuir P temporal removal models both have fewer input parameters than the other acceptable models and would be preferred for modeling purposes. The two 5.5 m long filters were in operation for a shorter time period (September 2007 – October 2011) and received a lower STE hydraulic loading rate of 100 L d^{-1} causing the P sorption and precipitation processes to possibly be at a different stage than the 8 m filters. Visual comparison of the observed cumulative P treatment relationships in Figures 2.4 and 2.5 for all LFSFs shows that the 5.5 m long filters have not yet undergone the observed reduction in the P removal rate observed in the 8 m LFSFs.

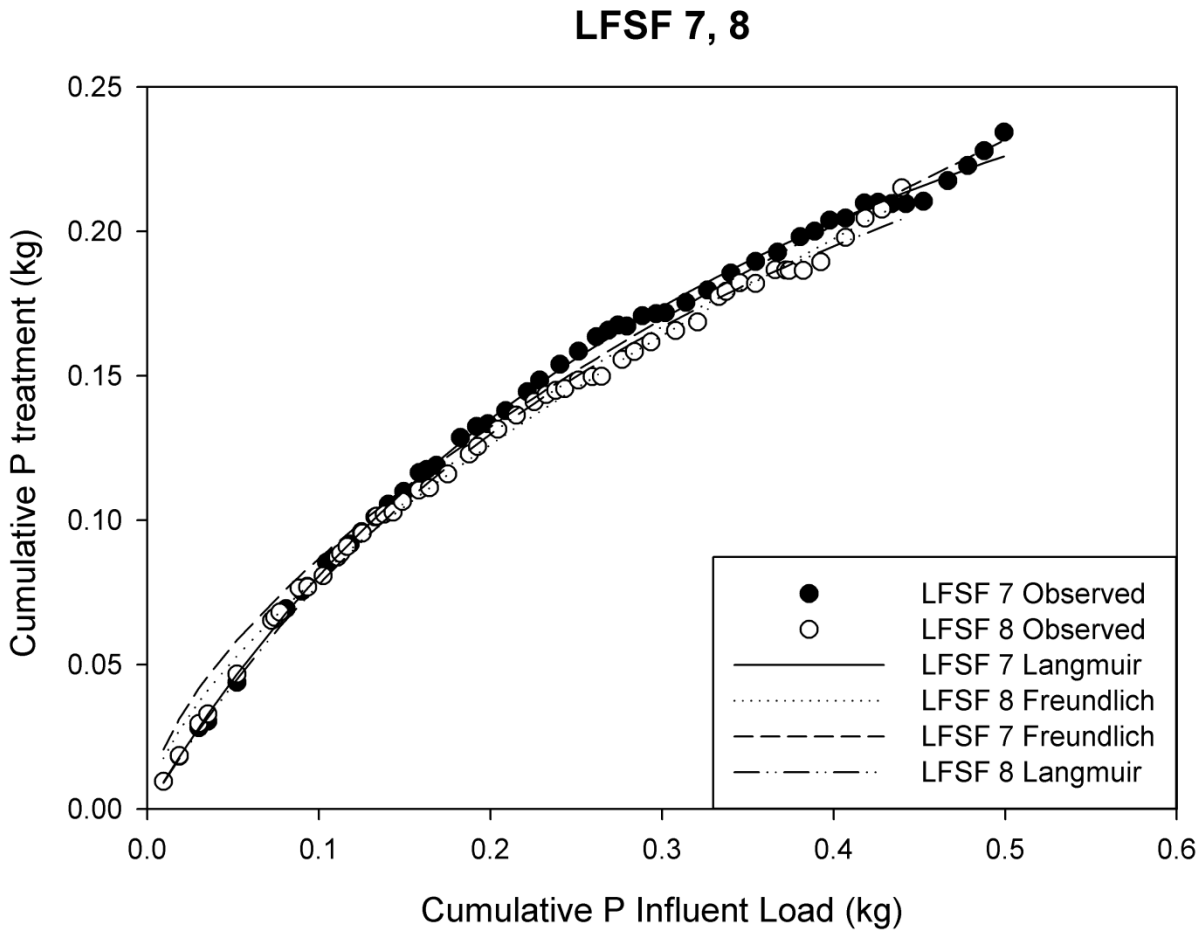

Figure 2.5 Cumulative observed and selected temporal removal modeled phosphorus treatment for LFSFs 7 and 8.

The average P temporal removal models were developed based on sand grain-size and filter length using the 2-part piecewise linear for the fine, medium and coarse sand 8 m long filters, and Freundlich for the 5.5 m long LFSFs. The average P temporal removal models for the 8 m long LFSFs had very good NSE (>0.95) and RMSE (≤0.10) for the Part I datasets, but performed poorly for the Part II dataset with NSE values below 0 as shown in Table 2.8. The average Freundlich P temporal removal model for LFSFs 7 and 8 had very good model performance for both the Part I and II datasets, although both LFSFs have the same designs. The use of the average Freundlich P temporal removal model for LFSF7 and 8 would be satisfactory to predict P sorption and precipitation for the 2007 to 2011 time period. Prediction using the average LFSF7 and 8 Freundlich temporal removal model for cumulative P influent loads greater than the observed dataset should be verified with continued monitoring as the two filters have not undergone the reduction in the P removal rate observed in the 8 m long filters.

Table 2.8 Average phosphorus temporal removal model performance results for the Part I and II observed datasets for each lateral flow sand filter.

Parameter	LFSF1		LFSF2		LFSF3		LFSF4		LFSF5		LFSF6		LFSF7		LFSF8	
	I	II	I	II	I	II	I	II	I	II	I	II	I	II	I	II
Model Type	2-Part Piecewise Linear												Freundlich			
NSE	0.99	-4.92	0.99	-6.73	0.95	-68.36	0.99	-7.50	1.00	-5.90	0.96	-135	0.98	0.96	0.99	0.94
RMSE (kg)	0.07	0.10	0.04	0.08	0.10	0.10	0.05	0.09	0.04	0.08	0.09	0.11	0.01	0.00	0.00	0.00

A possible reason for the poorer performance of the 8 m long LFSF average P temporal removal model is the normalization of the P influent loads using the average P treatment sand mass predicted by the calibrated HYDRUS-2D models. The predicted active P treatment sand masses for the 8 m long LFSFs with the same sand grain-size, but different slopes differ by 1.5 to 4.2×10^3 kg. These differences in P treatment sand masses translate into an increase in the maximum amount removed just by sorption processes of 0.1 to 0.5 kg P, which is significant when the total P influent load for each 8 m long LFSF is approximately 2.2 kg P. A method that could be alternatively used instead of the average P temporal removal models based on sand grain-size and filter length is linear interpolation based on design slope for filters with the same sand grain-size and filter-length.

A visual examination of the observed cumulative P amounts retained in the 8 m LFSFs with the same sand grain-size, but different slopes shows that they are performing similarly (Figure 2.4). The percent TP reductions for the LFSFs with the same sands, but different slopes in Table 2.6 also demonstrate this similar level of P treatment. The LFSFs 1 and 4 have an approximately 10% difference in treatment performance, which potentially can be attributed to the 1.5 day difference in observed mean RTD from the rhodamine WT tracer studies. Lower contact time with the filter media is known to reduce the amount of P removed by sorption and/or precipitation (Fuchs et al., 2009). Although the medium and coarse sand LFSFs have similar observed and predicted mean RTDs for 5 and 30% slopes, internal flow and moisture content distributions are different, which appears to have an influence on P retention processes, contributing to the poorer fit of the averaged temporal removal models.

2.4 Conclusions

This study evaluated seven different P temporal removal modeling approaches for simulating P sorption and precipitation processes in eight LFSFs and found at least one type of temporal removal model for each LFSF that satisfactorily predicted cumulative P treatment. For the six 8 m long LFSFs the 2-part piecewise linear P temporal removal models had the best model performance. This suggests that both fast reacting sorption to

a finite maximum and long-term precipitation reactions are occurring within the LFSFs, and that the P temporal removal model needs to represent both processes well. The P treatment processes in the medium sand, 5.5 m long LFSFs 7 and 8 were best modeled by the Langmuir and Freundlich temporal removal models, but all seven models had satisfactory model performance. Phosphorus temporal removal models constructed with average fitted input parameters, based on the sand grain-size and filter length, did not perform as well, especially with respect to predicting P treatment for the last 20 sampling months of the 8 yr study period in the 8 m long LFSFs. The average Freundlich P temporal removal model for the two 5.5 m long filters had very good model performance, but both filters have the same design specifications. Estimation of active treatment areas within lateral flow disposal fields is needed to predict long-term P treatment performance, and the physically-based HYDRUS-2D model proved useful in deriving this information. Further tracer studies should be conducted using a conservative tracer (e.g. bromide) to remove uncertainty created by tracer sorption when calibrating the HYDRUS-2D LFSF models. None of the eight LFSF designs were effective at long-term P treatment with effluent concentrations at the end of the study period >1 mg P L^{-1}. The medium and fine sand 8 m long LFSFs for both slope classes had the best P reductions rates of the designs studied. Overall, the LFSFs are not effective as a long-term P treatment technology for STE, and different design regulations may be required, particularly for P sensitive watersheds that are already experiencing accelerated eutrophication caused water quality issues. One method would be a sand filter media replacement program that periodically replaces the sand media bed every 5 to 10 yrs. Alternatively, a sand media that is Fe or Al enriched and has a higher P sorption capacity than the sand currently used in Nova Scotia could be used to increase P treatment capacity in the LFSFs. Further research studies should be done to examine how the 2-part piecewise linear P temporal removal model performs for longer monitoring periods and for different disposal field technologies. The results of this study will be used to develop disposal field input parameters for a watershed-scale model simulating long-term OWS P loading in a rural, mixed land-use watershed in Nova Scotia.

CHAPTER 3 A WATERSHED MODELING FRAMEWORK FOR PHOSPHORUS LOADING FROM RESIDENTIAL AND AGRICULTURAL SOURCES

Materials in this chapter are drawn from a manuscript that has been submitted for publication in the **Journal of Environmental Quality**.

Sinclair, A., R. Jamieson, A. Madani, R.J. Gordon, W. Hart, and D. Hebb. 2013. A watershed modeling framework for phosphorus loading from residential and agricultural sources. J. Environ. Qual. (In Review).

3.1 Introduction

Watersheds with sparse human populations typically use on-site wastewater systems (OWS) to treat residential wastewater, and these systems can be a source of phosphorus (P) loading to aquatic systems. In the United States, Canada, and the province of Nova Scotia (NS) the percentage (%) of the population who live in rural areas and would potentially use OWSs are 19 (United States Census Bureau, 2012), 19 (Statistics Canada, 2012a) and 45% (Nova Scotia Environment, 2011), respectively. A conventional OWS design involves a septic tank that discharges into a tile drainage disposal field underlain by native soil or imported filter media. At the tile drain and native soil or filter media interface a biomat often develops with a lower hydraulic conductivity than the underlying soil or filter media (Radcliffe and West, 2009). The P removal primarily occurs in the septic tank by settling out of particulate forms of P created by sorption and precipitation processes; resulting in septic tank effluent (STE) where 85% of the total P (TP) is in the form of soluble orthophosphate (McCray et al., 2005). The two P treatment mechanisms in the filter media and native soil are sorption and precipitation (McCray et al., 2009).

The USEPA (2002) identified OWS disposal field hydraulic failure, and the inability of the disposal field or surrounding soil to retain P, as the main reasons for OWS P loading to surface water bodies. Several studies have tried to quantify the significance of OWS P loads at the watershed-scale. The amount of P loading that results from OWSs in agricultural watersheds is often assumed to be relatively small compared to agricultural

P loads (Withers et al., 2011). Withers et al. (2009) found investigation of P surface runoff sources in a small agricultural watershed to be difficult because of the various unknown and combined drainage sources. Surface runoff from roads and septic tank discharges however, had more biologically available P than agricultural runoff. Lombardo (2006) reviewed case studies for six North American lakes and found OWS contributed between 4 and 55% of the TP loads. In the UK, a study of OWS discharges into a stream network found increased P concentrations during low flow conditions and ineffective P treatment in OWS disposal fields in impermeable clay soils (Withers et al., 2011). A review of five watersheds from across Europe found OWS P loads contributed <10% of the watershed P load, but caused increased in-stream P concentrations during the summer months (Withers et al., 2012).

The most common site constraints impacting OWS design in NS are low permeability soils, shallow bedrock and high water tables (Havard et al., 2008). The majority of OWS disposal field designs in the province are either contour trenches or lateral flow sand filters (LFSFs) (L. Boutilier, personal communication, 2013). Both rely on imported sand filter media beds and lateral STE flow through the media (Nova Scotia Environment, 2009). Sinclair et al. (2013a) studied LFSFs that differed in design by sand type, slope and width, and were continuously loaded with municipal wastewater for eight years. All of the LFSFs were not effective at long-term P treatment with TP effluent concentrations at the end of the study >1 mg TP L^{-1}; this exceeds the minimum Bureau de Normalisation du Québec (BNQ) OWS effluent guideline requirement of 1 mg TP L^{-1} (BNQ, 2009). A three year study of two C2 type raised contour trenches in NS that differed by loading method (gravity vs. periodic pressure loading) had TP effluent concentrations of <0.3 and >1.0 mg P L^{-1}, respectively (Bridson-Pateman, 2013). The results of these two studies align with the Cucarella and Renman (2009) classification of sand as a low P sorption capacity filter material (0.1 – 0.5 g P kg^{-1} material).

An important watershed management tool to assist with prevention and reduction of point and non-point source pollution of water systems is watershed-scale computer modeling. Jeong et al. (2011) and McCray et al. (2009) identified that the majority of computer models of OWS P treatment and transport processes have been conducted at the lab- and field-scales with few at a watershed scale. Two such models that include

algorithms specifically simulating OWS P treatment, failure, and transport processes are the Watershed Analysis Risk Management Framework (WARMF) (Weintraub et al., 2002) and the SWAT (version 2009 [SWAT2009]) model (Jeong et al., 2011). Both utilize a modified version of a biozone algorithm (Siegrist et al., 2005) that simulates P removal as occurring in and native soil layers below the disposal field using a linear sorption isotherm. A maximum sorption capacity value is used to cap off the linear isotherm when the biozone and disposal field layers are P saturated. SWAT2009 allows P leaching to lower soil layers before P saturation is reached using a linear relationship function (Bond et al., 2006). Phosphorus transport via lateral flow is not simulated in SWAT2009 (Neitsch et al., 2011). Lateral flow of P to surface water systems occurs in WARMF when the water content of a soil layer reaches or exceeds field capacity (Siegrist et al., 2005).

Both WARMF and SWAT2009 simulate STE P treatment as occurring within a thin biozone layer (0.5 – 10 cm) and the native soil layers vertically below it (Siegrist et al., 2005; Jeong et al., 2011). An OWS disposal field with imported filter media cannot be directly simulated in WARMF or SWAT2009. Both WARMF and SWAT2009 represent residential land-uses areas in a sub-basin as conglomerated areas that are typically at least several hectares in size with the same soil type and slope class, which are then classed as lumped computational units. In comparison, an individual OWS or cluster of OWSs will be only several hundred square meters in area. It then becomes a scale and geometry issue where the smaller imported sand media areas cannot be adequately represented in these larger lumped land-use computational units. Both require adjustments to STE P concentration and P treatment input parameters to approximate P treatment in the imported material. The OWS designs used in NS rely on lateral flow of STE through imported sand filter media and surrounding native soils; instead of the assumed vertical flow systems that are simulated in the WARMF and SWAT2009 models. There is a need to develop more appropriate algorithms to represent P treatment and transport processes for NS OWS designs in watershed-scale models. The objectives of this research were: (i) To design a P on-site wastewater simulator (POWSIM) to simulate P loads from individual or clusters of residential OWS typically used in NS; and (ii) to simulate OWS P loads in the Thomas Brook Watershed (TBW), NS using the

SWAT2009 model in conjunction with POWSIM, to concurrently predict and compare P loading from agricultural and residential sources.

3.1.1 Background to the SWAT Model

The SWAT2009 model is a process-based hydrological-water quality computer simulation model that operates on a daily time step (Arnold et al., 1998). It has been widely used for the assessment of hydrology, as well as sediment, nutrient, bacteriological, and pesticide loading at various spatial and temporal scales throughout the world (Douglas-Mankin et al., 2010; Gassman et al., 2007; Tuppad et al., 2011). The SWAT2009 model was chosen over the WARMF model for this study because SWAT2009 is an open source program that allows full user access to the various P transport algorithms in the source code; while WARMF is a proprietary model with no user access to assess how the algorithms are functioning (Weintraub et al., 2002; Neitsch et al., 2011). The WARMF model also does not have as an expansive and diverse publication record as the SWAT model, particularly for North America (Gassman et al., 2007; Dayyani et al., 2013). The SWAT2009 model is semi-distributed with the watershed spatially partitioned into discrete subbasins, which are then further sub-divided into non-spatial, lumped hydrologic response units (HRUs). Each HRU represents a user-defined homogeneous area of land-use, slope classification and soil type that discharges directly into the stream network at the subbasin outlet (Gassman et al., 2007).

The P routines within the SWAT2009 model are based on the EPIC model (Jones et al., 1984), and use solution, active, and stable inorganic, and fresh and humic organic pools to simulate P movement in the soil layers (Vadas and White, 2010). Phosphorus transport to the water course in each subbasin is simulated in the SWAT2009 model by surface runoff algorithms, which assume that the solution P pool is only mobile in the top 10 mm of soil and use a partitioning factor with the surface runoff volume (Equation 3.1) (Neitsch et al., 2011).

$$P_{surf} = \frac{P_{sol,surf} * Q_{surf}}{\rho_b * depth_{surf} * k_{d,surf}} \tag{3.1}$$

where P_{surf} (kg P ha^{-1}) is the soluble P lost via surface runoff, $P_{sol,surf}$ (kg P ha^{-1}) is the amount of soluble P in the top 10 mm of the top soil layer, Q_{surf} is the given daily amount

of surface runoff (mm H_2O), ρ_b (Mg m^{-3}) is the soil bulk density of the top soil layer, $depth_{surf}$ (mm) is the 10 mm depth of soil involved in surface runoff, and $k_{d,surf}$ (m^3 Mg^{-1}) is the phosphorus soil partitioning coefficient, also referred to as PHOSKD. Another equation in the SWAT2009 model that controls the value of $P_{sol,surf}$ is the leaching of soluble P below the 10 mm soil depth (Equation 3.2).

$$P_{perc} = \frac{P_{sol,surf} * w_{perc,surf}}{10 * \rho_b * depth_{surf} * k_{d,perc}} \tag{3.2}$$

where P_{perc} (kg P ha^{-1}) is the amount of soluble P leaching out of the top 10 mm of the top soil layer to the lower part of the layer, $w_{perc,surf}$ (mm_{H2O}) is the amount of water percolating from the top 10 mm of the soil layer into the lower part of the layer, and $k_{d,perc}$ (m^3 Mg^{-1} soil) is the user defined watershed-scale P percolation coefficient, also referred to as PPERCO.

The other transport algorithm in SWAT is P attachment to sediment in surface runoff using an enrichment ratio. Similar to the surface runoff algorithm the active, stable, and fresh and humic organic P pools in the top 10 mm of the top soil layer represent the only P available for sediment attachment (Equations 3.3, 3.4).

$$sedP_{surf} = 0.001 * \left(conc_{sed,P}\right) * \frac{sed}{area_{hru}} * \varepsilon_{P:sed} \tag{3.3}$$

$$conc_{sed,P} = 100 * \frac{\left[minP_{act,surf} + minP_{sta,surf} + orgP_{hum,surf} + orgP_{frsh,surf}\right]}{\rho_b * depth_{surf}} \tag{3.4}$$

where $sedP_{surf}$ (kg P ha^{-1}) is the amount of P transported with the sediment in the surface runoff, $conc_{sed,P}$ (g P Mg^{-1} soil) is the concentration of P attached to the sediment in the top 10 mm of the top soil layer, *sed* (Mg) is the sediment yield on a given day, $\varepsilon_{P:sed}$ is the P enrichment ratio, $area_{hru}$ (ha) is the area of the HRU, $minP_{act,surf}$ (kg P ha^{-1}) is the amount of P in the top 10 mm of the top soil layer in the active inorganic P pool, $minP_{sta,surf}$ (kg P ha^{-1}) is the amount of P in the top 10 mm of the top soil layer in the stable inorganic P pool, $orgP_{hum,surf}$ (kg P ha^{-1}) is the amount of P in the top 10 mm of the top soil layer in the humic organic P pool, and $orgP_{frsh,surf}$ (kg P ha^{-1}) is the amount of P in the top 10 mm of the top soil layer in the fresh organic P pool. The $\varepsilon_{P:sed}$ can be either user defined or calculated in the SWAT model for a given day using the following logarithmic equation (Neitsch et al., 2011):

$$\varepsilon_{P:sed} = 0.78 * \left(\frac{sed}{10 * area_{hru} * Q_{surf}} \right)^{-0.2468} \quad (3.5)$$

The SWAT model simulates lateral flow P loading to the water course as a user-defined constant shallow groundwater soluble P concentration (GWSOLP [mg P L^{-1}]) (Neitsch et al., 2011).

Within the channel, P can be removed from the water column through sedimentation or transformed using the algorithms originally derived from the QUAL2E model (Brown and Barnwell, 1987). The $\varepsilon_{P:sed}$ regulates the amount of P removed from the water column through sedimentation. Simplified Bagnold (default), Kodatie, Molinas and Wu, Yang sand and gravel are sediment routing in steam channel algorithms available in the SWAT2009 model (Neitsch et al., 2011).

In eastern Canada, the SWAT model has been successfully used to simulate flow diversion terraces in the Black Brook Watershed in northwestern New Brunswick that was dominated by potato cropping systems (Yang et al., 2009). Frey et al. (2013) used SWAT to model hydrologic flow, sediment, nutrients, and fecal indicator bacteria in the South Nation River Watershed in eastern Ontario and had satisfactory results for flow and nutrients, and inadequate results for the other parameters. The 630 km^2 Pike River Watershed in southern Quebec was adequately modeled using SWAT for flow, sediment and phosphorus yields (Deslandes et al., 2007). Ahmad et al. (2011) successfully calibrated and validated the SWAT model for hydrologic flow, sediment and nitrogen transport in the mixed land-use TBW in the Annapolis Valley region of Nova Scotia.

3.2 Materials and Methods

3.2.1 POWSIM Components and Algorithms

The POWSIM loading tool simulates P removal and transport from an individual or cluster of OWS to the neighboring surface water system using three separate computational components: (i) an OWS disposal field design selection and mass of treatment media calculation, (ii) disposal field P treatment dynamics, and (iii) soil subsurface plume P treatment dynamics. Figure 3.1 is a diagram of the P removal and transport process being modeled by POWSIM for an example OWS disposal field with

predominantly lateral flow. The selection of an OWS disposal field design in NS requires site slope, soil hydraulic conductivity, depth of permeable soil, and total soil depth to groundwater (Nova Scotia Environment, 2009). The OWS disposal field designs that can be chosen are the most commonly used in the province with sand filter media and include the mound, contour trench and lateral flow sand filter (LFSF) systems. The five different types of contour trenches approved for use in NS are C1, C1 raised, C2, C2 raised and C3 with the designs increasing in complexity and amount of sand filter media above the existing soil surface as the names increase in numeric value. Table 3.1 shows the initial selection criteria used by POWSIM to choose a group of OWS disposal field designs that potentially will be appropriate for the site.

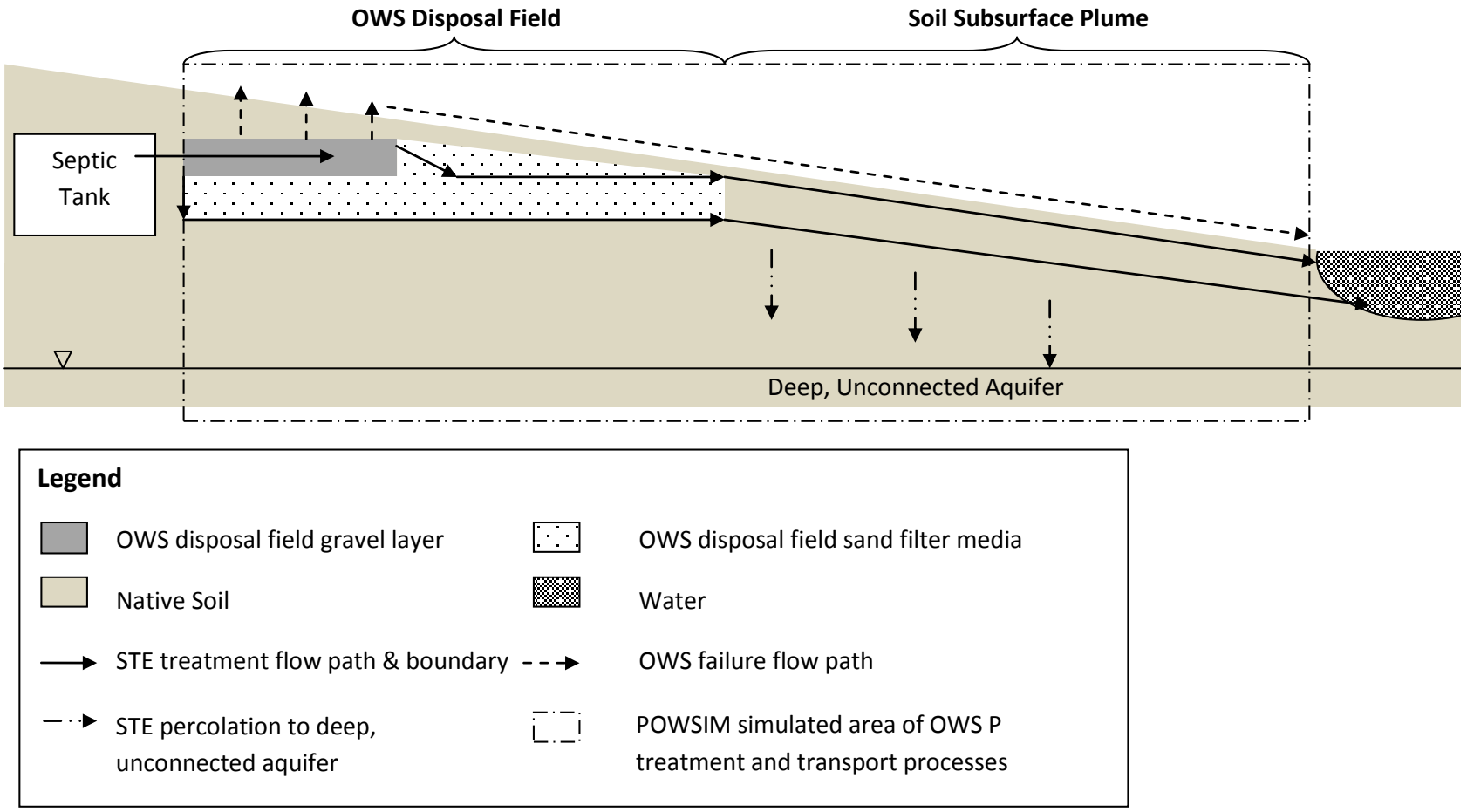

Figure 3.1 Profile diagram of phosphorus transport from a lateral flow on-site wastewater system to the nearest surface water body.

Table 3.1 Design selection criteria for on-site wastewater systems in Nova Scotia (adapted from Nova Scotia Environment (2009)).

Permeable Soil Depth*	Slope		
	<0.03	**0.03 – 0.3**	**>0.3**
mm		m m^{-1}	
0 - <300	Mound	C2 raised, C3	LFSF
300 - <750		C2, C2 raised ,C3	
750 - >1300		C1, C1 raised, C2, C2 raised, C3	

* Soil hydraulic conductivity (K_s) – 5 x 10^{-4} to 3 x 10^{-6} m s^{-1}

As shown in Figure 3.2, the POWSIM model (flow chart) calculates the dimensions of the sand filter portion of the simplest OWS disposal field design in the group selected. The OWS disposal field dimension calculations were adapted from the Nova Scotia OWS Technical Guidelines (Nova Scotia Environment, 2009). One of the input parameters required for POWSIM to calculate these dimensions is sand type, with three choices (fine, medium and coarse). These three sand types encompass the range of materials used in contour trenches, mounds and LFSFs in NS, and have been studied by Havard et al. (2008) and Bridson-Pateman et al. (2013). The soil depth below the OWS disposal field design to the groundwater table is calculated and if there is less than 1 m separation the dimensions of the next most complex OWS disposal field in the design class are calculated.

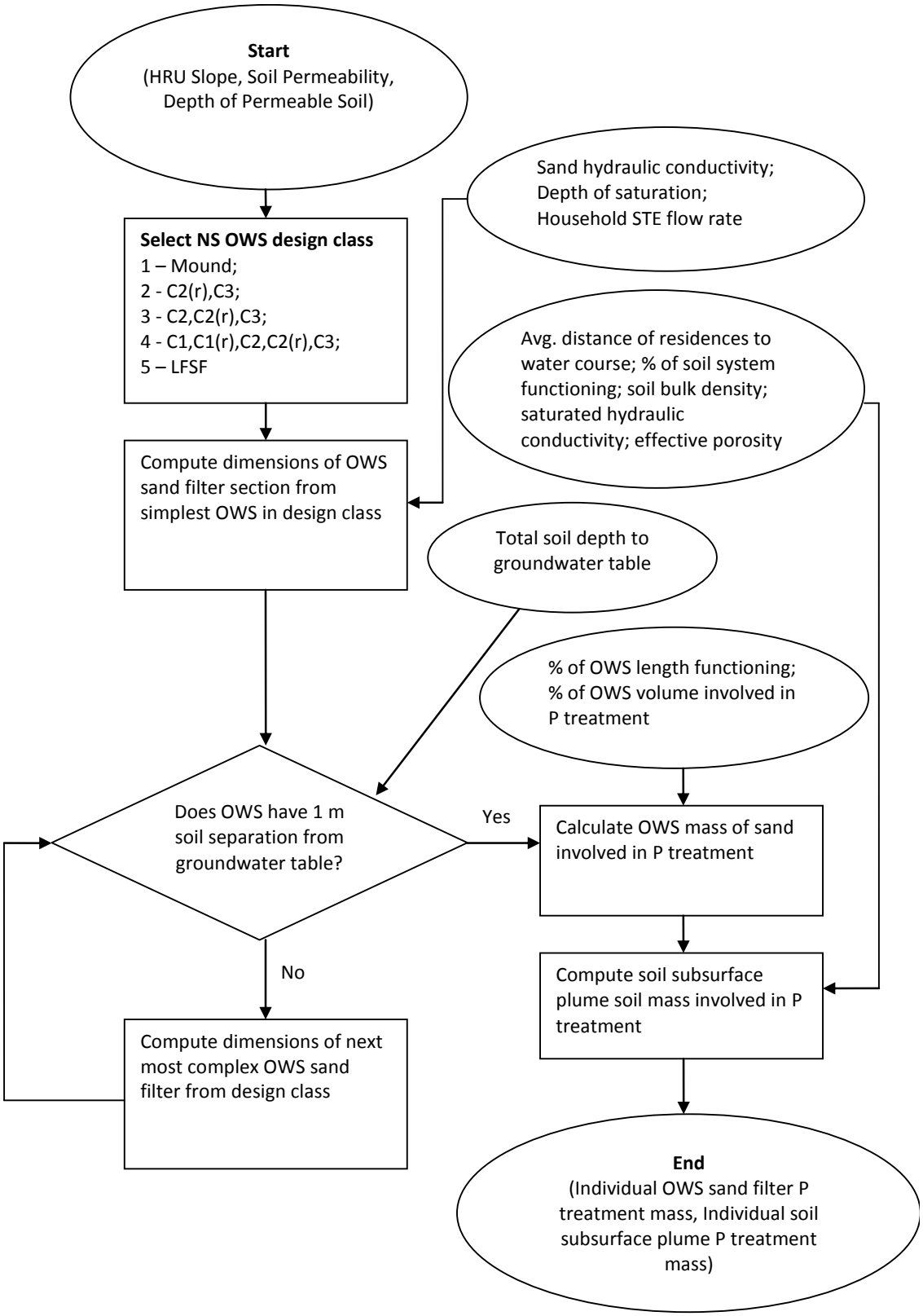

Figure 3.2 POWSIM flowchart for computing masses of sand filter and soil involved in active phosphorus treatment.

When an OWS disposal field design meets the groundwater separation criteria, the mass of sand involved in P treatment is calculated using two different parameters. The first is the percentage (%) of the OWS filter media volume involved in P treatment. The % volume of sand involved in P treatment was adapted from Sinclair et al. (2013a). The model calculates the % of filter volume involved in P treatment by interpolation of the Sinclair et al. (2013a) LFSF dataset using sand type and OWS slope. The other parameter is how much of the disposal field length is receiving septic tank effluent (STE). Distribution trenches can become clogged with solids in the STE and may not allow uniform STE distribution throughout the trench length (Patel et al., 2008; Bridson-Pateman et al., 2013). The mass of sand involved in P treatment is then calculated using the sand bulk density.

The effluent is assumed to move laterally through the imported sand media and into the surrounding soil. The final operating dimensions of the OWS disposal field sand filter are used to calculate the mass of soil involved in P treatment in the soil subsurface plume (M_{SSP} [kg]) using the following equations from Appelo and Postma (2005):

$$M_{SSP} = \rho_b * D * \left[\left(W_{sys} * L_{path} \right) + \frac{\left(\sigma_T * L_{path} \right)}{2} \right] \tag{3.6}$$

where p_b (kg soil m^{-3}) is the soil bulk density, D (m) is the saturation depth of effluent leaving the disposal field, W_{sys} (m) is the active width of the OWS, L_{path} (m) is the distance from the OWS to the water course, and σ_T (m) is the standard deviation of the plume width that is calculated by:

$$\sigma_T = \sqrt{2 D_T \frac{L_{path}}{v_x}} \tag{3.7}$$

where v_x (m s^{-1}) is the Darcy velocity and D_T (m^2 s^{-1}) is the hydrodynamic dispersion coefficient perpendicular to the principal direction of flow, which is transverse and computed by:

$$D_T = 0.1 D_L \tag{3.8}$$

where D_L (m^2 s^{-1}) is the hydrodynamic dispersion coefficient parallel to the principal direction of flow, which is longitudinal and calculated using the following equation:

$$D_L = v_x \alpha_L \tag{3.9}$$

where α_L is the longitudinal dynamic dispersivity (m) and calculated by:

$$\alpha_L = 0.83(\log_{10} L_{path})^{2.414} \tag{3.10}$$

The Darcy velocity (v_x) is calculated by:

$$v_x = \left(\frac{K_s}{n}\right) * \left(\frac{dh}{dx}\right) \tag{3.11}$$

where K_s is the saturated hydraulic conductivity (m s^{-1}), n is the effective porosity and dh/dx is the slope of the soil subsurface plume.

As with the OWS P treatment sand mass calculations, the mass of soil involved in P treatment in the soil subsurface plume is multiplied by a % functioning factor to allow a treatment mass reduction or expansion (Figure 3.2). The newly reduced or expanded soil mass becomes the active P treatment soil subsurface plume. In heterogeneous soil conditions the plume may change shape because of non-uniform flow.

The OWS disposal field computational component calculates P removal for a given time step by first calculating the STE TP load entering the disposal field (Figure 3.3). The POWSIM model simulates all P transport and removal processes using the TP form as it is preferred for estimating long-term P loading and impacts on surface water systems (McDowell et al., 2004). A % of the STE TP load in the individual or cluster of OWS is assumed to go directly to the water course. This represents OWS disposal field surface hydraulic failure where the STE would percolate to the surface because of a blocked or non-functional disposal field. POWSIM assumes that the STE TP load from OWS failure receives no treatment before it enters the water course. The surface hydraulic failure represents a conservative assumption that the STE TP load travels unimpeded to the water course in a completely dissolved inorganic form. In reality the surface hydraulic failure TP load would be affected by filtering and uptake from surface vegetation and sediment transport processes. One cause of OWS hydraulic failure is improper septic tank maintenance, such as infrequent pumping (USEPA, 2002). As septic tanks can take several years to fill up with solids and subsequently fail, the POWSIM model assumes a linear increase in the OWS failure rate over a user-defined time period when the final failure rate is reached.

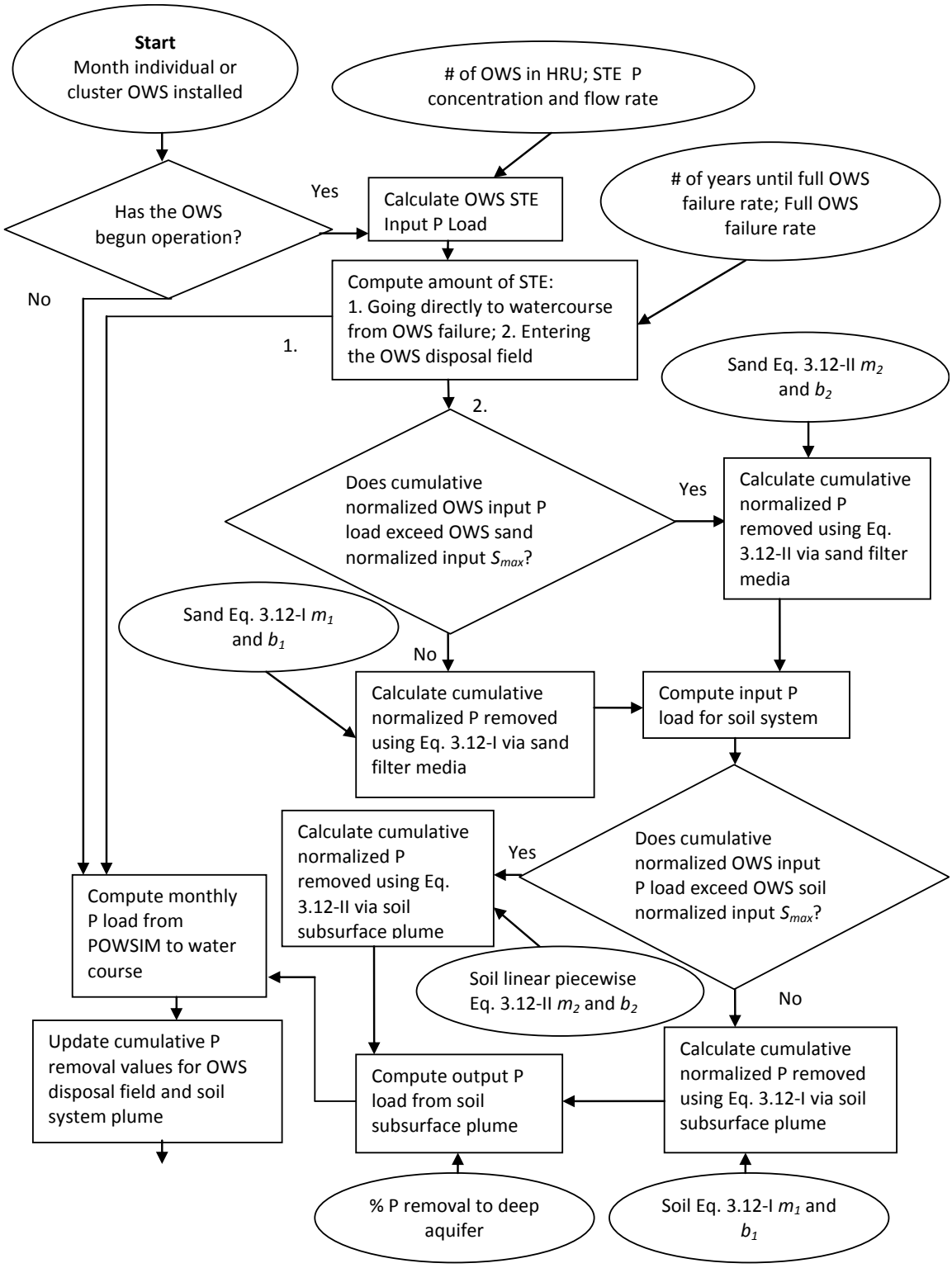

Figure 3.3 POWSIM on-site wastewater system disposal field and soil subsurface plume phosphorus treatment component flowchart.

The TP removal processes by sorption and precipitation in the OWS disposal field are calculated using a 2-part piecewise linear equation (Sinclair et al., 2013a); they developed different TP temporal removal models, including linear, Langmuir and Freundlich, using inflow and outflow P loads for six LFSFs in NS that had been receiving STE for eight years (2004 – 2011). The 2-part piecewise linear P temporal removal model was found to have the best performance of the models developed and is represented by the following equation:

$$\frac{P_{removed}}{M_{treatment}} = \begin{cases} \frac{P_{STE}}{M_{treatment}} * m_1 + b_1, when \frac{P_{STE}}{M_{treatment}} < S_{\max,STE} & (I) \\ \frac{P_{STE}}{M_{treatment}} * m_2 + b_2, when \frac{P_{STE}}{M_{treatment}} \geq S_{\max,STE} & (II) \end{cases} \quad (3.12)$$

where P_{STE} (mg P) is the STE P load entering the OWS disposal field, $M_{treatment}$ (kg sand) is the mass of sand involved in P treatment, m is the equation slope, b (mg P kg^{-1} sand) is the equation y-intercept and $S_{max,STE}$ (mg P kg^{-1} sand) is the normalized maximum P sorption capacity. The normalized maximum sorption capacity is the equivalent influent STE TP load divided by the mass of filter media involved in TP treatment when the maximum P sorption capacity is reached. When the $S_{max,STE}$ value is reached the 2-part piecewise linear equation switches from linear equation 3.12-I to equation 3.12-II, where precipitation is the predominant removal mechanism. The linear equation 3.12-I represents when both sorption and precipitation processes are occurring and linear equation 3.12-II represents when maximum sorption capacity has been reached in the filter media and precipitation is the dominant treatment process. The six LFSFs studied by Sinclair et al. (2013a) differed by sand type (fine, medium, coarse) and slope (0.05, 0.3) and each had its own 2-part piecewise linear equation (Table 3.2). Average P temporal removal models were developed by averaging the individual 2-part piecewise linear equation fitted parameters based on sand type and filter length, but different design slopes; they did not adequately represent P treatment in the LFSFs. As all of the OWS disposal field designs rely on sand filter media and lateral flow for P treatment, POWSIM assumes that the linear 2-part piecewise equations developed for the six research LFSFs will adequately represent TP removal in contour trenches and mounds with the same slopes and sand types. Although both the LFSFs with the same sand type and filter

length, but different slopes experienced the same reductions in the STE TP loading, they were estimated as having different masses of sand filter media involved in active TP treatment, and therefore different removal rates (kg TP kg^{-1} sand) related to design slope. If the OWS disposal field in POWSIM has a slope that is between the two slope choices (0.05, 0.3) then the fitted parameters (m_1, m_2, b_1, and b_2) are calculated by interpolation based on slope values and sand type.

Table 3.2 The 2-part piecewise equation parameters used in POWSIM representing filter media type and slope which is adapted from Sinclair et al. (2013a).

Filter Media Type	S_{max}	$S_{max,STE}$	OWS Slope	m_1	b_1	m_2	b_2
	mg P kg^{-1} sand		m m^{-1}				
Fine Sand	74.7	79.1	0.05	0.94	0.41	0.52	65
			0.3	0.92	-0.16	0.37	77.2
Medium Sand	134.5	148.8	0.05	0.91	-0.47	0.34	91.4
			0.3	0.89	1.13	0.27	89.9
Coarse Sand	46.8	64.4	0.05	0.74	-1.12	0.14	89.2
			0.3	0.75	-0.25	0.1	78.0
Soil	237	276	-	0.86	0.00	0.29	157

The outflow TP load from the OWS disposal field component is then input into the soil subsurface plume model component, as shown in Figure 3.3. A 2-part piecewise linear equation is used to represent P treatment in the soil subsurface plume; this equation was adapted from the six LFSF equations developed by Sinclair et al. (2013a). In Nova Scotia, there was not soil specific data related to P treatment for OWS, so the LFSF TP treatment equations were adjusted appropriately. The 2-part piecewise linear equation uses normalized TP influent load values where the influent P load is divided by the mass of soil involved in TP treatment in the soil subsurface plume. The m_1 and m_2 values are the average of same parameters from the six LFSF equations (Sinclair et al., 2013a). The b_1 value was assumed to be 0, representing no initial TP content in the soil profile, and b_2

is calculated based on where the two linear equations intersect at the $S_{max,STE}$ value. There is potential for vertical percolation of TP out of the soil subsurface plume and into a groundwater layer that is not connected with the surface water system being modeled, which is represented in POWSIM using a user-defined percent removal value. The outflow TP load from the soil subsurface plume component is then added to the OWS failure TP load to calculate the total OWS TP load input for each subcatchment within the watershed-scale model. The POWSIM model then updates the cumulative TP removal values for the OWS disposal field and soil subsurface plume for the next time step calculation.

3.2.2 Case Study Watershed

Thomas Brook Watershed in the Annapolis Valley of NS (45˚03' to 45˚06'N lat, 64˚44' to 64˚46'W long) was selected to test the SWAT and POWSIM modeling approach (Figure 3.4). The 665 ha rural watershed has previously been modeled using the SWAT model (Ahmad et al., 2011; Goulden et al., 2013). The main TBW land-uses are rotational and permanent crop agriculture (~60% area), forest (~34%) and residential (~4%) (Figure 3.5). Rotational cropping systems in the TBW include corn, winter and spring wheat, barley, alfalfa and strawberries in various rotations, while permanent crops predominantly consist of pasture, grazing lands, timothy and corn. There are 81 residences in the watershed all with OWS. There is also a ~186 cow dairy farm, and two beef operations with ~36 and 16 cows, respectively (Sinclair et al., 2009). None of the farming operations or residential dwellings has point sources discharging pollutants directly into the water course. From 2004 to 2013 the TBW was part of the Watershed Evaluation of Beneficial Management Practices (WEBs) program through Agriculture and Agri-Food Canada (AAFC) (AAFC, 2013). The program established five permanent monitoring stations collecting flow, sediment and nutrient data from the water course with Station (Stn) 3 representing a subbasin with an area of 118 ha that was predominantly forest and residential land-use (Figure 3.5). The Stn 4 subcatchment has an area of 492 ha and contains both the dairy and two beef farm operations. Station 4 has the most complete flow, sediment and nutrient dataset of the five stations and has previously been used to calibrate and test the SWAT (version 2005 [SWAT2005]) model (Ahmad et al., 2011). The number of residences in the Stn 3 and 4 subcatchments are 17 and 66, respectively. The hydrological and water quality monitoring data used in this study for model calibration and validation were from Stns 3 and 4 for five years between January 2004 and December 2008.

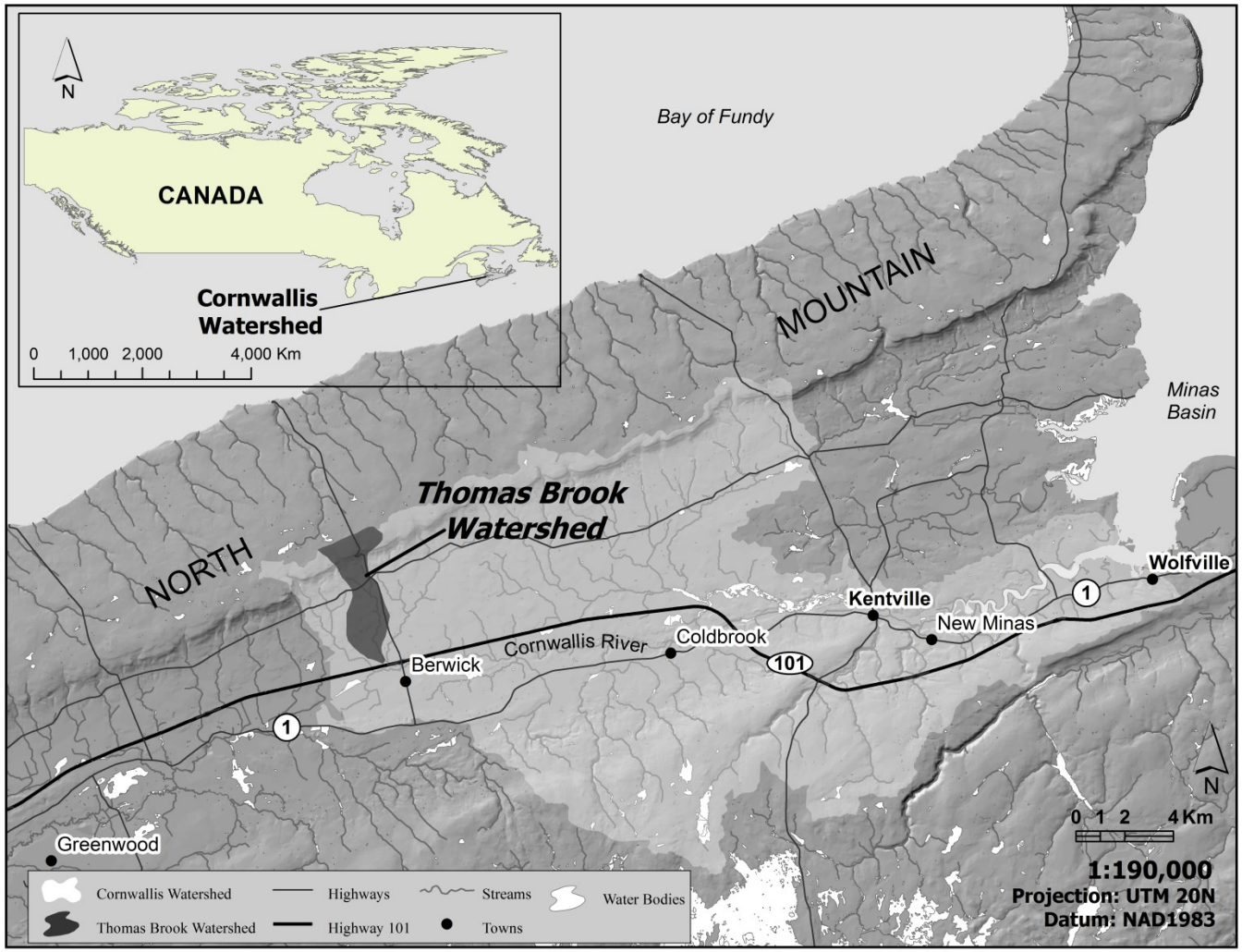

Figure 3.4 Location of Thomas Brook Watershed in Nova Scotia, Canada.

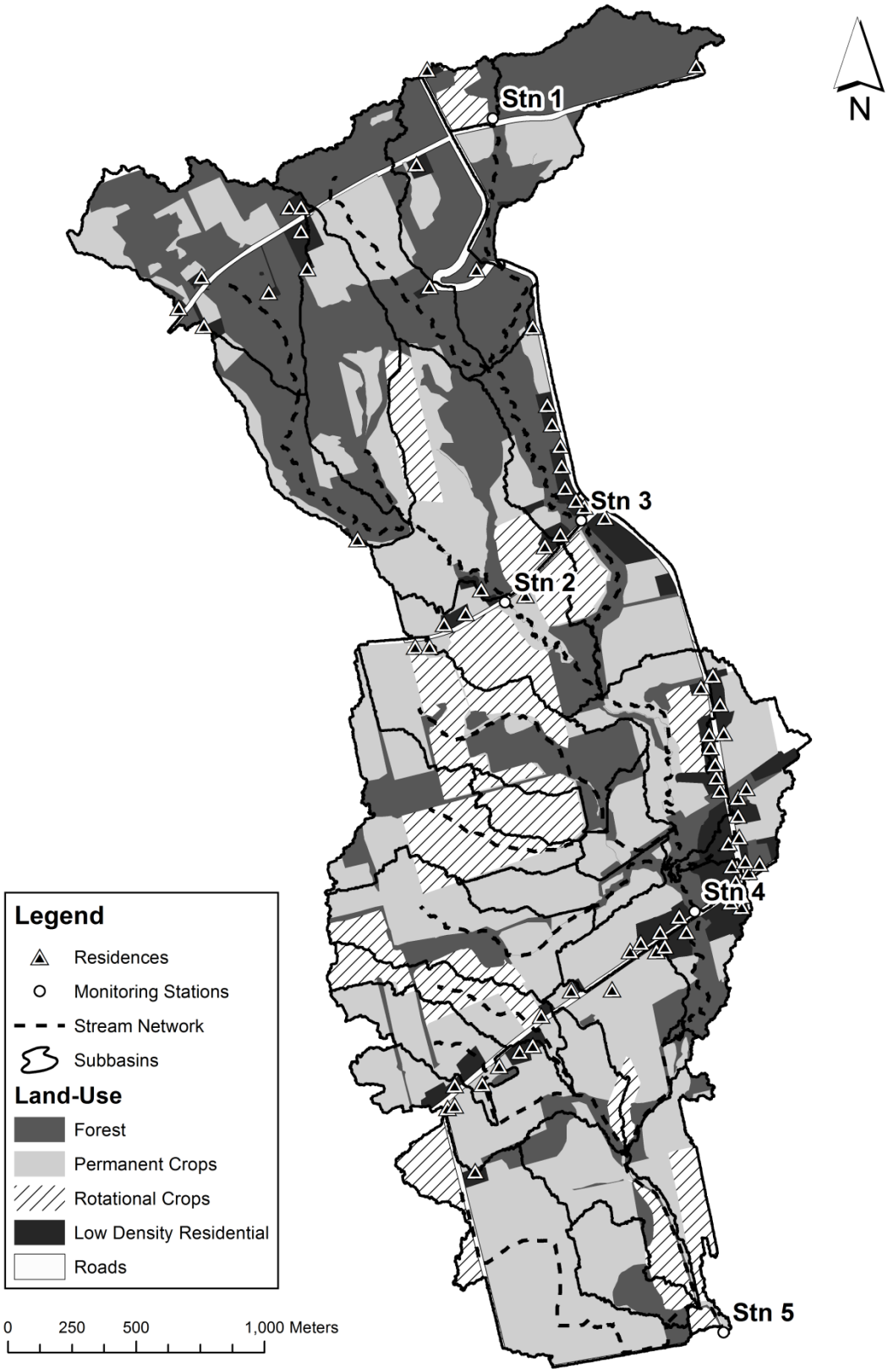

Figure 3.5 Thomas Brook Watershed with residence locations and major land-uses.

Flow (m^3 d^{-1}) was calculated on a daily basis using stage discharge relationships developed from stage and discharge measurements (Sinclair et al., 2009; Goulden et al., 2013). The stage measurements were collected using pressure transducers that recorded water depths on 60 s intervals. The discharge measurements were made periodically throughout the year using the velocity area method (Canadian General Standards Board, 1991). Water samples were collected at each of the monitoring stations using ISCO 6700 autosamplers during the non-winter (April-December) and by weekly discrete grab sampling in the winter (January-March). The autosamplers collected 200-mL samples every 6 h and composited every four samples into an 800-mL bottle. A three day representative sample was formed by combining three consecutive 800-mL samples (Ahmad et al., 2011). The water samples were analyzed for total suspended solids (TSS) and total phosphorus (TP) using APHA standard methods 2540D and 4500-P (1999 revision), respectively (APHA, 2000).

3.2.3 SWAT Model Setup

The SWAT2009 ArcSWAT model was used to simulate flow, sediment and P in the TBW from 2004 through 2008 with a 15-yr model parameterization (warm-up) period. The geographic information system (GIS) data layers used for the SWAT2009 model include land-use classified through aerial photographs and field validation, soil from the Canadian Soil Information Service (CANSIS) database (AAFC, 2010) and topography using a 1-m resolution digital elevation model (DEM) (Goulden et al., 2013). Based on the results of Goulden et al. (2013) the spatial distribution of the slope classes was calculated from a 25-m resolution DEM derived from the 1-m DEM to improve simulation of sediment transport processes. The water course and subbasin delineation for the initial SWAT model setup were conducted using the 1-m DEM. The subbasin outlets were manually adjusted to match the approximate location of the WEBs monitoring stations. Observed daily precipitation and temperature data from the nearby (~17 km away) Environment Canada weather station in Greenwood, NS were input into the model. Crop rotation and fertilizer application data was used from the SWAT2005 model operation schedule developed by Ahmad et al. (2011).

3.2.4 POWSIM Inputs

The OWS TP loading in the TBW was simulated by developing a POWSIM model for each of the four monitoring stations (Stns 2, 3, 4, 5) in the watershed with residences in their subcatchments. The OWSs within each monitoring station subcatchment were grouped together and each POWSIM model simulated the OWSs in the subcatchment as a cluster with a single distance to the water course, site slope and soil type. This user-definition method for POWSIM inclusion into the SWAT model was chosen because the monitoring station subcatchments were already defined within the TBW SWAT model, and were relatively small in area (<200 ha). The representative OWS distance to the water course for each POWSIM subcatchment was determined using ArcGIS 9.3 (ESRI, Redlands, CA) by first calculating the centroid of each residential land-use polygon from the land-use shapefile. It was assumed, for each residential lot, that the centre of the property would be the location of the residence. The shortest straight line distance between each centroid point shapefile and the water course was then determined using ArcGIS and the median value for each monitoring subcatchment selected. A value of 20 m was subtracted from the median subcatchment value to represent the approximate length from the house to the down gradient end of the OWS disposal field. The OWS distances to the water course for each individual residence within a cluster were calculated and then averaged together to compute the POWSIM input parameter for the length of the soil subsurface plume. The representative soil type and site slope for each subcatchment was determined from the attributes of the subcatchment SWAT2009 model residential HRU that represented the largest number of residences.

In July 2011 a mail-in survey on OWS usage and maintenance practices, and OWS failure was sent out to ~300 residences in the Upper Cornwallis River Watershed of which the TBW is a subcatchment. There was a 30% reply rate and the results were averaged to provide the number of residents per household, age of OWS and % of OWS failed, which were used as inputs into POWSIM. In May 2011 a sampling study was also conducted on 11 septic tanks in the TBW and the average soluble reactive P concentration was used as the POWSIM STE TP concentration input. The rest of the input parameters for the four POWSIM models were taken from relevant literature or

assumptions based on the experience of the authors (Table 3.3). The soils within the TBW were assumed to have no initial P concentrations in the soil subsurface plume (soil b_1) and no deep aquifer P removal based on the results of the sensitivity analysis of the POWSIM input parameters. The results of the four POWSIM models were input as text files into the SWAT2009 ArcSWAT model representing monthly time step soluble P point sources at manually chosen points along the stream reach that were closest in distance to the highest densities of residences in each subcatchment. It was assumed that the OWS TP load would be all in the form of soluble P as the SWAT2009 model does not accept point source loads in the form of TP. This soluble P load includes the OWS failure load, which was assumed to be only in the soluble form when percolating to the surface and flowing to the water course. This is a conservative worst-case scenario as the soluble P form arriving into the water body or stream network is the most bioavailable form of P. In reality the OWS surface hydraulic failure TP load would interact with the surface environment and be impacted by precipitation events, which would partition P into sediment bound and organic forms.

Table 3.3 POWSIM input parameters with Thomas Brook Watershed values, and results of the two sensitivity analyses (18 and 50 yr OWS operation periods for Stns 3 and 4 (2004-2008) total outflow total phosphorus loads.

Parameter	Thomas Brook Watershed Value	Information Source	Sensitivity Analysis Range	Sensitivity Class*			
				1991 (18 yrs)		1959 (50 yrs)	
				Stn 3	Stn 4	Stn 3	Stn 4
Operation Start Year	1991	Cornwallis Headwaters Survey	1981 – 2001; 1948 – 1958	III	III	I	I
# of residences	Stn 2 – 8; Stn 3 – 17; Stn 4 – 41; Stn 5 - 15	AAFC WEBs program	-	-	-	-	-
Soil Type	Stn 2 – Cumberland; Stn 3 – Woodville; Stn 4,5 - Cornwallis	Thomas Brook SWAT2009 HRUs	-	-	-	-	-
OWS Failure Rate (%)	15	Cornwallis Headwaters Survey	0 - 30	III	III	II	II
STE TP Concentration, mg P L^{-1}	18.5	Thomas Brook STE sampling	3.5 - 33.5	III	III	III	III
STE outflow, L d^{-1}	1200 (3 people)	Cornwallis Headwaters Survey	1000 - 2000	III	III	III	III
Distance to water course, m	Stn 2 - 29.1; Stn 3 - 35.7; Stn 4 - 32.2; Stn 5 – 40.3	Median shortest straight-line distance from residence to water course	Default ±25	III	III	II	II
OWS & plume slope, m m^{-1}	Stn 2, 3 - 0.06; Stn 4 - 0.05; Stn 5 – 0.03	Thomas Brook SWAT2009 HRUs	0.05 - 0.35	III	III	II	II
# of years until full failure	10	Assumed	0 - 20	I	I	I	I
% OWS length functioning	75	Assumed	50 - 100	I	I	I	I
% of OWS involved in P treatment	76	Sinclair et al. (2013a)	50 - 100	I	I	I	I
% of soil subsurface plume functioning	100	Assumed	50 - 100	II	II	I	I
Sand hydraulic conductivity, m $x10^{-4}$ s^{-1}	2.53	Sinclair et al. (2013a)	2.5 – 12.5	I	I	I	I
Sand S_{max}, mg P kg^{-1} sand	74.69	Sinclair et al. (2013a)	24.69 – 124.69	I	I	I	I
Sand m_1	0.94	Sinclair et al. (2013a)	0.44 - 1.44	I	I	I	I
Sand b_1	0.44	Sinclair et al. (2013a)	-0.56 - 1.44	I	I	I	I

Parameter	Thomas Brook Watershed Value	Information Source	Sensitivity Analysis Range	Sensitivity Class*			
				1991 (18 yrs)		1959 (50 yrs)	
				Stn 3	Stn 4	Stn 3	Stn 4
Sand m_2	0.52	Sinclair et al. (2013a)	0.27 – 0.77	III	III	III	III
Sand b_2	64	Sinclair et al. (2013a)	14 - 114	I	I	I	I
Depth of permeable soil, mm	Stn 2, 4, 5 - 1000; Stn 3 – 400	CANSIS Database (AAFC, 2010)	500 - 1500	I	I	III	III
Total soil depth to bedrock/ groundwater, mm	1000	CANSIS Database (AAFC, 2010)	1000 - 2000	I	I	I	III
Soil hydraulic conductivity, m $x10^{-5}$ s^{-1}	Stn 2, 3 - 1.94; Stn 4, 5 - 6.94	CANSIS Database (AAFC, 2010)	±1	I	I	I	I
Soil $S_{max,}$ mg P kg^{-1} soil	237	McCray et al. (2005)	87 - 387	II	II	III	II
Soil m_1	0.86	Avg. Sinclair et al. (2013a)	0.16 - 1.56	III	II	I	I
Soil b_1	0	Assumed	0 - 20	I	I	I	I
Soil m_2	0.29	Avg. Sinclair et al. (2013a)	0 - 0.59	I	I	II	II
Soil b_2	157	Calculated	7 - 307	I	I	I	I
Deep aquifer P removal, %	0	Assumed	0 - 10	I	I	I	I

* – Sensitivity classes – Class I – Small to negligible; Class II – Medium; Class III – High (adapted from Lenhart et al. (2002)).

3.2.5 Calibration, Sensitivity Analysis and Evaluation

The TBW SWAT2009 model was auto-calibrated in SWAT-CUP (version 4.3.7.1) using the parallel Sequential Uncertainty Fitting Version 2 (SUFI-2) method for flow and sediment (Abbaspour, 2011). The observed datasets used for daily flow multi-site auto-calibration were from Stns 3 and 4 from January 2004 to December 2006. The hydrologic flow input parameters that were auto-calibrated and their ranges are listed in Table 3.4. Only flow, sediment and nutrient data from Stns 3 and 4 were used for SWAT2009 model calibration as they had the most complete datasets of the five TBW monitoring stations. The validation period for the SWAT2009 model was January 2007 to December 2008. The range of annual precipitation values for the calibration and validation periods were 961 to 1194 mm and 897 to 1175 mm, respectively; these ranges when compared against the 1981 to 2010 climate normal (1117 mm) for the Greenwood weather station (Government of Canada, 2013) represent both wet and dry years. Moriasi et al. (2007) recommended that data sets used for watershed model calibration and validation include both wet and dry years to improve model robustness in representing a wide range of hydrological events.The auto-calibration used SUFI-2 to search for input parameter values within physically plausible user-defined ranges that optimized the value of an objective function (Gupta et al., 1999). The objective function used for flow, sediment and TP calibrations was the Nash-Sutcliffe efficiency (NSE) (Nash and Sutcliffe, 1970), as represented in the following equation:

$$NSE = 1 - \left[\frac{\sum_{i=1}^{n} \left(O_i - X_i \right)^2}{\sum_{i=1}^{n} \left(O_i - O_{avg} \right)^2} \right] \tag{3.13}$$

where O_{avg} is the average of observed values, and O_i and X_i are the observed and simulated values, respectively. The optimal NSE value is 1 and auto-calibration was terminated when further variation of the input parameter values within increasingly optimized and narrow ranges did not improve the Stn 3 and 4 NSE values.

Table 3.4 Hydrologic flow input parameters, calibration ranges, and calibrated values for SWAT and SWAT with POWSIM.

Parameter*	Parameter Description	Land-use/ Subbasin	Default Value	Calibration Range	Subbasin 1-9 Calibrated Value	Subbasin 10-28 Calibrated Value
Alpha_BF.gw	Baseflow alpha factor, d	All	0.014	0.001 – 0.1	0.00824	0.00619
GW_DELAY.gw	Groundwater delay time, d	All	30	1 - 4	1	1
GWWQMN.gw	Threshold depth for shallow aquifer return flow, mm H_2O	All	0	0 – 450	176.25	390.10
GW_REVAP.gw	Groundwater revap coefficient	All	0.1	0.02 – 0.2	0.0645	0.1293
RCHRG_DP.gw	Deep aquifer percolation fraction	All	0.05	0 – 0.15	0.0145	0.0500
CN2.mgt	Initial NRCS runoff curve number	All	0	±15%	-14.49	-7.13
USLE_P.mgt	USLE equation support practice factor	Agriculture	1	0.75 – 1	0.75	0.75
ESCO.hru	Soil evaporation compensation factor	All	0.95	0.5 – 1	0.653	0.504
EPCO.hru	Plant uptake compensation factor	All	1	0.9 – 1	0.975	0.936
CANMX.hru	Maximum canopy storage, mm H_2O	Forest	0	4 – 7	6.55	5.36
OV_N.hru	Manning's n value for overland flow	Forest	0.14	-	0.7	0.7
OV_N.hru		AGRL, GRAZ, PAST, RNGE, URLD†	0.14	-	0.41	0.41
CH_N(2).rte	Manning's n value for the main channel	All	0.014	-	0.1	0.05
CH_K(2).rte	Effective hydraulic conductivity in main channel, mm hr^{-1}	All	0.5	-	0	0
CH_W(2).rte	Average width of main channel, m	1 – 4, 6	‡	-	1.7	1.7
CH_W(2).rte		5,7 – 9	‡	-	2.3	2.3
CH_W(2).rte		10 – 19	‡	-	4	4
CH_W(2).rte		20 – 28	‡	-	5.1	5.1
CH_D(2).rte	Average depth of main channel, m	1 – 4, 6	‡	-	1.2	1.2
CH_D(2).rte		5,7 - 9	‡	-	1.3	1.3
CH_D(2).rte		10 – 19	‡	-	1.2	1.2
CH_D(2).rte		20 – 28	‡	-	2.1	2.1

Parameter*	Parameter Description	Land-use/ Subbasin	Default Value	Calibration Range	Subbasin 1-9 Calibrated Value	Subbasin 10-28 Calibrated Value
CH_N(1).sub	Manning's n value for tributary channel	All	0.014	-	0.1	0.05
CH_K(1).sub	Effective hydraulic conductivity for tributary channel, mm hr^{-1}	All	0.5	-	0	0
PET Method.bsn	Potential evapotranspiration method	All	-	-	Hargreaves	
SURLAG.bsn	Surface runoff lag coefficient	All	4	-	0.8	
SFTMP.bsn	Snowfall temperature, ˚C	All	1	-2 – 2	-0.204	
SMTMP.bsn	Snow melt base temperature, ˚C	All	0.5	-2 – 2	-1.823	
SMFMX.bsn	Snow melt factor on June 21, mm H_2O $˚C^{-1}$ d^{-1}	All	4.5	2 – 8	4.005	
SMFMN.bsn	Snow melt factor on Dec 21, mm H_2O $˚C^{-1}$ d^{-1}	All	4.5	2 – 8	3.367	
TIMP.bsn	Snow pack temperature lag factor	All	1	0.01 – 0.99	0.635	
SNOCOVMX.bsn	Minimum snow water content at 100% snow cover, mm H_2O	All	1	0 – 250	118.129	
SNO50COV.bsn	Fraction of snow volume represented by SNOCOVMX for 50% snow cover	All	0.5	0.01 – 0.99	0.317	

* gw – groundwater; mgt – management; hru – hydrologic response unit; rte – route; sub – subbasin; bsn – basin.

† AGRL – general agriculture; GRAZ – grazing; PAST – pasture; RNGE – rangelands; URLD – low-density residential.

‡ Calculated by ArcSWAT.

Table 3.4 lists a number of parameters that had fixed values that were not calibrated. The OV_N values were fixed at user-defined values for the forest, general agriculture, grazing, pasture, rangeland, and low-density residential land-uses as these were assumed to have higher OV_N values than the default parameters because of little change in vegetation cover throughout the year. The CH_N(2) values describing the main channel Manning's n value were verified by visually inspecting the quality of stream bed at each of the five monitoring stations in the TBW and using expert judgement to calculate an appropriate value. The CH_K(2) value for the effective hydraulic conductivity of the main channel was assumed to be 0 mm H_2O hr^{-1} as the water course does not disappear below the ground surface anywhere in the TBW. The CH_W(2) and CH_D(2) parameters correspond to main channel width and depth, respectively, and were physically measured at each of the five monitoring stations. The tributary CH_N(1) and CH_K(1) values were assumed to be the same as the values for the main channel. The Hargreaves potential evaportranspiration method was chosen as only minimum and maximum daily observed temperature data was available for the TBW. The surface runoff lag coefficient (SURLAG) was fixed at 0.8 d because of the small size of the TBW (<700 ha) and observed storm events typically peak within one day or less at the watershed outlet. The minimum daily time step for the SWAT2009 model makes modeling a SURLAG value substantially less than 1 d unrealistic.

One of the outputs of the SWAT-CUP program after each auto-calibration run is a sensitivity analysis of the calibrated input parameters. Not shown in this present study are the sensitivity analysis results, which were incorporated into subsequent auto-calibration runs by reducing the calibration ranges for the least sensitive parameters around the SWAT2009 model default values, and keeping larger value ranges for the most sensitive parameters. Although this methodology does not address a common problem in computer modeling of non-uniqueness of input parameter in producing the same model results, it does produce more modeler confidence that the most sensitive input parameters are being more thoroughly investigated during the auto-calibration process.

After completion of the flow auto-calibration, the SWAT-CUP sediment auto-calibration was performed on a monthly time step. Sediment was included in the calibration process because one of the main P transport pathways to the water course in

SWAT2009 is sediment-attached organic and soluble P in surface runoff (Neitsch et al., 2011). The input parameters and their calibration ranges are shown in Table 3.5. A monthly time step was chosen for the sediment and P calibrations as the water quality samples were collected using autosamplers on 6 h intervals that were composited to represent 3-d periods.

Table 3.5 Sediment input parameters, calibration ranges, and calibrated values for SWAT2009 and SWAT2009 with POWSIM.

Parameter*	Parameter Description	Default Value	Calibration Range	Subbasin 1-9 Calibrated Value	Subbasin 10-28 Calibrated Value
SPCON.bsn	Linear parameter for calculating maximum amount of sediment reentrained during channel routing	0.0001	0.0001 – 0.01	0.0001	
SPEXP.bsn	Exponent parameter for calculating sediment reentrained during channel routing	1	1 – 2	2	
PRF.bsn	Peak rate adjustment factor for main channel routing	1	0.5 – 2	0.5	
ADJ_PKR.bsn	Peak rate adjustment factor for tributary channel routing	1	0.5 – 2	0.5	
USLE_P.mgt†	USLE equation support practice factor	1	0.75 – 1	0.75	0.75
CH_EROD.rte	Channel erodability factor	0	0 – 1	0	0
CH_COV.rte	Channel cover factor	0	0 – 1	0	0

* bsn – basin; mgt – management; rte – route

† applied only to tillage crops.

The TBW water quality monitoring program sampled for TP, however, the SWAT2009 model does not directly provide TP as an output and instead calculates soluble P and organic P loads, which when summed together equal the TP load. Therefore, the SWAT2009 model without POWSIM was calibrated for P on a monthly time step by manually adjusting the appropriate input parameter values within physically plausible ranges (Eckhardt et al., 2005), as shown in Table 3.6. Other evaluation statistics used in this study to examine SWAT2009 model performance for flow, sediment and TP included percent bias (PBIAS) (Equation 3.14) and ratio of root mean square error to the standard deviation of measured data (RSR) (Equation 3.15) (Moriasi et a al., 2007). The guidelines developed by Moriasi et al. (2007) for evaluating the watershed model performance indicators NSE, PBIAS, and RSR were used in this study.

Table 3.6 Phosphorus input parameters, calibration ranges, and calibrated values for SWAT2009 and SWAT2009 with POWSIM.

Parameter*	Parameter Description	Default Value	Calibration Range	SWAT Calibrated Value	SWAT+ POWSIM Calibrated Value
PSP.bsn	P sorption coefficient	0.4	0.2 – 0.7	0.7	0.7
PHOSKD.bsn	P soil partitioning coefficient	175	100 - 200	200	200
PUPDIS.bsn	P uptake distribution factor	20	10 – 60	20	20
PPERCO.bsn	P percolation coefficient	10	10 – 17.5	10	10
SOL_LABP .chm	Initial soluble P concentration in soil layer, mg P kg^{-1}	0	0 – 100	0	0
SOL_ORGP .chm	Initial organic P concentration in soil layer, mg P kg^{-1}	0	0 - 100	0	0
ERORGP.hru	Organic P enrichment ratio	0	0 – 5	0	0

* bsn – basin; chm – soil chemistry; hru – HRU.

$$PBIAS = \left[\frac{\sum_{i=1}^{n} (O_i - X_i) * 100}{\sum_{i=1}^{n} (O_i)} \right] \tag{3.14}$$

$$RSR = \frac{\left[\sqrt{\sum_{i=1}^{n} (O_i - X_i)^2} \right]}{\left[\sqrt{\sum_{i=1}^{n} (O_i - O_{avg})^2} \right]} \tag{3.15}$$

The outputs from the four POWSIM models representing the Stns 2 to 5 subcatchments were entered as point sources in the calibrated TBW SWAT2009 model. The SWAT2009 model was manually re-calibrated for all the P input parameters in SWAT2009 (Table 3.6) using NSE as the objective function. Evaluation of the SWAT2009 model and SWAT2009 with POWSIM results included comparing NSE, PBIAS and RSR values for the calibration and validation periods. Further comparisons were made by running the calibrated SWAT2009 and SWAT2009 with POWSIM models on a daily time step to allow differentiation of simulated P loads into baseflow and stormflow. The observed and simulated daily flow data was differentiated into stormflow and baseflow using the straight-line baseflow separation method (McCuen, 1989).

The relative contributions of TP for each type of land-use (forest, permanent and rotational crops, residential, transportation) and POWSIM for the Stn 3 and 4 subcatchments were also compared. The SWAT2009 model does not track the relative TP load from each land-use after they have entered the water course at the subbasin level. Therefore, the relative TP contributions of each different land-use and the OWSs prior to entering the water course were determined for each subcatchment. The first step to calculate the average annual SWAT2009 land-use loads was to transform the HRU P loads from kg P ha^{-1} to kg P by multiplying them by their respective HRU surface areas (ha). The annual soluble, organic and sediment P loads for the HRUs with the same land-use classification were summed together for each subcatchment to get the TP load. The five-year average (2004-2008) TP load was then calculated for each land-use classification. The Stn 3 POWSIM five-year average TP load was calculated by first computing the annual soluble P loads for 2004 to 2008 from the Stn 3 point source input file and then averaging the results. The same methodology was applied to the Stn 4 POWSIM average load calculation, except the Stn 2, 3 and 4 monthly soluble P loads were first summed together.

A watershed-scale POWSIM input parameter sensitivity analysis was completed on the calibrated SWAT2009 model with POWSIM for the 2004 to 2008 time period. The POWSIM input parameters were varied individually within physically plausible value ranges with all other input parameters at fixed values (Table 3.3). The cumulative P loads at Stns 3 and 4 for the five year (2004–2008) time period were used for the

sensitivity analysis calculations. The dimensionless sensitivity index and classification method used by Lenhart et al. (2002) was applied to calculate POWSIM input parameter sensitivity.

To examine the impacts on POWSIM input parameter sensitivity of older OWS in the TBW, a second sensitivity analysis was completed. POWSIM models were developed assuming all OWS in the TBW had been in operation for 50 yrs, instead of the 18 yrs used in the calibrated POWSIM model. The same sensitivity analysis methodology described earlier in this section was used on the SWAT2009 model with the 50-yr POWSIM inputs. The POWSIM input parameter sensitivity ranking results for the SWAT2009 models with 18 and 50-yr POWSIM inputs were compared.

3.2.6 Export Coefficient Model

A commonly used method for determining P loads from various land-uses to a surface water system is to us an export coefficient modeling approach, particularly for ponds and lakes (Robertson et al., 1998; Brylinksy, 2004; Matias and Johnes, 2012). In Nova Scotia the 'User's Manual for Prediction of Phosphorus Concentration in Nova Scotia Lakes: A Tool for Decision Making, Version 1.0' (Brylinksy, 2004) is used to calculate annual P loads to lakes from agricultural, residential and forest land-uses using export coefficients. Annual TP loads (kg P yr^{-1}) from OWS in the Stn 3 and 4 subcatchments were calculated using the export coefficient method outlined by Brylinksy (2004). The input parameters for the export coefficient method are shown in Table 3.7. High and low input values were used for annual TP load per capita and adsorption capacity parameters to calculate a range of values to compare against the SWAT2009 with POWSIM results. The TP load output to the watercourse for the Stn 3 and 4 subcatchments from POWSIM for the 2004 to 2008 time period were averaged annually to allow direct comparison against the export coefficient method results. The results of the two methods were compared directly against each other using percent difference.

Table 3.7 On-site wastewater system input parameters for Nova Scotia export coefficient method for predicting phosphorus concentrations in lakes (Brylinksy, 2004).

Input Parameter	Parameter Description	Stn 3 value	Stn 4 value
N_d	# of dwellings	17	66
N_u	avg. # of people per dwelling	3	3
N_{pc}	avg. fraction of year dwelling occupied	1	1
S_i	annual P load per capita (kg P capita yr^{-1})	0.3*, 0.8†, 1.8‡	0.3*, 0.8†, 1.8‡
R_{sp}	adsorption capacity	0§, 0.5‖	0§, 0.5‖
Residential Area	Area (ha)	3.01	21.93

* Uttormark (1974).
† Dillon et al. (1986).
‡ Reckhow et al. (1980).
§ Conservative (Brylinksy, 2004).
‖ Hart et al. (1978).

3.3 Results and Discussion

3.3.1 Hydrology and Sediment

The calibration period (2004–2006) hydrologic flow simulations for SWAT2009 without POWSIM for Stns 3 and 4 were rated satisfactory with NSE (≥0.5), PBIAS (±25%), and RSR (<0.75) as shown in Table 3.8. Table 3.4 and 3.5 show the calibrated input parameters for hydrologic flow and sediment, respectively. The Stn 4 validation period (2007–2008) hydrologic flow simulation results were also rated satisfactory. The hydrologic flow simulation for the Stn 3 validation period did not perform to a satisfactory level with a positive PBIAS value of 38.3% representing a general under-prediction of observed flow. However, the Moriasi et al. (2007) model performance evaluation criteria were developed specifically for a monthly time step, which typically has better performance statistic results than a daily time step model. Therefore, the hydrologic flow auto-calibration results were considered satisfactory for the TBW SWAT2009 model.

Table 3.8 Flow, sediment, and total phosphorus (TP) calibration (2004-2006) and validation (2007-2008) statistical results for SWAT and SWAT with POWSIM calibrations for Stns 3 and 4.

Stn	Model Run	Simulation Period	Flow (Daily)			Sediment (Monthly)			TP (Monthly)		
			NSE	PBIAS	RSR	NSE	PBIAS	RSR	NSE	PBIAS	RSR
				%			%			%	
3	SWAT	Calibration	0.56	11.8	0.66	-2.35	-127.8	1.83	-1.96	86.9	1.72
		Validation	0.38	38.3	0.78	-0.21	-4.9	1.10	-0.47	82.9	1.21
	SWAT+	Calibration	0.57	10.7	0.66	-2.35	-127.9	1.83	-0.48	43.7	1.22
	POWSIM	Validation	0.39	37.5	0.78	-0.21	-4.9	1.10	-0.30	64.0	1.14
4	SWAT	Calibration	0.64	-25.0	0.60	0.19	-4.8	0.9	-0.14	76.5	1.07
		Validation	0.59	-2.0	0.64	-2.26	-65.9	1.81	-1.04	-4.7	1.43
	SWAT+	Calibration	0.64	-26.3	0.60	0.19	-4.8	0.9	0.05	59.1	0.98
	POWSIM	Validation	0.59	-3.7	0.64	-2.26	-65.9	1.81	-1.58	-50.3	1.61

Sediment monthly auto-calibration statistical evaluation results for the calibration and validation periods had both satisfactory and unsatisfactory PBIAS results (satisfactory ±50%), and unsatisfactory NSE and RSR values at Stn 3 and 4 (Moriasi et al., 2007). The negative PBIAS results show over-estimation of sediment loads for both the calibration and validation periods at both stations (Table 3.8). Ahmad et al. (2011) had unsatisfactory monthly manual sediment calibration NSE values of 0.45 and 0.27 for the same calibration and validation periods, respectively for Stn 4 with the TBW SWAT2005 model. The poor NSE values for simulation of sediment loading for both TBW SWAT models, is potentially explained by the less than 1-d time of concentration for the Stn 3 and 4 catchments and the daily time step resolution of the SWAT2005 and SWAT2009 models (Ahmad et al., 2011). If travel times in the watershed are less than one day, then there is potential for the peak flows to be smoothed out within both SWAT2005 and 2009 resulting in lowered estimated storm even sediment loads than are actually occurring in the TBW.

When the POWSIM point sources were introduced into the auto-calibrated SWAT2009 model there was little to no change in the hydrology and sediment statistical evaluation results for the Stns 3 and 4 calibration and validation periods. Therefore, the TBW SWAT2009 model with POWSIM point source inputs was not re-calibrated for hydrology and sediment.

3.3.2 Phosphorus

The monthly TP manual calibration model performance results for Stns 3 and 4 were similar to those for the sediment auto-calibration with mixed PBIAS (satisfactory ±75%) and unsatisfactory NSE and RSR values as shown in Table 3.8 (Moriasi et al., 2007). The two TP calibration input parameters that were changed from their default values to produce the best NSE objective function values were the P sorption coefficient (PSP) and P soil partitioning coefficient (PHOSKD) (Table 3.6). The annual SWAT2009 simulated TP loads, divided into the proportion attributed to baseflow and stormflow, are both generally under predicted for each year in the calibration and validation periods, particularly the Stn 4 stormflow TP loads (Figure 3.6). As sediment is the main P transport mechanism in SWAT2009, the issue of less than 1-d time of concentration and

model daily time step is possibly contributing to the unsatisfactory simulation of TP. The OWS TP load from the soil subsurface plume and surface hydraulic failure is continuously input into the water course for both the stormflow and baseflow period with the surface hydraulic failure TP load assumed to not be interacting with surface runoff sediment transport processes in the SWAT2009 model.

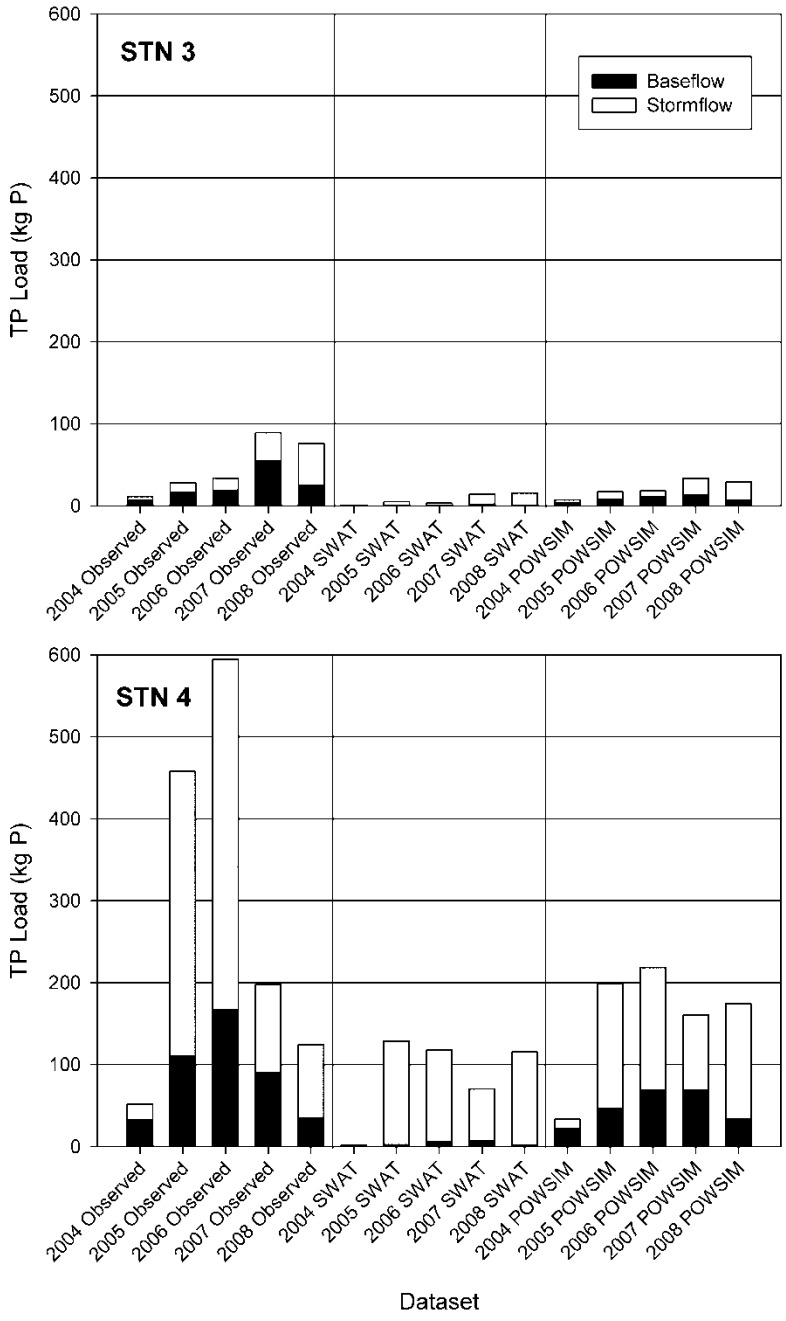

Figure 3.6 **Observed, SWAT, and SWAT with POWSIM annual baseflow and stormflow phosphorus loads for Stns 3 and 4.**

The POWSIM models developed for Stns 2, 3, 4 and 5 all selected the C3 type contour trench disposal field design based on the input parameters. Figure 3.7 shows the outputs from the Stn 3 POWSIM model with a total simulation time period of 50 yrs. A 50 yr simulation period was chosen to capture all the simulated changes in TP loading rate to the water course for the lifespan of a TBW OWS. The annual TP output loads for the different model components undergo significant changes at several points in time. The OWS disposal field to soil subsurface plume TP load shows the relatively quick (<5 yr) transition from Equation 3.12-I to 3.12-II as the maximum sorption capacity of the OWS disposal field sand is reached. There is then a discernible decrease in the disposal field to soil subsurface plume TP loading rate until year 10 as more of the STE is diverted to OWS failure and not the disposal field. The influence of the number of years until full failure rate input parameter is also illustrated in the linear increase in the failed OWS TP loading rate for the first 10 yrs. The annual TP output from the soil subsurface plume shows the switch from Equation 3.12-I to 3.12-II at ~ year 33. Until year 35 the OWS failure is the main contributor of TP to the water course when it is surpassed by the soil subsurface plume. Based on these POWSIM simulation results land-use planning in the TBW would need to focus on evaluating TP loading for time periods greater than 30 yrs of OWS operation to include peak TP loading to fully assess impacts of management practices. As the TBW OWS were, on average, installed in 1991, the POWSIM model outputs at the end of the SWAT2009 validation period (2008) are only at simulation year 18 in Figure 3.7.

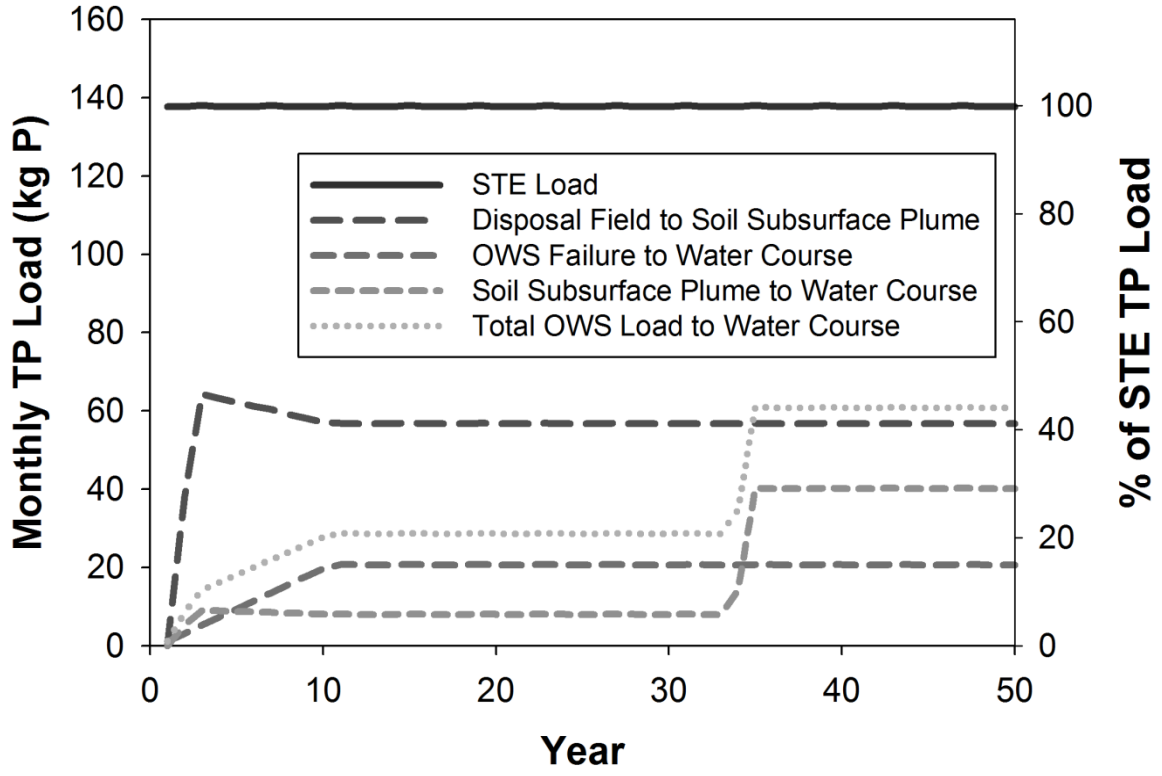

Figure 3.7 POWSIM annual incremental results for 17 residences in Stn 3 subbasin for a 50 year period.

The addition of the POWSIM point source inputs into SWAT2009, and the subsequent TP re-calibration of the TBW SWAT2009 model, produced improved statistical model performance results for the Stn 3 calibration and validation, and Stn 4 calibration periods (Table 3.8). None of the SWAT2009 input parameters were changed in value for the SWAT2009 with POWSIM re-calibration. The daily TP loading from POWSIM into the SWAT model caused a visual increase in the annual TP baseflow loads for both Stns 3 and 4 that better match the observed dataset (Figure 3.6). Withers et al. (2011; 2012) observed increased in-stream TP concentrations during baseflow periods because of OWS P loading. Therefore, improved simulation of baseflow TP outflows by including OWS P inputs suggests that OWS are a possible P source in the TBW. These results are contrary to Geza and McCray (2010) who calibrated the WARMF model for hydrology, sediment and P for the non-agricultural Turkey Creek Watershed in Colorado for the time period 1996 to 2005 with a residential population of 11,000. The model also included five centralized wastewater treatment plants that were simulated as point sources that served 10% of the watershed population. They found that OWS were minimally contributing to the in-stream TP concentration and concluded that native soils were providing adequate P treatment.

Although the annual baseflow and stormflow TP contributions simulated by the SWAT2009 model with POWSIM better fit the observed datasets they are still typically under-predicting (Figure 3.6). An obvious reason for the under-prediction is that the OWS are contributing more P than is simulated in the TBW. Further OWS field studies, particularly related to P treatment and transport in the soil subsurface plumes, would need to be conducted to warrant changing the POWSIM input parameters. Another reason is that the model is under-estimating the amount of P applied to agricultural lands. Nutrient management plans (NMPs) were used to calculate the P input fertilizer and manure application rates in SWAT2009, and actual fertilization rates in the TBW may be higher. Thirdly, there are a number of fields in the TBW underlain with tile drainage systems that are possibly contributing P to the water course. Currently, the TBW SWAT2009 model is not setup to simulate tile drainage; however, the SWAT2009 model does not simulate P movement through tile drainage (Neitsch et al., 2011). The constant soluble P shallow aquifer concentration parameter (GWSOLP) can be potentially used in SWAT2009 to

represent tile drainage, but was not used in this study as the number and types of fields underlain with tile drainage in the TBW is unknown, and so is their mean effluent P concentration

The TBW SWAT with POWSIM average annual (2004–2008) land-use TP loads for the Stns 3 and 4 subcatchments are shown in Figure 3.8. On-site wastewater systems and agriculture were the two main TP sources in both subcatchments, but were ranked differently for each subcatchment. The main reason for the ranking reversal between the two subcatchments is the difference in percentage of the drainage area that is classified as agriculture, which for Stn 3 and 4 is 34 and 51%, respectively. The housing densities for Stn 3 and 4 of 0.14 and 0.13 houses ha^{-1} subcatchment, respectively, are relatively close in value. The POWSIM inputs represent 48 and 39% of the total average annual TP loads for Stns 3 and 4, respectively; the values fall within the 4 to 55% range reported by Lombardo (2006), but exceed the 10% value found by Withers et al. (2012). The simulated OWS and agricultural TP loads for both the Stn 3 and 4 subcatchments are the same order of magnitude, so TBW management strategies should focus on both of these land-uses to reduce TP pollution.

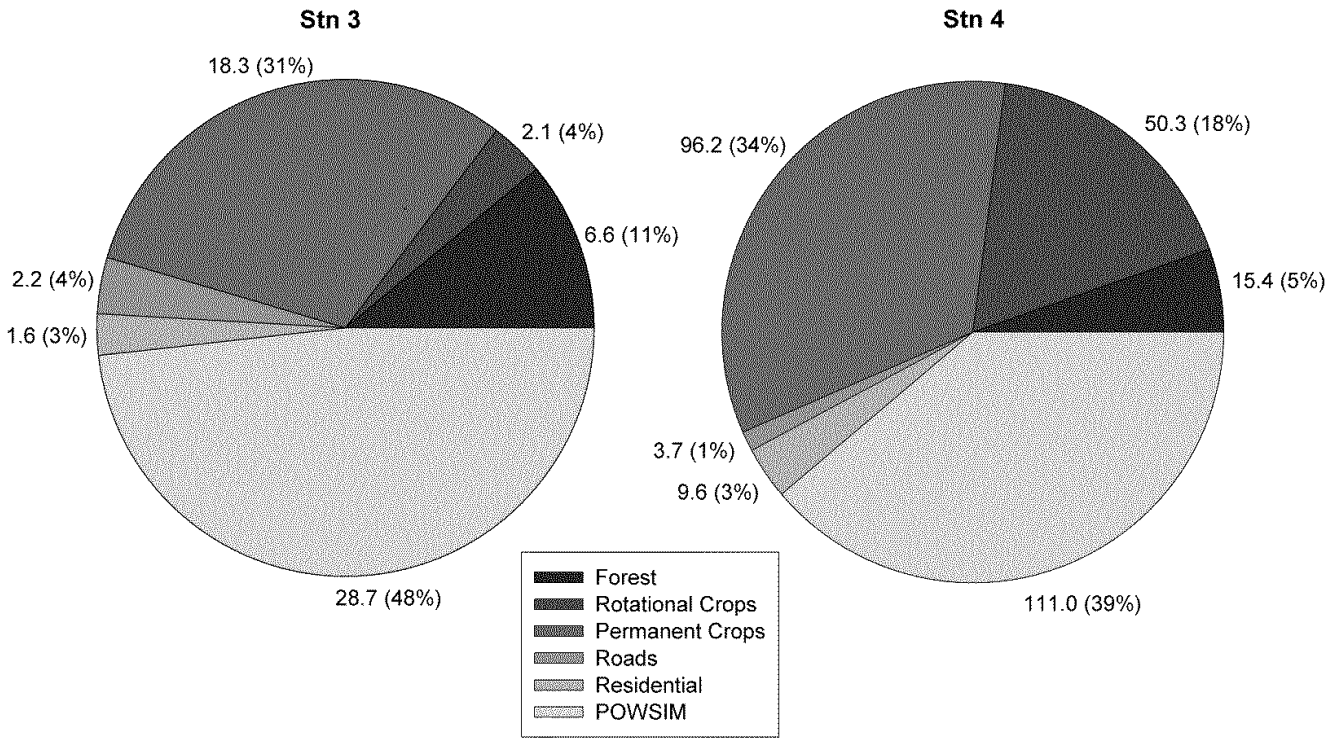

Figure 3.8 Average annual (2004 – 2008) simulated land-use total phosphorus loads (kg TP) and percent contributions at Stn 3 and 4.

3.3.3 POWSIM Sensitivity Analysis

The results of the two watershed-scale POWSIM input parameter sensitivity analyses for TBW Stns 3 and 4 are shown in Table 3.3. The sensitivity analysis results for each individually manipulated input parameter are ranked from I to III, with III being the highest (Lenhart et al., 2002). Parameters in class II or III are the most important, and improved accuracy in their estimation would provide increased confidence in the model results. The majority of parameters that had a medium (class II) or high (class III) sensitivity POWSIM model with OWS starting operation in 1991 (18 yrs) also had a class II or III sensitivity in POWSIM model with OWS starting operation in 1959 (50 yrs). The most sensitive parameters from both analyses were associated with the STE TP loading rate (STE TP concentration, outflow volume), disposal field sand Equation 3.12-II slope (m_2), soil maximum P sorption capacity (S_{max}) and the volume of the soil subsurface plume (distance to water course, plume slope). Operation start year, percent of soil subsurface plume active in treatment, and the soil Equation 3.12-I slope (m_1) were inputs with medium or high sensitivity only in the 1991 model as the soil subsurface plume has not switched from P removal Equation 3.12-I to 3.12-II (Figure 3.7). The soil Equation 3.12-II slope (m_2) was sensitive in the 1959 POWSIM model, which controls long-term P treatment in the soil subsurface plume. The 1959 POWSIM model also displayed high sensitivity to the depth of permeable soil and the total depth of soil to bedrock/groundwater parameters, which change the OWS disposal field design and volume of the soil subsurface plume. Some of the input parameters that were interestingly found not to be sensitive in this study were the % parameters affecting the amount of the OWS involved in P treatment, number of years until full OWS failure and percent removal to the deep aquifer.

Geza and McCray (2010) conducted an watershed-scale in-stream P concentration sensitivity analysis at three monitoring sites on OWS input load and soil P removal parameters for the WARMF model in the Turkey Creek Watershed, CO. They found that soil S_{max}, initial soil P concentration (soil b_1), and plant uptake had high sensitivity rankings. The STE P concentration was ranked as having a low sensitivity. Only the soil S_{max} ranking corresponds with the rankings from the TBW sensitivity analysis.

Based on the results of the two sensitivity analyses, obtaining accurate information on OWS design, installation times, operation and maintenance would be the most important inputs for the TBW POWSIM model. The household OWS operation and maintenance surveys, and STE sampling programs used in this study would be useful tools for collecting information to populate the POWSIM input parameters in other watersheds. The two most important P treatment input parameters are the Equation 3.12-II slopes for disposal field sand media and native soils that govern the long-term P removal rate, particularly for simulations greater than 30 years. Of the most sensitive POWSIM input parameters identified in the TBW study, only those associated with the soil subsurface plume were based predominantly on literature values and general assumptions. Investigations of P treatment in soil subsurface plumes in the TBW and other watersheds in NS would help improve that computational component in POWSIM.

3.3.5 Export Coefficient Method Comparison

The POWSIM results recalculated as annual average TP loads per year were closet in value (absolute average 18% difference) to export coefficient method for Stns 3 and 4 that used an annual P load per capita (S_i) value of 0.8 kg P capita^{-1} yr^{-1} and a conservative adsorption capacity (R_{sp}) of 0.5 (Table 3.9). The Stn 3 and 4 POWSIM average annual TP loads for 2004 to 2008 were equivalent to 1.4 and 1.5 kg P house^{-1} yr^{-1}, respectively. The POWSIM household annual TP loading rates were relatively close in value to the export coefficient used by Whitehead et al. (2011) of 1.25 kg P house^{-1} yr^{-1} to estimate OWS TP loads into the Black River in the Lake Simcoe Watershed, ON assuming a 57% P removal rate by the OWS. The POWSIM annual TP loading rate was higher than several other OWS TP export coefficient loading rates of 0.5, 0.72 and 0.78 kg P house^{-1} yr^{-1} used by Mattson and Issac (1999), Johnes (1996) and Greene et al. (2011), respectively. The relative proximity of the annual average POWSM TP loading rates to the export coefficient values reported in the literature and the current export coefficient method used in NS to predict P concentrations in lake environments suggests that the P loads predicted by the POWSIM model are reasonable.

Table 3.9 **Annual TP export loads and percentage differences for POWSIM and Brylinksy (2004) export coefficient method with different input parameters.**

Method	Stn 3		Stn 4		Abs. Average % Difference
	TP Load Rate (kg P yr^{-1})	% Difference	TP Load Rate (kg P yr^{-1})	% Difference	
POWSIM	23.6	-	102.6	-	-
Export Coefficient					
S_i – 0.3; R_{sp} – 0	15.3	-35	59.4	-42	38
S_i – 0.3; R_{sp} – 0.5	7.6	-68	29.7	-71	69
S_i – 0.8; R_{sp} - 0	40.8	73	158.4	54	63
S_i – 0.8; R_{sp} – 0.5	20.4	-13	79.2	-23	18
S_i – 1.8; R_{sp} – 0	91.8	289	356.4	247	268
S_i – 1.8; R_{sp} – 0.5	45.9	95	178.2	74	84

3.4 Conclusions

Overall the POWSIM model used in conjunction with the SWAT2009 model shows potential for improving the watershed scale simulation of P loading from OWS designs with pre-dominantly lateral flow based on the model simulations in this study. Land-use planning using POWSIM in the TBW requires simulating >30 yrs OWS operation periods to fully evaluate the impact of OWS beneficial management practices (BMPs) on peak P loading. Agricultural and OWS land-uses were simulated as the largest P sources in the TBW and their TP loads were the same order of magnitude even though residential land-uses are only 4% of the watershed area compared to 60% for agriculture. This suggests management strategies focus on both agricultural and residential OWS land-use types. The TBW SWAT2009 with POWSIM generally under-predicted baseflow and stormflow TP loads for both subcatchments studied, but performed better than the SWAT2009 model without POWSIM. The relative TP contribution from agricultural tile drainage systems is not known within the TBW and field studies would assist with better representing these systems in watershed-scale models. Field studies in the TBW and other NS watersheds examining soil subsurface plume P treatment and transport would likely help improve the POWSIM input parameterization and

computational component algorithms. To develop and gain greater confidence in the POWSIM model it should be calibrated and tested in other watersheds in NS and used at larger watershed-scales.

CHAPTER 4 MODELING IMPACTS OF RESIDENTIAL AND AGRICULTURAL DEVELOPMENT AND BENEFICIAL MANAGEMENT PRACTICE SCENARIOS ON PHOSPHORUS DYNAMICS IN A SMALL WATERSHED

4.1 Introduction

Two potential non-point phosphorus (P) sources in rural mixed land-use watersheds are agricultural fields and residential wastewater (Carpenter et al., 1998). Phosphorus loading from anthropogenic sources is the primary cause of accelerated eutrophication in freshwater systems (Schindler 1977; Carpenter et al., 1998). Eutrophic conditions can cause toxic algal blooms, oxygen depletion, and loss of aquatic habitat (Chambers et al., 2001). Sharpley et al. (2001) identified that particulate and dissolved forms of P enter freshwater systems from agricultural fields through attachment to eroded soil particles, surface and irrigation runoff, and subsurface flow. Residential wastewater in rural United States and Canada is generally treated using on-site wastewater systems (OWS) (Lowe et al., 2007). In these systems residential wastewater is first treated in a septic tank to settle out particulate forms of P; the effluent is then drained into a disposal field. The disposal field allows the effluent to percolate through either imported filter media or native soil, with treated water discharging into the surrounding soil profile. Finally, further treatment is provided by the soil profile before reaching neighbouring surface water systems by means of lateral flow. Surface hydraulic failure of the disposal field due to improper drainage or clogging can cause effluent discharge at the ground surface, thus reducing the amount of P treatment prior to discharge into a freshwater system. The two main P treatment processes that occur in a disposal field and its surrounding soil profile are sorption and precipitation (Robertson, 2008; McCray et al., 2005). Because Nova Scotia (NS), Canada is characterized by low permeability soils, shallow bedrock, and high water tables, disposal fields are most commonly constructed of imported filter media, typically sand (Havard et al., 2008).

There have been numerous studies which have documented substantial P loading from agricultural fields at the field- and watershed-scales (Sims et al., 1998; Sharpley et al., 2001; Hart et al., 2004; McDowell et al., 2004; McDowell, 2013). For example, McDowell (2013) found that grassland catchments in New Zealand with either intensive dairy or low-intensity drystock (red deer, sheep or beef) operations contributed 44 and 69% to the median stream filterable reactive P and total P (TP) concentrations, respectively. In contrast, there is routinely no monitoring of OWS P loads at the watershed-scale and loads are assumed to be relatively small compared to agricultural land-use (Withers et al., 2009, 2011; Badruzzaman et al., 2012). However, several recent studies have indicated that OWS can be significant non-point source P sources in mixed land-use watersheds. A study conducted in small United Kingdom (UK) agricultural watersheds (6.5 to 9.9 km^2) found that farmyard runoff and septic tank discharges had higher P concentrations compared to agricultural field runoff, and contained greater proportions of bioavailable P (Withers et al., 2009). Withers et al. (2011) found elevated soluble reactive P concentrations in a UK stream downstream of a group of OWS, with the highest P concentrations occurring during low or baseflow conditions; it was suggested in this study that the OWS were experiencing hydraulic failure. Others have estimated that OWS P loads represent 4 to 55 (Lombardo, 2006), 14 (Dudley and May, 2007), and 10% (Withers et al., 2012) of the total P load in a watershed. In general, the contributions of OWS to the total P load in a watershed tend to be poorly understood.

Watershed management plans address eutrophication related water quality issues by implementing practices and constructing engineered structures to reduce P loading from surface runoff or groundwater (Chambers et al., 2012). These practices and structures are commonly referred to as beneficial management practices (BMPs). The implementation of agricultural BMPs for reducing nutrient loading has been studied extensively for the past 15 yr. Both the United States and Canadian federal governments have administered research programs (US: Conservation Effects Assessment Project [CEAP] from 2002 to present; Canada: Watershed Evaluation of Beneficial Management Practices [WEBS] from 2004 to 2013) to evaluate the environmental impacts of different agricultural BMPs in various North American ecosystems (AAFC, 2013; USDA NRCS, 2013). Rao et al. (2009) conducted a literature review of agricultural field land-use BMPs

for reducing P loads and reported a wide range of P percent reductions for plot-, field- and watershed-scale studies. They identified that most agricultural BMPs reduced P loads by either altering hydrologic pathways away from P sources, reducing surface runoff and soil erosion, or decreasing P fertilizer application rates.

Compared to agricultural BMPs there has been significantly less research conducted on OWS BMPS. Much of the OWS P loading research to date has focused on evaluating P treatment and transport processes, and removal rates, in existing OWS technologies and soil subsurface plumes (McCray et al., 2009; Motz et al., 2012; Robertson, 2012; Bridson-Pateman et al., 2013). An OWS P BMP could either improve the P removal rate and treatment capacity, or reduce the hydraulic failure rate. The only OWS P BMP that has been evaluated through lab- and plot-scale experiments is improving P removal rates and treatment capacity in disposal field media (Johansson Westholm, 2006; Cucarella and Renman, 2009; Vohla et al., 2011). Plot- or field-scale investigations have not been performed on other potential OWS P BMPs, such as increased water course set-backs, disposal field replacement, and scheduled OWS maintenance and inspection programs. To the knowledge of the authors there have been no peer-reviewed studies published to date examining the environmental impacts of OWS P BMPs at the watershed-scale. In mixed land-use watersheds there is a need to compare the efficacy of both agricultural and OWS BMPs to develop watershed management plans that target the appropriate land-uses uses to reduce P transport to fresh water bodies.

A commonly used tool in watershed management to evaluate BMP scenarios prior to implementation at the watershed-scale is the integrated hydrological-water quality computer model. Conducting field- or watershed-scale investigations of BMP effectiveness can be difficult and costly to perform, so computer models are often used to estimate the spatial and temporal environmental impacts of candidate BMPs. The Soil and Water Assessment Tool (SWAT) is a frequently used watershed-scale model for evaluating sediment and nutrient load reductions from agricultural BMPs (Gassman et al., 2007). The SWAT model has previously been calibrated and tested in the Thomas Brook Watershed (TBW) in NS, which is the same watershed used in this present study (Ahmad et al., 2011; Sinclair et al., 2013b). The calibrated model has also been used to evaluate

the impact of different nutrient management plans and tillage practices on crop yields, and nitrate and sediment loading in the TBW (Amon-Armah et al., 2013).

The majority of OWS P treatment and transport modeling has been conducted at the lab- and field-scales (Jeong et al., 2011; McCray et al., 2009). Lemonds and McCray (2003) used the SWAT model to simulate OWS P loads in the Blue River Watershed in Colorado by adapting the fertilizer management practices and found OWS were not the primary source of P loading. The SWAT model (version 2009 [SWAT2009]) was recently updated to include an OWS algorithm that uses a linear P sorption model to simulate P removal (Jeong et al., 2011). However, P transport via lateral flow in the soil profile is not simulated in SWAT 2009 (Neitsch et al., 2011); representation of this process is critical for simulating OWS typically used in eastern Canada. To address this issue, Sinclair et al. (2013b) developed a P on-site wastewater simulator (POWSIM) to use in conjunction with the SWAT model to simulate OWS P loads at the watershed-scale and applied it to the TBW.

The objectives of this research were to: (i) investigate impacts of different agricultural and residential development scenarios on sediment, P loading and trophic status at the watershed outlet in the TBW using POWSIM and SWAT2009; and (ii) assess, rank and combine several agricultural (crop replacement, no-tillage) and OWS (reduced failure rates, increased water course set-backs, high P sorption filter media, and disposal field replacement) BMPs and evaluate their potential impact on water quality metrics with POWSIM and SWAT.

4.2 Materials and Methods

4.2.1 Case Study Watershed

Thomas Brook Watershed is located in the Annapolis Valley region of the province of NS, Canada. The TBW is an approximately 665 ha headwater subcatchment for the Cornwallis River. The headwaters of the TBW begin on the north side of the Annapolis Valley, referred to as the North Mountain, and are characterized by two distinct stream branches that converge approximately one third of the distance through the watershed (Jamieson et al., 2003). The TBW undergoes an elevation change from 212

m on North Mountain to 7 m on the valley floor. Goulden et al. (2013) determined from a 1 m digital elevation model (DEM) that the majority of the TBW landscape slope was between 0 and 7% with 95% existing below 20%. The stream network has an average slope of 3.5% with a maximum of 30% on North Mountain and a minimum of 0.5% on the valley floor (Goulden et al., 2013; Sinclair et al., 2009). The width of the stream varies between 2 and 3 m with sections on the valley floor incised because of mechanical straightening (Brisbois et al., 2008; Goulden et al., 2013). The main soil type in the TBW is reddish brown sandy loam (Jamieson et al., 2003).

The main land-uses within the TBW are agriculture, forest, and residential representing 60, 34, and 4% of the total watershed area, respectively. As shown in Figure 4.1 the main types of agricultural field land-uses are rotational and permanent crops, such as corn (*Zea mays* L.), timothy (*Phleum pratense* L.), and alfalfa (*Medicago sativa* L.) for producing animal fodder, and strawberries (*Fragaria* L.) for human consumption. The average agricultural field size in the TBW is 2 ha. The major agricultural BMP that is utilized in the TBW is the nutrient management plan (NMP), which was implemented in 2005 for approximately 80% of the agricultural crops (Nunn, 2007). Both rotational and permanent crops are fertilized with animal manure and/or chemical fertilizers. Table 4.1 lists the agricultural field land-uses, P fertilizer application rates and tillage operations within the TBW. The main sources of animal manure come from approximately 186 bovines on a dairy farm with manure storage, and two beef farms with 36 and 16 animals, respectively (Sinclair et al., 2009). The two beef farms pasture their cattle during the growing season (May to October) in various fields throughout the watershed. There are 81 residences in the TBW that treat their household wastewater using on-site wastewater systems (OWS) (Sinclair et al., 2013b).

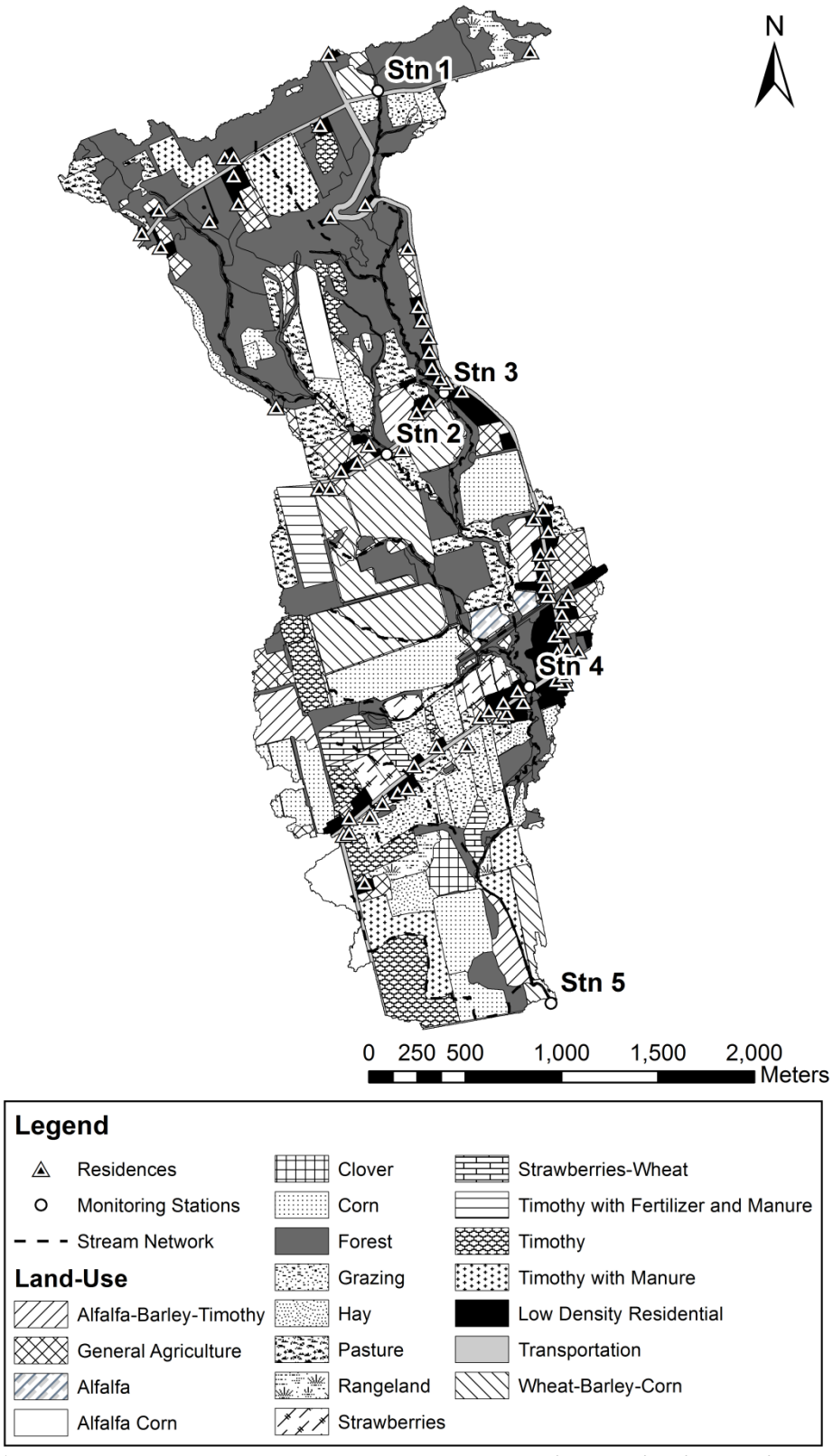

Figure 4.1 Thomas Brook Watershed land-use map with monitoring station locations.

Table 4.1 Agricultural field land-uses with crop rotations, P fertilizer application timing and rates, and types and timing of tillage.

Land-use	Land-use Abbreviation	Type of Rotation Schedule	Crop Rotation Schedule*	TP Fertilizer Application Rate (kg ha^{-1})*	TP Fertilizer Application Month(s)*	Type of Tillage*,†	Tillage Month(s)*
Alfalfa-Barley-Timothy	ABBT	4 y	A-B-B-T	A – 9.68; B – 20.55; T – 0	A – May; B – May/ June	A, T – 96; B – 43, 96	A, B – May; T - Oct
Alfalfa	ALFA	Cont	A	9.68	May	96	May
Alfalfa-Corn	ALFC	4 year	A-A-A-C	A – 9.68; C - 30	A,C - May	A – 96; C – 43, 96	A,C – May
Clover	CLVR	Cont	R	9.68	May	96	May
Corn	CORN	Cont	C	30	May	43, 96	May
Grazing	GRAZ	Cont	G	1.48	June - Oct	No Till	-
Hay	HAY	Cont	T	16.5	May	96	Oct
Pasture	PAST	Cont	Pa	1.48	June - Oct	No Till	-
Strawberries	STRW	4 y	S-S-S-S	0	-	S (1^{st} y) – 33; S (2^{nd} & 3^{rd} y) – No Till; S (4^{th} y) - 1	S (1^{st} y) – May; S (4^{th} y) - Oct
Strawberries-Wheat	STWH	4 y	S-S-S-W_s	0	-	S (1^{st} y) – 33; S (2^{nd} y) – No Till; S (3^{rd} y) – 1; W_s – 43, 96	S (1^{st} y) – May; S (3^{rd} y) – Oct; W_s - May
Timothy with Fertilizer and Manure	TFRM	Cont	T	30	May/ June	96	Oct
Timothy	TIMO	Cont	T	0	-	No Till	-
Timothy with Manure	TMAN	Cont	T	16.5	May	96	Oct
Wheat-Barley-Corn	WBBC	4 y	W_w-B-B-C	W_w – 24; B – 20.55; C – 30	W_w – Sept; B – May/ June; C - May	W_w – 1; B,C – 43, 96	W_w – Oct; B,C - May

Source: Ahmad et al. (2011).* A, alfalfa (*Medicago sativa* L.); B, barley (*Hordeum* L.); C, corn (*Zea mays* L.); G, grazing; Pa, pasture; R, red clover (*Trifolium pratense* L.); S, strawberry (*Fragaria* L.); T, timothy (*Phleum pratense* L.); W_s, spring wheat (*Tricticum aestivum* L.); W_w, winter wheat (*Tricticum aestivum* L.).† 1, Fall Plow; 33, Roller Harrow; 43, Springtooth Harrow; 96, Tandem Disk.

Two water quality studies have been conducted in the TBW examining P concentrations in the stream network to assess its trophic state. Brisbois et al. (2008) collected weekly grab samples from TBW monitoring stations (Stns) 1 - 5 (Figure 4.1) from May to September 2006 that were analysed for total phosphorus (TP). Only samples collected from Stn 2, which was directly downstream of a dairy farm, were consistently in the eutrophic range of 0.035 to 0.1 mg TP L^{-1} outlined by the Canadian Council of the Ministers of the Environment (CCME) freshwater guidelines (2004). However, the TP methodology used by Brisbois et al. (2008) had a detection limit of 0.06 mg P L^{-1} which is above the minimum range limit for the CCME eutrophic classification. Brisbois et al. (2008) compared the TBW TP results against those from a forested reference watershed in the Annapolis Valley region that was studied during the same time period. The TBW was identified as having elevated TP concentrations compared to the reference watershed, and had typical TP concentrations for a stream impacted by agricultural activities. Nunn (2007) collected samples using auto-samplers every 6 hours, which were then combined to form three day composite samples during the growing season (May to October) from 2001 to 2005 at TBW Stns 2, 4 and 5. Stations 4 and 5 are located on the low slope (0.5%) valley floor where 85% of the corn and rotational crop land area is located. The Stn 4 subcatchment also has 35 OWS in relatively close proximity to the station (Figure 4.1). The 5 yr mean TP concentrations at Stns 4 and 5 fell within the eutrophic range, while Stn 2 mean TP concentrations were in the hyper-eutrophic range (>0.1 mg P L^{-1}). The TP concentrations observed by the two studies show an impacted stream network, presumably caused by agricultural and residential activities.

4.2.2 Watershed and On-Site Wastewater System Models

The two computer models used in conjunction in this study were the SWAT2009 (Neitsch et al., 2011) and POWSIM (Sinclair et al., 2013b) models. The SWAT2009 model is a continuous, process-based, watershed-scale model that was developed to simulate long-term land management practices and has been widely-used to simulate hydrology, sediment, nutrient, pesticide and bacteria transport (Gassman et al., 2007). The monthly time step POWSIM loading tool simulates lateral-flow P removal and transport from an individual or cluster of OWS to the nearest surface water system, which

are then input into SWAT2009 as point-source loads (Sinclair et al., 2013b). The OWS designs that can be simulated by the POWSIM loading tool are the most commonly used in NS containing sand filter media, which are contour trenches and, lateral flow sand filters and mound systems according to L. Boutilier (personal communication, September 9, 2013). The POWSIM loading tool utilizes slope and soil data from the SWAT2009 model and user-defined OWS operation and maintenance inputs to choose the types of OWS designs that would be present in the watershed. These OWS designs and input parameters are then used to calculate the mass of disposal field treatment media and soil that will be involved in P treatment for each individual OWS or cluster of OWSs. Only one type of OWS disposal field design is selected by the POWSIM model to represent the cluster of OWSs option. The other two computational components of POWSIM simulate P treatment dynamics in the OWS disposal field and the soil subsurface plume that would exist down gradient of the disposal field. Phosphorus sorption and precipitation processes are simulated in POWSIM using a 2-part piecewise linear equation that uses the treatment media or soil maximum P sorption capacity as a trigger to switch from linear equation part I to II. The POWSIM model simulates OWS failure as direct transmission of P loading to the nearest surface water system. The POWSIM loading tool is described in further detail in Sinclair et al. (2013b).

Sinclair et al. (2013b) calibrated and tested the SWAT2009 model in conjunction with the POWSIM model at Stns 3 and 4 in the TBW for simulation of hydrology, and sediment and phosphorus transport processes. The daily time step hydrologic flow simulations had satisfactory Nash-Sutcliffe efficiency (NSE) and ratio of root mean square error to the standard deviation of the measured data (RSR) for both the calibration and validation periods at both stations (Table 4.2). However, the Stn 3 validation and Stn 4 calibration period percent bias (PBIAS) values were outside the acceptable range of ±25% as outlined by Moriasi et al. (2007); these values were considered acceptable as the evaluation criteria developed by Moriasi et al. (2007) were specifically for a monthly time step, which typically has better performance statistical results than a daily time step model. The sediment statistical results had both satisfactory and unsatisfactory results for PBIAS at Stns 3 and 4 for the calibration and validation periods. A previous simulation of sediment transport by Ahmad et al. (2011) using SWAT (version 2005 [SWAT2005]) at

TBW Stn 4 also had unsatisfactory results. The unsatisfactory simulation of sediment transport at Stns 3 and 4, particularly for the NSE evaluator is potentially caused by the less than one day time of concentrations for both of these sub-catchments; both SWAT2009 and SWAT2005 utilize daily time steps (Ahmad et al., 2011; Sinclair et al., 2013b). The TP calibration results in Table 4.2 show satisfactory PBIAS results, and unsatisfactory NSE and RSR for Stns 3 and 4 for both the calibration and validation periods that are possibly explained by the less than one day time of concentration as sediment is the main P transport mechanism in SWAT2009. Sinclair et al. (2013b) found that the inclusion of POWSIM into the SWAT model produced higher annual baseflow TP loads at both stations and a better fit to the observed data, than just the SWAT model alone. Although Moriasi et al. (2007) was used as a benchmark in this study to evaluate the SWAT2009 with POWSIM model calibration and validation results, the range of satisfactory performance indicator values was developed from evaluating SWAT model results for watersheds with areas significantly larger than the TBW (e.g. Bosque River 4277 km^2 [Santhi et al., 2001]). As such, measuring the performance of the TBW SWAT2009 with POWSIM model against the Moriasi et al. (2007) rating system is possibly too stringent for such a small watershed area. Therefore the calibrated TBW SWAT2009 with POWSIM model was assumed to be acceptable to represent hydrologic flow, and sediment and TP transport processes and used to evaluate development and BMP scenarios. The calibrated SWAT2009 and POWSIM models developed by Sinclair et al. (2013b) were used in this study to simulate the reference, development and BMP scenarios.

Table 4.2 Statistical evaluation results for SWAT and POWSIM models for the Thomas Brook Watershed for flow, sediment and total phosphorus.

Stn	Model Run	Simulation Period	Hydrology (Daily)			Sediment (Monthly)			Total Phosphorus (Monthly)		
			NSE*	PBIAS† %	RSR‡	NSE*	PBIAS† %	RSR‡	NSE*	PBIAS† (%)	RSR ‡
3	SWAT+ POWSIM	Calibration (2004 – 06)	0.57	10.7	0.66	-2.35	-127.9	1.83	-0.48	43.7	1.22
		Validation (2007 – 08)	0.39	37.5	0.78	-0.21	-4.9	1.10	-0.30	64.0	1.14
4	SWAT+ POWSIM	Calibration (2004 – 06)	0.64	-26.3	0.60	0.19	-4.8	0.9	0.05	59.1	0.98
		Validation (2007 – 08)	0.59	-3.7	0.64	-2.26	-65.9	1.81	-1.58	-50.3	1.61

Source: Sinclair et al. (2013b).

* Nash-Sutcliffe efficiency (Satisfactory is >0.5; Source: Moriasi et al. [2007]).

† Percent bias (Satisfactory is ±25% Hydrology, ±55% Sediment, ±70% Phosphorus; Source: Moriasi et al. [2007]).

‡ Ratio of root mean square error to the standard deviation of measured data (Satisfactory is <0.7; Source: Moriasi et al. [2007]).

4.2.3 Development Scenarios

An objective of this study was to examine long-term impacts on sediment and P loading associated with different agricultural and residential development scenarios in the TBW. The agricultural development scenarios were: (i) replacement of existing pasture and grazing lands with corn-based crops (corn, alfalfa-corn, wheat-barley-corn), and (ii) replacement of existing timothy crops with corn-based crops (Table 4.3). Corn and corn-based cropping rotations were chosen for the agricultural development scenarios as they have high sediment and nutrient runoff associated with frequent tilling practices and poor cover characteristics (Bundy et al., 2001). Corn also has the highest P fertilizer application rate of all TBW agricultural field land-uses (Table 4.1). The corn-based rotations represent a "worst-case" agricultural development scenario for the TBW based on existing land-use practices. The residential development scenarios involved increasing the human population in the watershed by 25 and 50%. The TBW is part of the Municipality of Kings County, which had an 11.5% increase in population from 1986 to 2011 (Statistics Canada, 2012b). The Kings County population growth increase equals 24% for a 50 yr time period, which is represented by the 25% population increase scenario. Sinclair et al. (2013b) found that the calibrated the Stn 3 TBW POWSIM model reached P saturation in the soil subsurface plume component at ~33 yr, which occurs concurrently with peak OWS P loading to the water course. Therefore, a 50 yr simulation time period (1962 to 2011) was chosen for the SWAT and POWSIM models to evaluate long-term scenario impacts. The 1962 to 2011 time period was chosen because of the availability of daily precipitation and temperature data from the nearby (~17 km) Environment Canada meteorological station in Greenwood, NS to input into SWAT2009. The input climate data used for the 1962 to 2011 time period did not undergo any climate forcing or manipulation and represents a time period when the land-use change scenarios occurred and not future climate change forecasting scenarios for the TBW. The simulation period was preceded by a 5 yr parameterization period for the SWAT2009 model from 1957 to 1961. The calibrated SWAT2009 and POWSIM input parameters from Sinclair et al. (2013b) were used to develop a reference scenario model. All scenario models were developed using the reference scenario model and evaluated by comparing

results between the reference and scenario models. The OWS were all assumed to begin operation in 1962.

Table 4.3 Summary of development and BMP categories simulated with the SWAT and POWSIM models.

Development Category	**Scenarios**
Agriculture	corn-based crops replace hay corn-based crops replace pasture
Residential	+25% population +50% population
BMP Category	
Corn and rotational crop replacement	Timothy grazing/pasture rangeland
Tillage	no-till corn
On-site wastewater system failure rate	10% 5%
On-site wastewater system water course set-back	50 m
On-site wastewater system disposal field replacement	25 y cycle
On-site wastewater system high P sorption filter media	5000 mg P kg^{-1} media

The agricultural development scenarios were set-up in SWAT2009 by taking the input land-use shapefile geographic information system (GIS) layer, used to calculate the hydrologic response units (HRUs), and replacing the applicable land-uses with corn-based cropping systems. The existing corn-based crops in the TBW SWAT2009 model were wheat-barley-corn, corn, and alfalfa-corn with relative areal percentage breakdowns to each other of 47, 42 and 11%, respectively. The replacement of hay fields or pastures with corn-based crops maintained this relative areal percentage breakdown by first computing the area of each field requiring replacement. A manual "mix and match" method was used to place the corn-based cropping systems into the applicable fields until the development scenario land-use layer had approximately the same relative areal percentage breakdown as the existing TBW corn-based cropping systems.

Residential scenarios were setup in POWSIM by increasing the population in each monitoring station subbasin by either 25 or 50%. The SWAT model land-use GIS layer was updated by replacing pasture, grazing or general agricultural fields in each monitoring station subcatchment with low-density residential to obtain an approximately 25 or 50% increase in residential area. Pasture, grazing or general agricultural fields were chosen for residential land-use replacement because they are not corn or rotational crop operations and require less site development than forest for residence construction.

4.2.4 Beneficial Management Practice Scenarios

The agriculture and residential OWS BMP scenarios were run for the same simulation period (1962 to 2011) as the development scenarios. The SWAT and POWSIM models were parameterized using the calibrated inputs from Sinclair et al. (2013b) for the BMP scenarios. The same reference SWAT and POWSIM models as the development scenario were used for BMP evaluation.

The two types of agricultural field BMPs simulated were corn and rotational crop replacement, and no-till corn (Table 4.3). Replacing corn and rotational crops with timothy grass, grazing/pasture and rangeland, which have no tillage and lower TP fertilization rates should lower sediment and TP surface runoff into the stream network. The corn and rotational crop replacement BMPs were set-up in the SWAT model using the same methodology as the crop replacement development scenarios. No-tillage practices are one of the most widely-used agricultural BMPs for reducing soil erosion and nutrient loading (Holland, 2004). However, no-till systems have been found to increase soluble nutrient losses, particularly P (Bundy et al., 2001; Tiessen et al., 2010). The no-till corn BMP was applied to the TBW because of its wide-spread adoption across North America as an agricultural BMP (Horowitz et al., 2010; Statistics Canada, 2012c), and 131 ha of the TBW is in some form of corn-based cropping system. The no-tillage BMP replaced the existing corn land-use tillage practices with generic no-till mixing in the management input files. The Natural Resource Conservation Service (NRCS) surface runoff curve number (CN2) was reduced by 3 points for each of the rotational crops with no-till (Chung et al., 1999).

The OWS BMPs examined in this study included: (i) increased water course set-backs for OWS, (ii) reduced OWS failure rates, (iii) periodic disposal field replacement, and (iv) utilizing high P sorption filter media in the disposal field. Sinclair et al. (2013b) estimated the distance from each OWS to the nearest water course as the straight line distance from the centre of the residential property, minus 20 m to represent the approximate length from the house to the down gradient end of the OWS disposal field. Increasing the distance of the OWS from the water course increases the mass of soil that could be involved in P treatment. All of the monitoring station subcatchments possessed an average OWS distance to the water course of less than 50 m therefore a scenario was run assuming the OWS set-back for each subcatchment was 50 m. OWS water course set-back distances greater than 50 m were not simulated because many of the residential lots were too close to the stream network to allow placement of an OWS on the property, while still meeting the higher distance criteria.

The default OWS failure rate for the TBW is 15% and is based on the results of a regional mail-in survey conducted by Sinclair et al. (2013b), which included the TBW area. One main cause of OWS failure is hydraulic failure of the disposal field caused by solids breakthrough from the septic tank. Solids breakthrough typically occurs because of infrequent pumping out of the solids that accumulate in the septic tank. Scheduled pumping of a septic tank every 3 to 5 yr in conjunction with a visual inspection of the septic tank can prevent hydraulic failure (Nova Scotia Environment, 2009). An OWS watershed management strategy that would require all homeowners to pump out and visually inspect their septic tanks every 5 yr would be expected to lower the hydraulic failure rate. Scenarios with OWS failure rates reduced to 10 and 5% from the reference scenario value of 15% were simulated.

Many studies have shown that OWS disposal fields and soil subsurface plumes experience reduced P removal efficiencies over time (Robertson et al., 1998; Robertson, 2008; Sinclair et al., 2013a). Sinclair et al. (2013a) found that six field-scale lateral flow sand filters that were continuously loaded with septic tank effluent for 8 yr (2004 to 2011) had TP removal efficiencies of 93 to 72% and 44 to 8% for the 2004 to 2006 and 2009 to 2011 time periods, respectively; both time periods received similar total TP influent loads. An OWS BMP that would require the disposal field filter media to be

excavated and replaced with new media would regenerate these P sorption sites and improve long-term P removal. Disposal field replacement is the most expensive and labour intensive of the OWS BMPs. Based on the author's experience, a disposal field replacement strategy of every 25 yr was chosen, since a higher frequency replacement schedule would be considered cost prohibitive to the homeowners.

All of the OWS disposal field designs that are commonly used in NS and simulated by POWSIM employ sand as the main filter media. Sinclair et al. (2013a) conducted batch P sorption capacity tests on three sand types typically used in NS OWS and found their maximum P sorption capacities ranged from 47 to 135 mg P kg^{-1} sand. A literature review of batch P sorption test results by Cucarella and Renman (2009) classified shell and iron enriched sands as having high maximum P sorption capacities (1000 to 10000 mg P kg^{-1} sand). To simulate the alternative filter media BMP, an average of the high P sorption capacity sand range reported in the literature (5000 mg P kg^{-1} media) was used, and it was assumed that these enriched sands would exhibit similar hydraulic properties to the media currently used in NS OWS.

4.2.5 Scenario Evaluation

The two main evaluation methods for the development and BMP scenarios were cumulative pollutant loading and trophic state frequency distribution. Both TP loads and in-stream trophic state (as determined from TP concentration) were assessed as they characterize different potential environmental impacts. The total load of TP is of interest with respect to management and protection of downstream water bodies (lakes, reservoirs, estuaries), while the in-stream TP concentration and associated trophic state characterize potential impacts to in-stream aquatic habitat within the watershed. Streams and rivers within the Annapolis Valley are also heavily used for irrigation and recreational purposes, and algae blooms could have negative impacts on these anthropogenic water uses. The 50 yr cumulative TP and sediment loads were calculated from the simulation results for each of the scenarios at the watershed outlet (Stn 5) and compared against the reference scenario loads. The BMPs were then ranked based on their percent reduction of sediment and TP. The best ranked residential and agricultural

BMPs were then combined and simulated using SWAT and POWSIM models using a sequential methodology adapted from Yang et al. (2012).

For each of the development and BMP scenarios, the daily TP concentrations were calculated for Stn 5. The daily TP concentrations for the growing season (May to October) were grouped into 5 yr interval periods, and used to develop frequency distributions representing the trophic status classifications. The trophic state classes were adapted from the CCME (2004) and were oligotrophic (<0.01 mg TP L^{-1}), mestrophic (0.01 to <0.035 mg TP L^{-1}), eutrophic (0.035 to <0.1 mg TP L^{-1}) and hyper-eutrophic (≥0.1 mg TP L^{-1}). Five year interval periods were chosen for the trophic state analysis to represent the conditions of a full 4 yr crop rotation cycle. The May to October growing season encompasses the annual time period when freshwater streams, rivers and lakes in NS are most used for livestock watering, agricultural irrigation and recreation. The trophic state analysis involved examining how the trophic state frequency distributions changed over the 50 yr simulation period for each scenario.

4.3 Results and Discussion

4.3.1 Development Scenarios

The simulated 50 yr cumulative sediment and TP loads for the agricultural and residential development scenarios are shown in Table 4.4. Both of the corn-based crop rotation replacement scenarios increased the sediment and TP loads compared to the reference. Pasture replacement had the largest increase in cumulative sediment loading of 58%, compared to 20% for hay field replacement (Table 4.4). Pasture and hay fields comprise 12.3 and 13.2% of the existing watershed area, respectively. A reason that corn-based crop replacement of pasture/grazing land-uses had a larger sediment load increase is that two of the hay cropping systems (timothy with manure, and timothy with fertilizer and manure) are tilled annually. An example of the relative differences in sediment loading between the two agricultural scenarios is in Subbasin 3 in the Stn 3 subcatchment when the timothy with manure/Kingsport/4-8 slope HRU was switched to corn a 89% increase in the average cumulative sediment load ha^{-1} (43 vs. 82 Mg ha^{-1}) was observed. In contrast when pasture/Kingsport/4-8 slope HRU in Subbasin 6 (Stn 3 subcatchment)

was switched to corn it resulted in a 710% increase in the average cumulative sediment load ha^{-1} (6 vs. 49 Mg ha^{-1}). The higher sediment loads for the corn-based crop rotation replacement scenarios are related to the higher TP loads as one of the main P transport mechanisms in SWAT is attachment to sediment particles in surface runoff (Neitsch et al., 2011).

Table 4.4 Simulated development and BMP scenario cumulative and average annual sediment and total phosphorus loads, percent differences, and rankings.

Scenarios	Sediment			Total Phosphorus			BMP Ranking
	Cumulative Load (Mg ha^{-1})	% Difference from Reference	Average Annual Load (Mg ha^{-1})	Cumulative Load (kg P ha^{-1})	% Difference from Reference	Average Annual Load (kg P ha^{-1})	
Reference	23.6	-	0.47	33.7	-	0.67	-
Development							
Corn-based crops replace hay	37.3	20	0.75	44.1	23	0.88	-
Corn-based crops replace pasture	28.3	58	0.57	41.5	31	0.83	-
+25% residential population	23.6	0	0.47	36.1	7	0.72	-
+50% residential population	23.6	0	0.47	38.9	15	0.78	-
Beneficial Management Practices							
Pastures replace corn and rotational crops (PRCRC)	12.8	-46	0.26	22.3	-34	0.45	1
Rangelands replace corn and rotational crops	12.4	-47	0.25	22.2	-34	0.44	1
Timothy replaces corn and rotational crops	20.5	-13	0.41	24.9	-26	0.5	3
No-till corn	22.7	-4	0.45	34.2	2	0.68	9
10% on-site wastewater system failure rate	23.6	0	0.47	32.6	-3	0.65	7
5% on-site wastewater system failure rate (OWS-FR)	23.6	0	0.47	31.5	-6	0.63	6
50 m on-site wastewater system water course set-back (OWS-SB)	23.6	0	0.47	30.6	-9	0.61	5
25 y disposal field replacement (DFR)	23.6	0	0.47	33.0	-2	0.66	8
High P sorption filter media (HPSFM)	23.6	0	0.47	28.8	-15	0.58	4
Combination Beneficial Management Practices							
PRCRC, HPSFM	12.8	-46	0.26	17.4	-48	0.35	3
PRCRC, HPSFM, OWS-SB	12.8	-46	0.26	17.4	-48	0.35	3
PRCRC, HPSFM, OWS-SB, OWS-FR	12.8	-46	0.26	14.2	-58	0.28	1
PRCRC, HPSFM, OWS-SB, OWS-FR, DFR	12.8	-46	0.26	13.8	-59	0.28	1

The two residential development scenarios did not increase the cumulative sediment loading, as shown in Table 4.4. Sinclair et al. (2013b) also found that inputting the POWSIM model results into the SWAT model did not change flow or sediment statistical evaluation results. However, the cumulative TP loads for both residential development scenarios increased compared to the reference, which was observed by Sinclair et al. (2013b) when the POWSIM model results were input into the TBW SWAT model. The increase in population from 25% to 50% was linearly related to the increase in cumulative TP loading from 7 to 15%.

The agricultural development scenarios had higher cumulative TP and sediment export loads than the residential development scenarios. Agricultural scenario cumulative TP loadings exhibited higher rates of increase compared to the residential scenarios (Figure 4.2.A). The agricultural scenarios would pose a higher risk to lakes, reservoirs or estuaries that are downstream of the TBW where sediment attached P would settle out. The increased P load into these water bodies would contribute to algal and macrophyte growth in the water column and accelerated eutrophication (Carpenter et al., 1998).

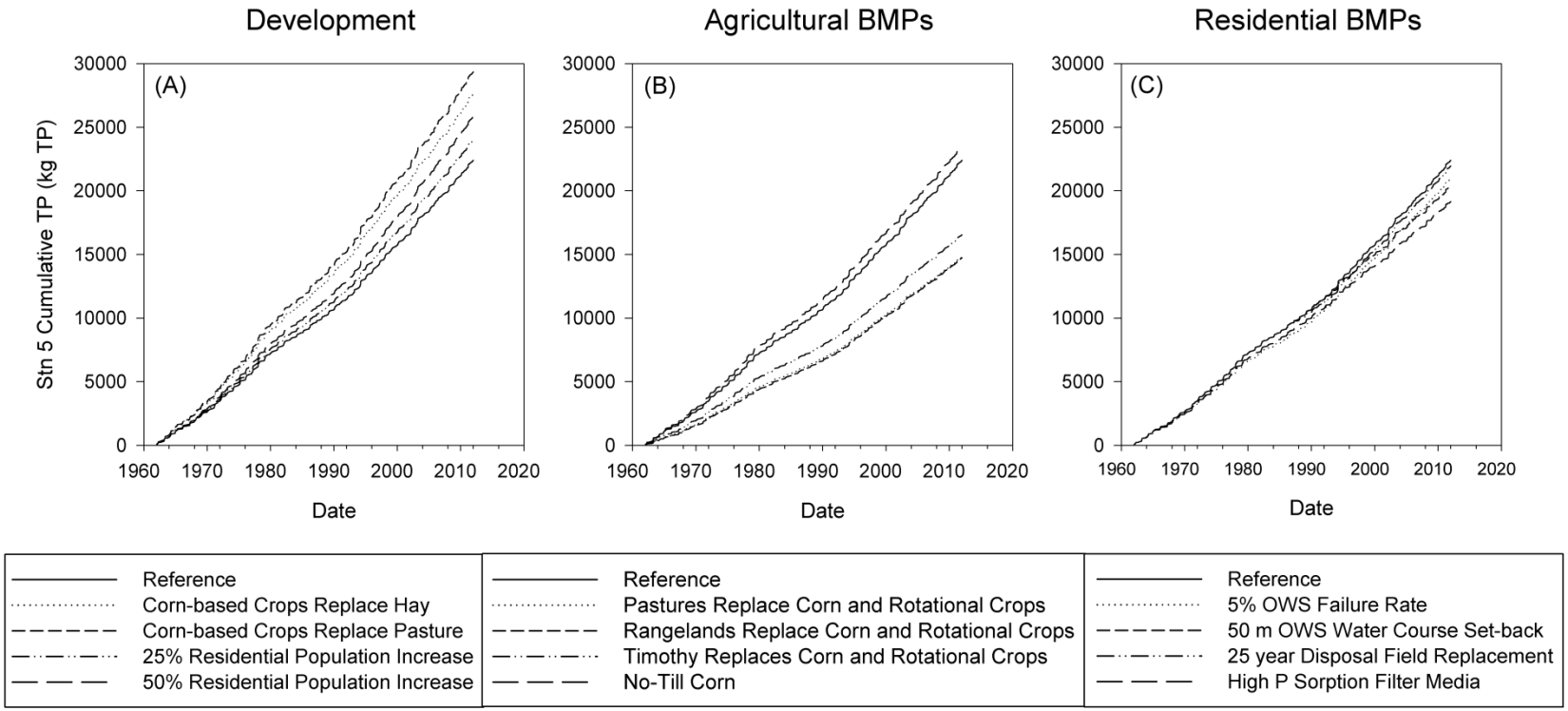

Figure 4.2 Cumulative total phosphorus loads for (A) development, and (B) agricultural and (C) residential beneficial management practice scenarios.

The trophic state frequency distributions (Figure 4.3) indicate that all of the residential and agricultural scenarios promote accelerated eutrophication, causing a shift from mesotrophic to eutrophic/hyper-eutrophic status over the 50 yr period. In the last 20 yr of all the scenarios, over 50% of the in-stream TP concentrations during the growing season fall in the hyper-eutrophic range as at ~30 yr the OWS soil subsurface plumes reach P saturation and peak OWS P loading occurs. The residential scenarios exhibited higher hyper-eutrophic frequencies than the agricultural. When the trophic state frequencies of the development scenarios are compared to the reference (Figure 4.4) both agricultural scenarios show only slight differences in trophic state frequencies. However, the residential scenarios produced a marked increase in the number of days exhibiting hyper-eutrophic conditions (>40% increase in the last 20 yr of the simulation period). As the OWS are a continuous source of TP loading, and agricultural loading is episodic during surface runoff events, it would be expected that OWS would contribute more to increased TP concentrations during baseflow conditions.

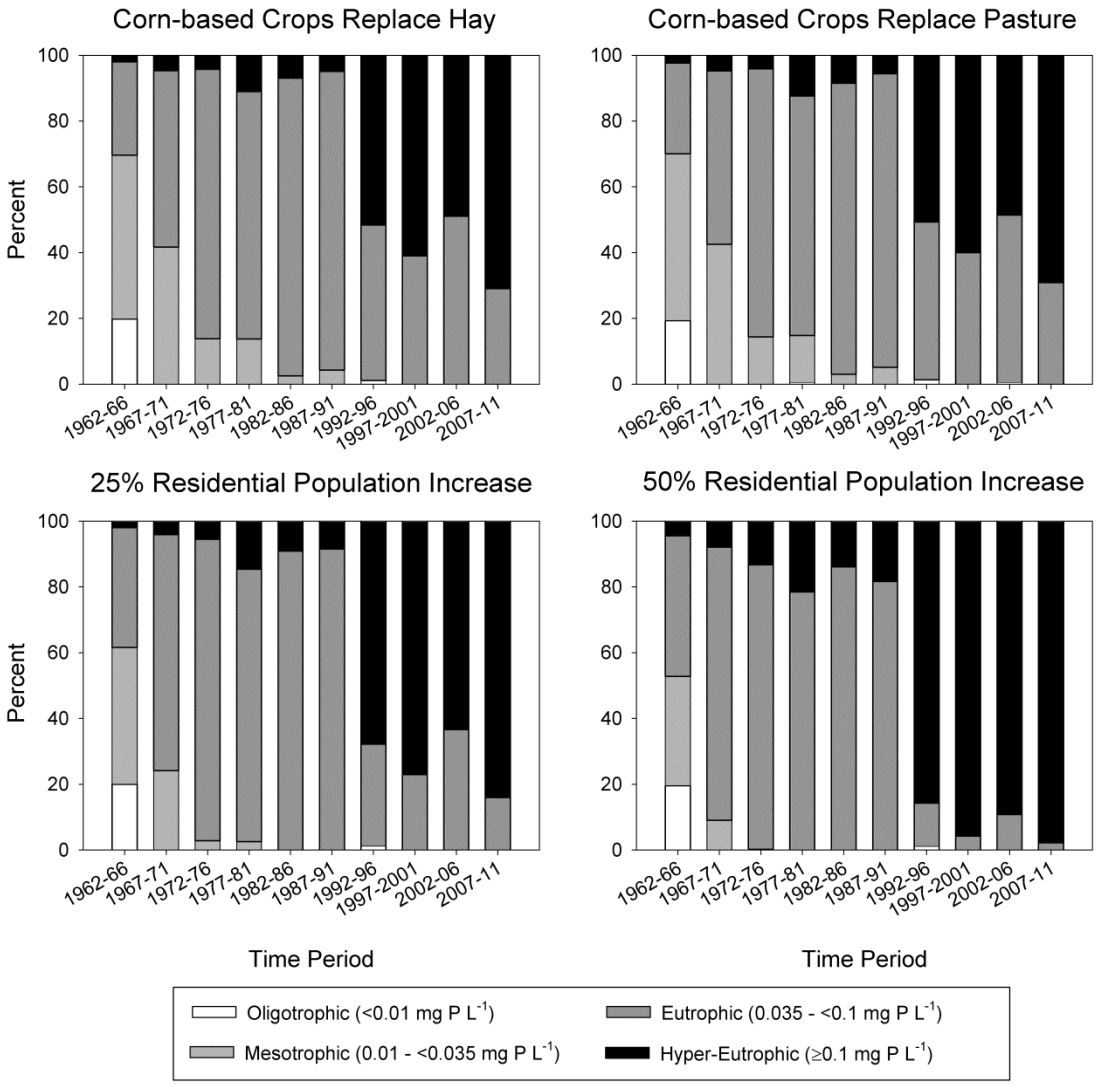

Figure 4.3 **Development scenario growing season trophic status percent breakdowns for 50 year simulation period.**

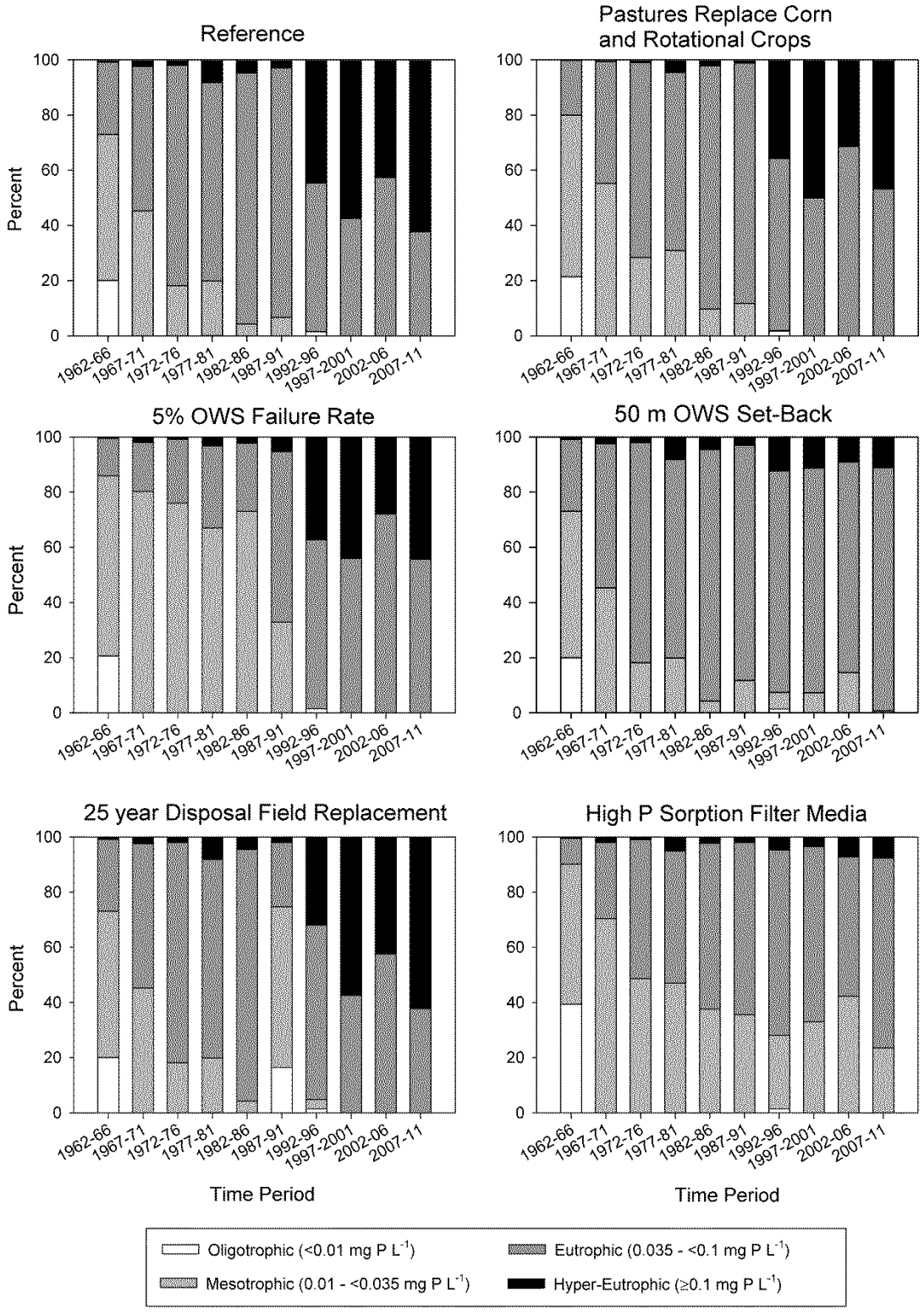

Figure 4.4 **Individual beneficial management practice scenario growing season trophic status percent breakdowns for 50 year simulation period.**

Geza and McCray (2010) modeled in-stream P concentrations from OWS P loading for three different population scenarios (pop. 0; 11,000; 22,000) in the predominantly residential and forest land-use Turkey Creek Watershed in Colorado using the Watershed Analysis Risk Framework (WARMF) model. It was assumed that 90% of the residences relied on OWS and the remainder used five centralized wastewater treatment plants that were simulated as point sources. The doubling of the population from 11,000 to 22,000 increased the in-stream TP concentration at three locations by only 1 to 4%. They hypothesized the relatively small increase in TP concentration was caused by dilution and settling out of sediment attached P in the stream network, leaching to the groundwater table, and increased surface runoff from land-use conversion to residential from forest. In general, the WARMF modeling study found that OWS contributed a relatively small proportion to the total P concentration.

4.3.2 Agricultural Beneficial Management Practices

Both the agricultural and OWS BMPs were analysed individually before ranking and simulating combinations of the highest ranked BMPs. The corn and rotational crop replacement BMPs resulted in the largest cumulative reductions in sediment and TP loads of the agricultural BMPs (Table 4.4, Figure 4.2.B). Replacement of corn and rotational cropping systems with pasture and rangeland were the highest ranked, producing approximately equivalent load reductions for both pollutants. The no-tillage corn BMP produced a relatively small decrease in cumulative sediment loading and a small increase in cumulative TP loading. Several SWAT modeling studies that simulated no-till BMPs observed increased P losses from agricultural fields, particularly organic P (Einheuser et al., 2012; Giri et al., 2012; Yang et al., 2012). Although the corn and rotational crop replacement BMPs had the largest cumulative TP reductions, there was relatively no change in the trophic state frequency distribution at Stn 5 (Figure 4.4) for the pastures replace rotational crops scenario when compared to the reference. The other agricultural BMP scenarios also exhibited relatively no change in the trophic state frequency distribution (results not shown).

All of the agricultural BMPs involved changing crop production practices to reduce or eliminate tillage and supplementary fertilization. The timothy replaces corn and

rotational crops BMP possibly did not have as large a decrease in cumulative sediment loading as the pasture and rangeland crop replacement scenarios because it undergoes a harvest and kill operation at the end of the growing season that reduces the amount of ground cover during the dormant season. The no-till corn BMP only had a relatively small decrease in sediment loading because only one of the three corn-based crops was non-rotational. Both alfalfa-corn and wheat-barely-corn cropping systems had tillage occur for 3 yr out of every 4 yr crop rotation cycle when corn was not grown and would not experience significant long-term reductions in sediment and TP runoff. There was relatively no change to the trophic state frequency distributions by the agricultural BMPs as they only reduced storm-event TP loads, and had little influence on baseflow in-stream TP concentrations. The corn and rotational crop replacement BMPs should presumably influence baseflow TP loads and the trophic status as lower P fertilization rates would reduce the amount of P available for transport through subsurface lateral flow. However, the SWAT2009 model does not simulate lateral flow P transport processes (Neitsch et al., 2011).

4.3.3 On-Site Wastewater System Beneficial Management Practices

The high P sorption filter media BMP had the highest cumulative TP reduction of the OWS BMPs at 15% (Table 4.4, Figure 4.2.C). The 10% OWS failure rate and 25 yr disposal field replacement BMPs were the worst ranked with cumulative TP load reductions of 3 and 2%, respectively. None of the residential BMPs changed the cumulative sediment load leaving the TBW. All of the OWS BMPs produced changes to the accelerated eutrophication rate for the 50 yr simulation period with high P sorption filter media having the greatest influence (Figure 4.4). The reference scenario trophic state changes from mesotrophic to eutrophic/hyper-eutrophic over the course of the simulation time period, while the high P sorption filter media has a lower eutrophication rate and mesotrophic conditions exist for at least 20% of the growing season. The 5% OWS failure rate and 50 m OWS set-back BMPs both exhibited reduced eutrophication rates, but had predominantly eutrophic conditions at the end of the simulation period. The 25 yr disposal field replacement scenario only differed from the reference trophic state

frequency distribution with improved trophic conditions for the 5 yr interval immediately following the 1986 replacement of the filter media.

One reason that the high P sorption filter media had the highest ranked cumulative TP reduction and reduced eutrophication rate was its assumed maximum P sorption capacity, which was 5000 mg P kg^{-1} media compared to 74.7 mg P kg^{-1} media for the reference filter sand. The maximum P sorption capacity changes when the POWSIM model switches from disposal field 2-part piecewise linear equation 3.12-I to 3.12-II with 3.12-I having a higher P removal rate than 3.12-II. Linear equation 3.12-I represents when both sorption and precipitation processes are occurring and 3.12-II represents when only precipitation occurs. In the reference scenario the POWSIM model for each monitoring station switches from linear equation 3.12-I to 3.12-II after approximately 1.8 yr of OWS operation when the disposal field maximum P sorption capacity is reached. The 25 y disposal field replacement BMP scenario illustrates this relatively short time period for the disposal field to reach P saturation. In Figure 4.4 the trophic status improves to mesotrophic from eutrophic for the 5 y interval immediately following the 1986 sand filter media replacement, which is then followed by a return to eutrophic dominated conditions for the remainder of the simulation period. The high P sorption filter media POWSIM models switch from Equation 3.12-I to 3.12-II after 58 to 64 yr of OWS operation, which contributes to the decreased eutrophication rate.

Both the 50 m OWS set-back and 5% OWS failure rate BMPs predominantly influenced P treatment in the soil subsurface plumes. The 50 m OWS set-back BMP increased the mass of soil involved in P treatment by approximately 52% compared to the reference scenario. This larger soil subsurface plume P treatment capacity increased the length of time until the maximum P loading rate was reached from 25 to 39 yr for the reference scenario to 45 to 50 yr (Sinclair et al., 2013b). Figure 4.4 illustrates when the P maximum loading rate is reached for the 50 m OWS set-back BMP as mesotrophic conditions were not present for the last 5 yr interval of the simulation period. The 5% OWS failure rate BMP did not change the mass of soil involved in P treatment, but did increase its influent P loading rate. The lower OWS failure rate reduced the total OWS P loading rate to the water course and decreased the eutrophication rate more than any other OWS BMP for the first 30 yr of the simulation period. However, the increased influent P

load to the disposal field and soil subsurface plume decreased the length of time until both components reached their maximum P sorption capacities and peak P loading rate to the water course, which was approximately 23 to 35 yr.

The individual OWS BMP cumulative TP loads and trophic state frequency distributions illustrate the importance in long-term simulation of OWS, such as the 50 yr period used in this study. Sinclair et al. (2013b) found that it generally takes 25 to 39 yr for soil subsurface plumes to reach P sorption saturation in the TBW. Two of the OWS BMP scenarios extended that time to peak P loading to 45 to 50 yr for the 50 m OWS water course set-back and 58 to 64 yr for the high P sorption filter media BMP scenario. If OWS are a potential P source in a watershed then simulation periods of 50 yr or more may be necessary to properly evaluate the maximum potential P loads into a freshwater system and the impacts of OWS BMP implementation.

4.3.4 Comparison of Agricultural and On-Site Wastewater System Beneficial Management Practices

As was observed in the development scenario comparison, the agricultural field BMPs had the largest reductions in cumulative sediment and TP loads (Table 4.4), and the residential BMPs produced greater changes to the trophic state frequency distributions (Figures 4.3, 4.4) . These results highlight the importance in identifying specific water quality issues that exist within a watershed prior to developing the watershed management and BMP plans. If the freshwater system is used directly for irrigation, human and animal drinking water, and/or recreation then implementing OWS BMPs would reduce the eutrophication rate and decrease the risk of harmful algal blooms, and improve water quality conditions in the stream network itself during periods of peak use. If the concern is P loading to downstream water bodies then agricultural BMPs would be better at addressing these long-term cumulative loads. As many watersheds have a variety of direct and downstream users combinations of agricultural and OWS BMPs would potentially address both water quality issues.

4.3.5 Combination Beneficial Management Practice Scenarios

The first combination BMP scenario was constructed by combining the highest ranked individual agricultural and OWS BMPs (pastures replace corn and rotational crops, and high P sorption filter media). The rangelands replace corn and rotational crops BMP had almost equivalent pollutant load reductions as pasture crop replacement, so it was assumed that a farmer would choose the active agricultural land-use of pasture over fallow rangeland. Other combination scenarios were developed by adding the next highest ranked BMP in sequence (50 m OWS set-back, 5% OWS failure rate and disposal field replacement) to the first combination scenario until all five individual BMPs were combined for a total of four combination scenarios (Table 4.4). Only OWS BMPs were able to be added to the first combination scenario as the other agricultural BMPs involved replacing cropping systems on the same fields utilized by the pasture replaces corn and rotational crops BMP. The better ranked 5% OWS failure rate was chosen over the 10% failure rate. The cumulative sediment load reductions of all combination scenarios were equivalent to the highest ranked agricultural BMPs as the OWS BMPs experienced no reduction in sediment loading. The cumulative TP loads were further reduced by 14 to 25% for the four combination BMPs compared to the individual pasture replaces corn and rotational crops BMP. As shown in Figures 4.4 and 4.5 all of the combination scenarios experienced greater reductions in the eutrophication rate compared to the individual high P sorption filter media BMP.

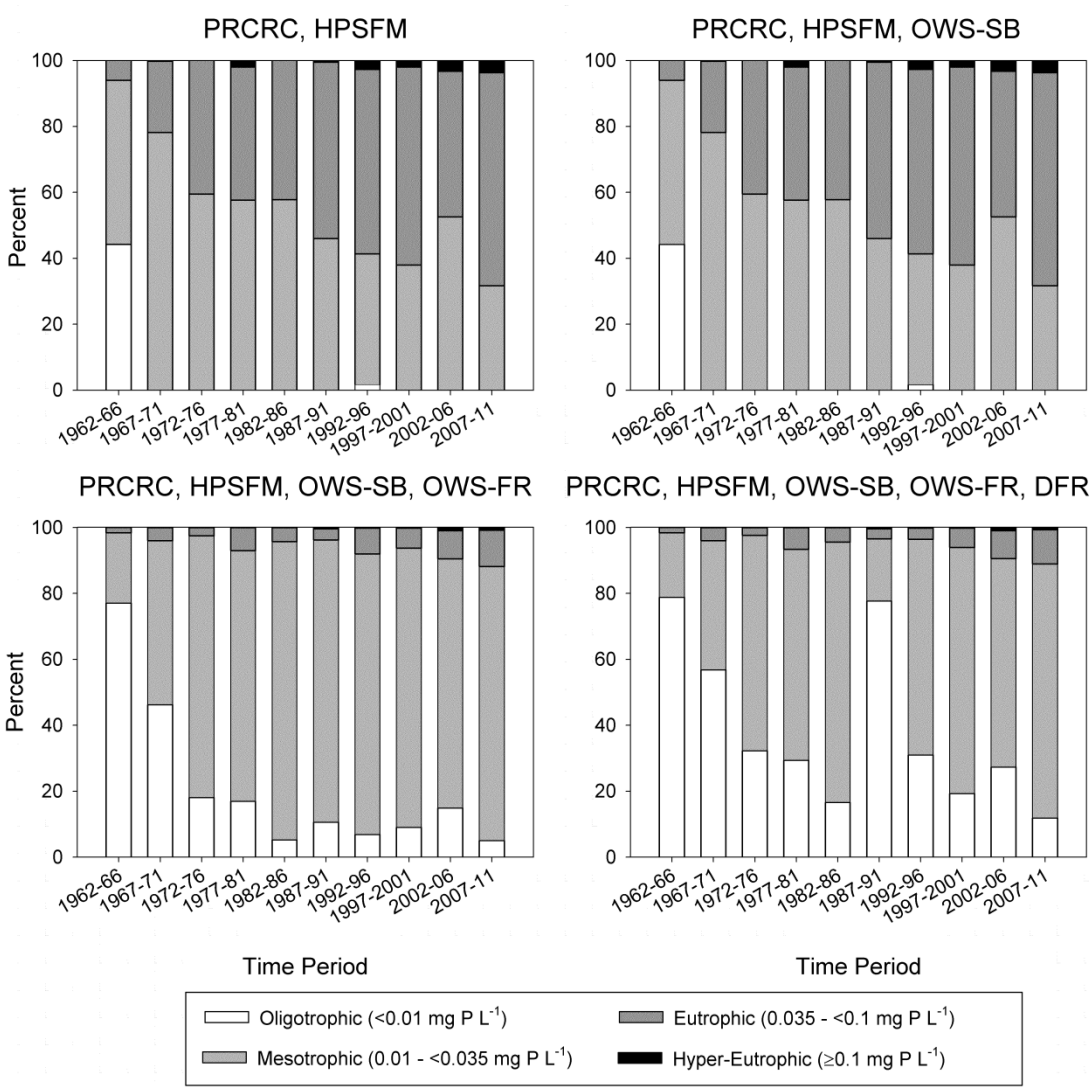

Figure 4.5 **Combination beneficial management practice scenario growing season trophic status percent breakdowns for 50 year simulation period. Note: PRRC, pasture replace rotational crops; OWS-SB, 50 m OWS water course set-back; OWS-FR, 5% OWS failure rate; HPSFM, high P sorption filter media; DFR, 25 year disposal field replacement.**

The combination scenarios with four and five BMPs were the highest ranked with both exhibiting the same relative reductions in cumulative TP loads (58-59%) and decreased eutrophication rates resulting in mesotrophic conditions for the last 20 yr of the simulation period. However, the influence of the 50 m OWS set-back when combined with the high P sorption filter media and pastures replace corn and rotational crops BMPs exhibited no change in the cumulative TP load and trophic state frequency distribution (Figure 4.5). One reason for the no change in TP load or trophic state by the 50 m OWS set-back BMP is the influence of the high P sorption filter media. As the high P sorption media disposal field does not reach P saturation until 58 to 64 yr there is a lower influent TP loading rate to the soil subsurface plume for the entire simulation period compared to the reference and other individual OWS BMP scenarios. This lower TP loading rate into the soil subsurface plume does not exceed the maximum P sorption capacity of the existing plume soil mass for the simulation period, so increasing the sorption capacity of the soil subsurface plume will not affect the P removal rate of the soil subsurface plume. As the 50 m OWS set-back when combined with high P sorption filter media does not improve P related water quality in the TBW it can be removed from the best ranked combination scenarios.

The main observable difference between the two highest ranked combination scenarios is the trophic state frequency distribution with the scenario including disposal field replacement exhibiting higher frequencies of oligotrophic conditions throughout the simulation period. However, the relative difference between the frequency distributions for the last 20 yr of the simulation period is small with the majority (>60%) of the growing season exhibiting mesotrophic conditions for both scenarios (Figure 4.5). Chambers et al. (2012) developed threshold TP criteria for Atlantic Maritime agricultural watersheds of 0.01 to 0.03 mg P L^{-1} to protect ecological conditions. The reference scenario eutrophic conditions (0.35 to 0.1 mg P L^{-1}) exceed the threshold criteria range. The mesotrophic conditions (0.01 to 0.035 mg P L^{-1}) for the best ranked combination scenarios would meet the threshold TP criteria and result in acceptable in-stream ecological conditions. Therefore, the combination scenario with pastures replace corn and rotational crops, high P sorption filter media and 5% OWS failure rate would be the

preferred scenario for reducing cumulative TP loads and maintaining an acceptable trophic state in the TBW.

A number of socio-political factors would also influence the implementation of the proposed agricultural and OWS BMPs in the TBW, and other similar watersheds in NS. As the TBW is not a designated protected water area, there are no existing regulations or financial incentives to assist with developing a BMP strategy (Nova Scotia Environment, 2006). The rotational crop replacement BMPs would presumably require financial incentives to compensate for the reduced farm income by switching from commodity crops (corn, wheat, barley) to pasture or fallow rangelands. A provincial and/or federal government crop replacement funding program would be most appropriate as they currently provide crop insurance, adaptation programs, and other financial services to farmers. Provincial regulations for agricultural BMPs may be required if the water quality issues are of a serious environmental or human health concern and voluntary participation does not meet water quality targets. For OWS BMP implementation the Nova Scotia Department of Environment will need to be involved as it is the OWS regulatory body (Nova Scotia Environment, 2009). Municipal government involvement may also be required as it is responsible for regulating development in the watershed area. Financial incentives may be required for the more intrusive and costly high P sorption filter media and disposal field replacement OWS BMPs through municipal and/or provincial programs. Specific P treatment targets for new OWS may be required to ensure appropriate disposal field designs and filter media are installed. Currently, there are no water quality targets for OWS disposal field effluent. The reduction in OWS failure rate through regular septic tank pumping and inspection may require regulation and enforcement by provincial or municipal authorities to ensure the program is properly enacted. An alternative failure rate reduction strategy could involve the establishment of a municipally managed Wastewater Management District. In this situation the municipal government would coordinate a scheduled septic tank pumping program. Watershed residents could be charged user fees, increased property tax rates and homeowner association fees for new developments, and incorporation of scheduled pumping programs in deeds for new homes to fund the maintenance program.

4.4 Conclusions

The evaluation of agricultural and OWS development scenarios simulated using the SWAT and POWSIM models in the TBW found that both would have long-term negative impacts on stream water quality. The agricultural development scenarios increased both cumulative sediment and TP loads at the watershed outlet. The OWS development scenarios produced changes in stream trophic conditions during the growing season by reducing the dissolved P entering the stream via groundwater transport from the soil subsurface plume.

Agricultural corn and rotational crop replacement BMPs were shown to produce the highest reductions in cumulative sediment and TP export loads, while most of the OWS BMPs had the greatest impact on growing season trophic state. The highest ranked combination of agricultural and OWS BMPs decreased the 50 yr cumulative sediment and TP export loads by 46 and 58%, respectively and included replacing corn and rotational crops with pastures, using high P sorption OWS filter media, and reducing the OWS failure rate to 5%. The reference scenario had consistently eutrophic conditions during the growing season for the last 20 yr of the simulation period, while the best combination BMP scenario had mesotrophic conditions for the same time period, representing a reduction in the eutrophication rate.

This study demonstrates that OWS development and BMP simulation periods need to exceed the length of time it takes for the OWS to reach P treatment saturation, which for the reference scenario in TBW is 25 to 39 yr. Simulation periods that do not include the maximum OWS P loading rate may miss a significant P source that will cause future water quality issues. Implementation of the agricultural and OWS BMPs in the TBW and other similar watersheds in NS will require working with several levels of government, and may require financial incentives and new regulations to achieve water quality targets. Biophysical field studies should be conducted at the watershed-scale in NS to evaluate the agricultural and OWS BMPs examined in this study individually and in various combinations.

CHAPTER 5 CONCLUSION

5.1 Summary and Conclusions

This thesis presents the development and evaluation of a computer modeling framework for simulating phosphorus (P) loading from agricultural land-uses and lateral flow dominated on-site wastewater systems (OWS) in rural watersheds, particularly in Nova Scotia (NS). The modeling framework used the P on-site wastewater simulator (POWSIM) loading tool, which was specifically designed in this study, in conjunction with the Soil and Water Assessment Tool (version 2009 [SWAT2009]) model to simulate P loads in the mixed land-use Thomas Brook Watershed (TBW). The framework was also used to assess different residential and agricultural development and beneficial management practice (BMP) scenarios in the TBW and their impacts on P loading and in-stream concentrations.

In Chapter 2, the P treatment algorithms for the lateral flow OWS designs simulated in the POWSIM model were developed and tested. The HYDRUS-2D modeling software was successfully used to simulate OWS hydraulics and to estimate the active P treatment mass in lateral flow sand filters (LFSFs), a NS approved OWS disposal field design. Seven different temporal removal models were developed and evaluated in their ability to simulate long-term P treatment in the LFSFs. The P temporal removal model with the best model performance for the six experimental LFSFs studied was found to be the 2-part piecewise linear temporal removal model. The 2-part piecewise linear equation switches from linear equation I to II when the maximum P sorption capacity of the filter media is reached. Linear equation I has a higher P removal rate than II and represents the time period when both sorption and precipitation are occurring. The P sorption process stops when the maximum P sorption capacity of the filter media is reached and precipitation becomes the dominant P treatment mechanism represented by linear equation II.

Chapter 3 focused on the development and testing of the POWSIM model in conjunction with the SWAT2009 model to simulate P loading in the TBW. The SWAT2009 model linked with POWSIM produced a better simulation of baseflow total

P (TP) loads at two monitoring stations in the TBW when compared with using the SWAT2009 model alone. The simulated OWS P loads were the same order of magnitude as the agricultural loads. A watershed-scale sensitivity analysis was also conducted of the POWSIM input parameters for 18 and 50 yr OWS operating periods. It was found that the septic tank effluent loading rate and P concentration, OWS failure rate, disposal field long-term P removal rate (linear equation II slope), soil maximum P sorption capacity and OWS distance to water course were the most sensitive parameters.

In Chapter 4, various residential and agricultural development and BMP scenarios were simulated in the TBW using the modeling framework. The various scenarios were assessed and compared based on their impacts on TP and sediment loads, and in-stream TP concentrations at the watershed outlet. Beneficial management practice scenarios, which involved replacing rotational crops with less intensive forages produced the highest variations to cumulative sediment and TP loads at the watershed outlet. The residential OWS development and BMP scenarios produced the greatest change in the eutrophication rate. The peak TP loading rates from OWS were predicted to occur between 23 and 64 yrs during the BMP simulations. The best BMP combination scenario had the highest reductions in the cumulative TP load (24%) and accelerated eutrophication rate, resulting in a mesotrophic class final trophic state. The BMPs in the best combination scenario were replace corn and rotational crops with pastures, use of high P sorption filter media and reducing the OWS failure rate to 5%.

5.2 Novel Contributions to Science

The computer modeling framework, POWSIM in conjunction with the SWAT2009 model, provides a new approach for simulating P loading in rural watersheds with both agricultural and residential land-uses. The POWSIM model simulates P treatment and transport in OWS disposal fields that rely on predominantly lateral flow and utilize sand media, which are typical in NS and other geographic areas with low permeability soils, shallow bedrock and high groundwater tables. Existing watershed-scale hydrological-water quality models, such as the SWAT2009 and Watershed Analysis Risk Framework (WARMF) models, simulate OWS P transport and treatment processes

via vertical percolation through native soil profiles. The POWSIM model also simulates lateral flow P transport to the nearest surface water body from the OWS through the soil profile. The 2-part piecewise linear P temporal removal models used in POWSIM to represent P sorption and precipitation processes in OWS disposal fields, and their soil subsurface plumes, are unique in their ability to represent long-term P removal. In comparison, existing watershed-scale computer models utilize linear equations that are interrupted once the maximum P sorption capacity is reached; after this point P removal via the disposal field and/or soil profile no longer occurs.

The testing and evaluation of the computer modeling framework in a small rural watershed with both agricultural and residential land-uses is another unique aspect of this study. The TBW had separate monitored subcatchments with different percent areas of dominant land-uses (e.g. Stn 3 was dominated by residential uses and Stn 4 was dominated by agriculture). The relative contributions to the total P load at Stns 3 and 4 were calculated for both residential OWS and agricultural land-uses. Although other watershed modeling studies have investigated P loading from both residential and agricultural land-uses, none have quantified their relative contributions at the watershed-scale. The improved simulation of baseflow TP loads in the TBW with the new modeling framework (SWAT2009 with POWSIM) highlights the importance in simulating P loads from OWS, particularly for baseflow periods. Many watershed-scale hydrological-water quality modeling studies negate OWS contributions to P loading in rural, mixed land-use watersheds and therefore are missing a potentially significant P source.

Evaluating the efficacy of both residential and agricultural BMPs in a rural watershed using the computer modeling framework is another novel contribution of this thesis. Other modeling studies have evaluated either agricultural or residential BMPs, but none have compared the two types against each other, or in combination. A first in this study is the simulation of OWS P loading for a 50 yr time period, which was required to capture the simulated peak OWS P loading in the TBW. Other OWS watershed modeling studies have simulated shorter time periods, and potentially have missed the occurrence of peak OWS P loading. Another unique aspect is the use of cumulative TP loads and changes to trophic state to evaluate the BMP and development scenarios in this study. Other studies typically examine changes in TP loads or in-stream concentrations. By

examining both cumulative TP loads and concentrations this study identified that different types of BMP and development scenarios impacted either in-stream or downstream water quality. This highlights the importance of identifying specific water quality issues prior to implementing a watershed BMP strategy.

5.3 Recommendations for Future Work

- The accuracy of the method for estimating the mass of filter media involved in active P treatment in LFSFs or other lateral flow dominated disposal field designs could be improved through the use of conservative (e.g. bromide) tracer studies. Rhodamine WT is known to undergo sorption processes in sand media and creates a level of uncertainty in both the observed and modeled results. Removal of tracer sorption as a model variable would allow for less uncertainty in the tracer calibration.
- The efficacy of the 2-part piecewise linear P temporal removal models for use in long-term simulation time periods and for lateral flow dominated OWS designs other than LFSFs should be investigated. This could be done through continued monitoring of input and output TP loads for the Bio-Environmental Engineering Centre (BEEC) LFSFs along with comparison and updating of the P temporal removal models. Conducting long-term monitoring studies of contour trench and mound OWS disposal field designs with the same sand grain-sizes as the BEEC LFSFs would create datasets for evaluating the use of this study's 2-part piecewise linear equations to represent P treatment in other OWS technologies.
- Field-scale studies of P treatment in OWS soil subsurface plumes in different watersheds would improve the estimation of input parameters and development of computational component algorithms in the POWSIM model.
- The robustness of using the POWSIM and SWAT2009 models in other watersheds should be examined as this study only conducted model calibration and validation in a single watershed. Testing in larger watersheds with time of concentrations greater than 1 d and covering a variety of geological and climatic conditions would assist with model development and validation. It is

hypothesized that the SWAT model calibration would be better in watersheds with flow travel times greater than 1 d.

- The OWS BMPs simulated in this study would benefit from biophysical studies as they have not been studied at either the field- or watershed scales individually or in combination. Research studies examining the impacts of BMPS on stream network water quality and OWS P treatment and transport would help make the POWSIM model more robust in simulating these BMPs and provide insight into achievable water quality targets. Agriculture and OWS BMPs in combination should also have biophysical studies conducted at the watershed-scale.

REFERENCES

AAFC. 2010. The national soil database. Agriculture and Agri-Food Canada. http://sis.agr.gc.ca/cansis/nsdb/index.html (accessed January 15, 2010).

AAFC. 2013. Watershed Evaluation of Beneficial Management Practices (WEBS). Agriculture and Agri-Food Canada. http://www.agr.gc.ca/eng/?id=1285354752471 (accessed September 10, 2013)

Abbaspour, K.C. 2011. User Manual: SWAT-CUP4 - SWAT calibration and uncertainty programs. EAWAG: Swiss Federal Institute of Aquatic Science and Technology, Dübendorf, Switzerland.

Ahmad, H.M.N., A. Sinclair, A., R. Jamieson, A. Madani, D. Hebb, P. Havard, and E.K. Yiridoe. 2011. Modeling sediment and nitrogen export from a rural watershed in Eastern Canada using the Soil and Water Assessment Tool. J. Environ. Qual. 40: 1182-1194.

Amon-Armah, F., E.K. Yiridoe, N.H.M. Ahmad, D. Hebb, R. Jamieson, D. Burton, and A. Madani. 2013. Effect of nutrient management planning on crop yield, nitrate leaching and sediment loading in Thomas Brook Watershed. Environ. Manage. 52. (in press).

APHA. 2000. Standard methods for examination of water and wastewater. 21st ed. APHA, Washington, DC.

Appelo, C.A.J., and D. Postma. 2005. Geochemistry, groundwater and pollution. 2nd ed. A.A. Balkema Publishers, Leiden, The Netherlands.

Arnold, J.G., R. Srinivasan, R.S., Muttiah, and J.R. Williams. 1998. Large area hydrologic modeling and assessment part I: Model development. J. Am. Water Resour. Assoc. 34(1): 73-89.

ASTM. 2006. Standard test method for permeability of granular soils (constant head). ASTM D2434-68, West Conshohocken, PA.

ASTM. 2008. Standard test methods for determination of the soil water characteristic curve for desorption using hanging column, pressure extractor, chilled mirror hygrometer, or centrifuge. ASTM D6836-02, West Conshohocken, PA.

Badruzzaman, M., J. Pinzon, J. Oppenheimer, and J.G. Jacangelo. 2012. Sources of nutrients impacting surface waters in Florida: A review. J. Environ. Manage. 109: 80-92.

Beal, C.D., D.W. Rassam, E.A. Gardner, G. Kirchof, and N.W. Menzies. 2008. "Influence of hydraulic loading and effluent flux on surface surcharging in soil adsorption systems." J. Hydrologic Eng. 13(8): 681-692.

Beach, D.N.H., and J.E. McCray. 2003. Numerical modeling of unsaturated flow in wastewater soil adsorption systems. Ground Water Monit. Rem. 23(2): 64-72.

Beggs, R.A., D.J. Hills, G. Tchobanoglous, and J.W. Hopmans. 2011. Fate of nitrogen for subsurface drip dispersal of effluent from small wastewater systems. J. Contam. Hydrol. 126(1-2): 19-28.

BNQ. 2009. Onsite residential wastewater treatment technologies, CAN/BNQ 3680-600/2009. Bureau de normalisation du Québec, QC.

Bolster, C.H., and G.M. Hornberger. 2007. On the use of linearized Langmuir equations. Soil Sci. Soc. Am. J. 71(6): 1796-1806.

Bond, C., R. Maguire, and J. Havlin. 2006. Change in soluble phosphorus in soils following fertilization is dependent on initial Mehlich-3 phosphorus. J. Environ. Qual. 35(5): 1818-1824.

Brady, N.C., and R.R. Weil. (2008). The Nature and properties of soil. 14th ed. Prentice Hall, Upper Saddle River, NJ.

Brisbois, M.C., R. Jamieson, R. Gordon, G. Stratton, and A. Madani. 2008. Stream ecosystem health in rural mixed land-use watersheds. J. Environ. Eng. Sci. 7: 439-452.

Bridson-Pateman, E., J. Hayward, R. Jamieson, L. Boutilier, and C. Lake. 2013. The effects of dosed versus gravity-fed loading methods on the performance and reliability of contour trench disposal fields used for onsite wastewater treatment. J. Environ. Qual. 42: 553-561.

Brown, L.C., and T.O. Barnwell. 1987. The enhanced water quality models QUAL2E and QUAL2E-UNCAS documentation and user manual. EPA document EPA/600/3-87/007. USEPA, Athens, GA.

Brylinsky, M. 2004. User's manual for prediction of phosphorus concentration in Nova Scotia lakes: A tool for decision making. Version 1.0. Nova Scotia Department of Environment and Labour, NS, Canada.

Bumgarner, J.R., and J.E. McCray. 2007. Estimating biozone hydraulic conductivity in wastewater soil-infiltration systems using inverse numerical modeling. Water Res. 41: 2349-2360.

Bundy, L.G., T.W. Andraski, and J.M. Powell. 2001. Management practice effects on phosphorus losses in run-off in corn production systems. J. Environ. Qual. 30: 1822-1828.

Burnham, K.P., and D.R. Anderson. 2002. Model Selection and Multi-model inference: A practical information-theoretic approach, 2nd Ed., Springer, New York, NY.

CCME. 2004. Canadian water quality guidelines for the protection of aquatic life: Phosphorus: Canadian guidelines framework for the management of freshwater systems. In Canadian Environmental Quality Guidelines. Canadian Council of the Ministers of the Environment, Winnipeg, MB.

Canadian General Standards Board. 1991. Liquid flow measurements in open channels – velocity area methods. CAN/CGSB-157.6-M/ISO 1088. National Standards of Canada, Ottawa, ON.

Carpenter, S.R., N.F. Caraco, D.L. Correll, R.W. Horwath, A.N. Sharpley, and V.H. Smith. 1998. Nonpoint pollution of surface waters with phosphorus and nitrogen. Ecol. App. 8(3): 559-568.

Carsel, R.F., and R.S. Parrish. 1988. Developing joint probability distributions of soil water retention characteristics. Water Resour. Res. 24(5): 755-769.

Chambers, P.A., M. Guy, E.S. Roberts, M.N. Charlton, R. Kent, C. Gagnon, G. Grove, and N. Foster. 2001. Nutrients and their impact on the Canadian environment. Agriculture and Agri-Food Canada, Environment Canada, Fisheries and Oceans Canada, Health Canada, and Natural Resources Canada, Ottawa, ON.

Chambers, P.A., D.J. McGoldrick, R.B. Brua, C. Vis, J.M. Culp, and G.A. Benoy. 2012. Development of environmental thresholds for nitrogen and phosphorus in streams. J. of Environ. Qual. 41:7-20.

Check, G.G., D.H. Waller, S.A.Lee, D.A. Pask, and T.D. Mooers. 1994. The lateral-flow sand-filter system for septic-tank effluent treatment. Water Environ. Res. 66(7): 919-928.

Chung, S.W., P.W. Gassman, L.A. Kramer, J.R. Williams, and R. Gu. 1999. Validation of EPIC for two watersheds in Southwest Iowa. Working Paper 99-WP 215. Center for Agricultural and Rural Development, Ames, IA.

Corwin, D.L. 2000. Evaluation of a simple lysimeter design modification to minimize sidewall flow. J. Contam. Hydrol. 42(1): 35-49.

Cucarella, V., and G. Renman. 2009. Phosphorus sorption capacity of filter materials used for on-site wastewater treatment determined in batch experiments – a comparative study. J. Environ. Qual. 38: 381-392.

Dayyani, S., S.O. Prasher, A. Madani, C.A. Madramootoo, and P. Enright. 2013. Evaluation of WARMF model for flow and nitrogen transport in an agricultural watershed under a cold climate. Water Qual. Res. J. Can. (in press).

Deslandes, J., I. Beaudin, A. Michaud, F. Bonn, and C.A. Madramootoo. 2007. Influence of landscape and cropping system on phosphorus mobility within the Pike River watershed of southwestern Quebec: Model parameterization and validation. Canadian Water Resour. Journal. 32: 21-42.

Dillon, P.J., K.H. Nicholls, W.A. Scheider, N.D. Yan, and D.S. Jefferies. 1986. Lakeshore capacity study – trophic status. Research and Special Projects Branch. Ontario Ministry of Municipal Affairs, Toronto, ON.

Douglas-Mankin, K.R., R. Srinivasan, and J.G. Arnold. 2010. Soil and Water Assessment Tool (SWAT) model: Current developments and applications. Trans. ASABE 53: 1423-1431.

Dudley, B., and L. May. 2007. Estimating the phosphorus load to waterbodies from septic tanks. Report to the Scottish Environmental Protection Agency and Scottish National Heritage. Centre for Ecology and Hydrology, Lancaster, UK.

Eckhardt, K., N. Fohrer, and H.G. Frede. 2005. Automatic model calibration. Hydrol. Processes 19:651-658.

Einheuser, M.D., A.P. Nejadhashemi, S.P. Sowa, L. Wang, Y.A. Hamaamin, and S.A. Woznicki. 2012. Modeling the effects of conservation practices on stream health. Sci. Total Environ. 435-436:380-391.

Elser, J., and E. Bennett. 2011. Phosphorus cycle: A broken biogeochemical cycle. Nature 478, 29-31.

Fogler, H.S. 1992. Elements of Chemical Reaction Engineering, 2nd ed., Prentice Hall, Upper Saddle River, NJ

Frey, S.K., E. Topp, T. Edge, C. Fall, V. Gannon, C. Jokinen, R. Marti, N. Neumann, N. Ruecker, G. Wilkes, D.R. Lapen. 2013. Using SWAT, Bacteroidales microbial source tracking markers, and fecal indicator bacteria to predict waterborne pathogen occurrence in an agricultural watershed. Water Res. (in press).

Fuchs, J.W., G.A. Fox, D.E. Storm, C.J. Penn, and G.O. Brown. 2009. Subsurface transport of phosphorus in riparian floodplains: influence of Preferential Flow Paths. J. of Environ. Qual. 38(2): 473-484.

Gassman, P.W., R. Reyes, C.H. Green, and J.G. Arnold. 2007. The soil and water assessment tool: Historical development, applications, and future research directions. Trans. ASABE 50:1211-1250.

Geza, M. and J.E. McCray. 2010. Model evaluation of potential impacts of on-site wastewater systems on phosphorus in Turkey Creek Watershed. J. Environ. Qual. 39: 1636-1646.

Giri, S., A.P., Nejadhashemi, S. Woznicki, and Z. Zhang. 2012. Analysis of best management practice effectiveness and spatiotemporal variability based on different targeting strategies. Hydrol. Processes DOI: 10.1002/hyp.9577 (in press).

Gooseff, M.N., S.M. Wondzell, R.Haggerty, and J. Anderson. 2003. Comparing transient storage modeling and residence time distribution (RTD) analysis in geomorphically varied reaches in the Lookout Creek Basin, Oregon, USA. Adv. Water Resour. 26(9): 925-937.

Goulden, T., C. Hopkinson, R. Jamieson, S. Sterling, A. Sinclair, and D. Hebb. 2013. Sensitivity of hydrological outputs from SWAT to DEM spatial resolution. Photogramm. Eng. Remote Sens. (in press).

Government of Canada. 2013. Canadian Climate Normals. Government of Canada. http://climate.weather.gc.ca/climate_normals/ (accessed Nov 9, 2013).

Greene, S., D. Taylor, Y.R. McElarney, R.H. Foy, and P. Jordan. 2011. An evaluation of catchment-scale phosphorus mitigation using load apportionment modelling. Sci. Total Environ. 409: 2211-2221.

Gupta, H.V., S. Sorooshian, and P.O. Yapo. 1999. Status of automatic calibration for hydrological models: Comparison with multilevel expert calibration. J. Hydrologic Eng. 4: 65-70.

Hanson, B.R., J. Šimůnek, and J.W. Hopmans. 2006. Evaluation of urea-ammonium-nitrate fertigation with drip irrigation using numerical modeling. Agric. Water Manage. 86: 102-113.

Harman, J., W.D. Robertson, J.A.Cherry, and L. Zanini. 1996. Impacts on a sand aquifer from an old septic system: nitrate and phosphate. Ground Water 34(6): 1105-1114.

Hart, M.R., B.F. Quinn, and M.L. Nguyen. 2004. Phosphorus runoff from agricultural land and direct fertilizer effects: A review. J. Environ. Qual. 33:1954-1972.

Hart, W.C., R.S. Scott, and J.G. Ogden III. 1978. A phosphorus loading model for lakes in the Shubenacadie headwaters. Technical Report No. 2. Dalhousie University, Halifax, NS.

Havard, P., R. Jamieson, D. Cudmore, L. Boutilier, and R. Gordon. 2008. Performance and hydraulics of lateral flow sand filters for on-site wastewater treatment. J. Hydrologic Eng. 13: 720-728.

Holland, J.M. 2004. The environmental consequences of adopting conservation tillage in Europe: Reviewing the evidence. Agric., Ecosyst. Environ. 103: 1-25.

Horowitz, J., R. Ebel, and K. Ueda. 2010. “No-till” farming is a growing practice. Economic Information Bulletin No. 70. United States Department of Agriculture Economic Research Service, Washington, DC.

Hutson, J.L., and R.J. Wagenet. 1991. Simulating nitrogen dynamics in soils using a deterministic model. Soil Use Manage. 7(2): 74-78.

Jamieson, R., R. Gordon, S. Tattrie, and G. Stratton. 2003. Sources and persistence of fecal coliform bacteria in a rural watershed. Water Qual. Res. J. Can. 38:33-47.

Jeong, J., C. Santhi, J.G. Arnold, R. Srinivasan, S. Pradhan, and K. Flynn. 2011. Development of algorithms for modeling onsite wastewater systems within SWAT. Trans. ASABE 54: 1693-1704.

Johansson Wesholme, L. 2006. Substrates for phosphorus removal – potential benefits for on-site wastewater treatment? Water Research 40: 23-36.

Johnes, P.J. 1996. Evaluation and management of the impact of land use change on the nitrogen and phosphorus load delivered to surface waters: The export coefficient modelling approach. Journal of Hydrology. 183: 323-349.

Jones, C.A., C.V. Cole, A.N. Sharpley, and J.R. Williams. 1984. A simplified soil and plant phosphorus model I: I. Documentation. Soil Sci. Soc. Am. J. 48: 800-805.

Kinley, R.D., R.J. Gordon, G.W. Stratton, G.T. Patterson, and J. Hoyle. 2007. Phosphorus losses through agricultural tile drainage in Nova Scotia, Canada. J. Env. Qual. 36:469-477.

Lemonds, P. J., and J. E. McCray. 2003. Modeling phosphorus transport in the Blue River watershed, Summit County, Colorado. In Proceedings of First Interagency Conference on Research in Watersheds, 272-277. United States Department of Agriculture – Agricultural Research Service, Washington, DC.

Lenhart, T., K. Eckhardt, N. Fohrer, and H.-G. Frede. 2002. Comparison of two different approaches of sensitivity analysis. Phys. and Chem. of the Earth 27: 645-654.

Langergraber, G., and J. Šimůnek. 2005. "Modeling variably saturated water flow and multicomponent reactive transport in constructed wetlands." Vadose Zone J. 4(4): 924-938.

Lombardo, P. 2006. Phosphorus geochemistry in septic tanks, soil absorption systems, and groundwater. Lombardo Associates, Inc., Newton, MA.

Lowe, K.S., N.K. Rothe, J.M.B Tomaras, K. DeJong, M.B. Tucholke, J. Drewes, and J. Munakata-Marr. 2007. Influent constituent characteristics of the modern waste stream from single sources: Literature review. 04-DEC-1a. Water Environment Research Foundation, Alexandria, VA.

Marshall, T.J. 1958. A relation between permeability and size distribution of pores. J. Soil Sci. 9(1): 1-8.

Matias, N.-G., and P.J. Johnes. 2012. Catchment phosphorus losses: An export coefficient modelling approach with scenario analysis for water management. Water Resources Management 26: 1041-1064.

Mattson, M.D., and R.A. Issac. 1999. Calibration of phosphorus export coefficients for total maximum daily loads of Massachusetts lakes. Lake Reservoir Manage. 15: 209-219.

McCray, J.E., S.L. Kirkland, R.L. Siegrist, and G.D. Thyne. 2005. Model parameters for simulating fate and transport of on-site wastewater nutrients. Ground Water 43: 628-639.

McCray, J.E., K. Lowe, M. Geza, J. Drewes, S. Roberts, A. Wunsch, D. Radcliffe, J. Amador, J. Atoyan, T. Boving, D. Kalen, and G. Loomis. 2009. State of the science: Review of quantitative tools to determine wastewater soil treatment unit performance. Publication Report #DEC1R06. Water Environment Research Foundation, Alexandria, VA.

McCuen, R.H. 1989. Hydrologic analysis and design. Prentice Hall, Englewood Cliffs, NJ.

McDowell., R.W. 2013. Estimating the mitigation of anthropogenic loss of phosphorus in New Zealand grassland catchments. Sci. Total Environ. (in press).

McDowell, R.W., B.J.F. Biggs, A.N. Sharpley, and L. Nguyen. 2004. Connecting phosphorus loss from agricultural landscapes to surface water quality. Chem. Ecol. 20: 1-40.

McGechan, M.B., and D.R. Lewis. 2002. Sorption of phosphorus by soil, part 1: Principles, equations and models. Biosyst. Eng. 82(1): 1-24.

Millington, R.J., and J.P. Quirk. 1959. Permeability of porous media. Nature 183: 387-388.

Moriasi, D.N., J.G. Arnold, M.W. Van Liew, R.L. Bingner, R.D. Harmel, and T.L. Veith. 2007. Model evaluation guidelines for systematic quantification of accuracy in watershed simulations. Trans. ASABE 50: 885-900.

Motz, E.C., E. Cey, M.C. Ryan, and A. Chu. 2012. Nutrient fate and transport in the vadose zone below and at-grade wastewater distribution system in a cold climate. J. Environ. Eng. 138: 1029-1039.

Murphy, J., and J. Riley. 1962. A modified single solution method for the determination of phosphorus in natural waters. Anal. Chim. Acta 27: 31-36.

Nair, V.D., K.M. Portier, D.A. Graetz, and M.L. Walker. 2004. An environmental threshold for degree of phosphorus saturation in sandy soils. J. Environ. Qual. 33(1): 107-113.

Nash, J.E., and J.V. Sutcliffe. 1970. River flow forecasting through conceptual models. Part I. A discussion of principles. J. Hydrol. 10(3): 282-290.

Neitsch, S.L., J.G. Arnold, J.R. Kiniry, and J.R. Williams. 2011. Soil and water assessment tool theoretical documentation. Version 2009. No. 406. Texas Water Resources Institute, College Station, TX.

Nelson, N.O., and J.E. Parsons. 2007. Basic Approaches to Modeling Phosphorus Leaching. Modeling Phosphorus in the Environment, D.E. Radcliffe and M.L. Cabrera, eds. CRC Press, Boca Raton, FL, 81-103.

Nova Scotia Environment. 2006. Developing a municipal source water protection plan: A guide for water utilities and municipalities. Step 4 – develop a source water protection management plan. Nova Scotia Environment, Halifax, NS.

Nova Scotia Environment. 2009. On-site sewage disposal systems: Technical guidelines. Nova Scotia Environment, Halifax, NS.

Nova Scotia Environment. 2011. Wastewater. Nova Scotia Environment. http://www.gov.ns.ca/nse/wastewater/ (accessed Sept 10, 2013).

Nunn L.-A.J. 2007. Nitrogen and phosphorus status in the Thomas Brook Watershed. Master's thesis, Dalhousie University, Halifax, NS.

Pang, L., M.E. Close, J.C.P. Watt, and K.W. Vincent. 2000. Simulation of picloram, atrazine, and simazine leaching through two New Zealand soils into groundwater using HYDRUS-2D. J. Contam. Hydrol. 44(1): 19-46.

Parkhurst, D.L., K.G., Stollenwerk, and J.A. Colman. 2003. Reactive-transport simulation of phosphorus in the sewage plume at the Massachusetts Military Reservation, Cape Cod, Massachusetts. Water-Resources Investigations Report 03-4017. Toxic Substances Hydrology Program. U.S. Geological Survey, Northborough, MA.

Patel, T., N., O'Luanaigh, and L.W. Gill. 2008. A comparison of gravity distribution devices used in on-site domestic wastewater treatment systems. Water Air Soil Pollut. 191: 55-69.

Radcliffe, D.E., and L.T. West. 2009. Design hydraulic loading rates for onsite wastewater systems. Vadose Zone J. 8: 64-74.

Rao, P.S.C., and J.M. Davidson. 1979. Adsorption and movement of selected pesticides at high concentrations in soils. Water Res. 13(4): 375-380.

Rao, N.S., Z.M. Easton, E.N. Schneiderman, M.S. Zion, D.R. Lee, and T.S. Steenhuis. 2009. Modeling watershed-scale effectiveness on agricultural best management practices to reduce phosphorus loading. J. Environ. Manage. 90: 1385-1395.

Reckhow, K.H. 1979. Empirical lake models for phosphorus: Development, applications, limitations and uncertainty. Perspectives in lake ecosystem modeling, D. Scavia and A.Robertson, eds. Ann Arbor Science Publishers, MI.

Richardson, S.D., C.S. Willlson, and K.A. Rusch. 2004. Use of rhodamine water tracer in the marshland upwelling system. Ground Water 42(5): 678-688.

Robertson, W.D. 2003. Enhanced attenuation of septic system phosphate in noncalcareous sediments. Ground Water 41(1): 48-56.

Robertson, W.D. 2008. Irreversible phosphorus sorption in septic system plumes? Ground Water 46(1): 51-60.

Robertson, W.D. 2012. Phosphorus retention in a 20-year-old septic system filter bed. J. Environ. Qual. 41: 1437-1444.

Robertson, W.D., S.L. Schiff, and C.J. Ptacek. 1998. Review of phosphate mobility and persistence in 10 septic system plumes. Ground Water 36(6): 1000-1010.

Sabatini, D.A. 2000.Sorption and intraparticle diffusion of fluorescent dyes with consolidated aquifer media. Ground Water 38(5): 651-656.

Schindler, D.W. 1977. Evolution of phosphorus limitation in lakes. Science 195 (4275): 260-262.

Schindler, D.W. 2006. Recent advances in the understanding and management of eutrophication. Limnol. Oceanogr. 51(1): 356-363.

Sharpley, A.N., H.P. Jarvie, A. Buda, L. May, B. Spears, and P. Kleinmann. 2013. Phosphorus legacy: Overcoming the effects of past management practices to mitigate future water quality impairment. J. Environ. Qual. 42: 1308-1326.

Sharpley, A.N., P.J.A. Kleinmann, A.L. Heathwaite, W.J. Gburek, G.J. Folmar, and J.P. Schmidt. 2008. Phosphorus loss from an agricultural watershed as a function of storm size. J. Environ. Qual. 37:362-368.

Sharpley, A.N., R.W. McDowell, P.J.A. Keinman. 2001. Phosphorus loss from land to water: integrating agricultural and environmental management. Plant Soil 237: 287-307.

Siegrist, R. L., J. McCray, L. Weintraub, C. Chen, J. Bagdol, P. Lemonds, S. Van Cuyk, K. Lowe, R. Goldstein, and J. Rada. 2005. Quantifying site-scale processes and watershed-scale cumulative effects of decentralized wastewater systems. Project No. WU-HT-00-27. Prepared by the Colorado School of Mines for the National Decentralized Water Resources Capacity Development Project, Washington University, St. Louis, MO.

Šimůnek, J., M. Th. van Genuchten, and M. Šejna. 2006. The HYDRUS software package for simulating the two- and three-dimensional movement of water, heat, and multiple solutes in variably-saturated media. Version 1.0. Technical manual. PC Progress. Prague, CZ.

Sims, J.T., R.R. Simard, and B.C. Joern. 1998. Phosphorus loss in agricultural drainage: Historical perspective and current research. J. Environ. Qual. 27: 277-293.

Sinclair, A., D. Hebb, R. Jamieson, R. Gordon, K. Benedict, K. Fuller, G.W. Stratton, and A. Madani. 2009. Growing season surface water loading of fecal indicator organisms within a rural watershed. Water Res. 43: 1199-1206.

Sinclair, A., R. Jamieson, R.J. Gordon, A. Madani, and W. Hart. 2013a. Modeling phosphorus treatment capacities of on-site wastewater lateral flow sand filters. J. Environ. Eng. (in press).

Sinclair, A., R. Jamieson, A. Madani, R. Gordon, W. Hart, and D. Hebb. 2013b. A combination watershed modeling approach for phosphorus loading from residential and agricultural sources in Nova Scotia. J. Environ. Qual. (Submitted).

Spiteri, C., C.P. Slomp, P. Regnier, C. Meile, and P. Van Cappellan. 2007. Modelling the geochemical fate and transport of wastewater-derived phosphorus in contrasting groundwater systems. J. Contam. Hydrol. 92(1): 87-108.

Statistics Canada. 2012a. Canada's rural population since 1851: Population and dwelling counts, 2011 Census, Cat no. 98-310-X2011003. Statistics Canada, Ottawa, ON.

Statistics Canada. 2012b. GeoSearch. 2011 Census. Statistics Canada Catalogue no. 92-142-XWE. Statistics Canada, Ottawa, ON. http://www12.statcan.ca/census-recensement/2011/geo/ref/geosearch-georesearche-eng.cfm (accessed on Oct 1, 2013).

Statistics Canada. 2012c. Snapshot of Canadian agriculture: Chapter 5. Statistics Canada, Ottawa, ON. http://www.statcan.gc.ca/pub/95-640-x/2012002/05-eng.htm#XV (accessed on Oct 1, 2013).

Tiessen, K.H.D., J.A. Elliott, J. Yarotski, D.A. Lobb, D.N. Flaten, N.E. Glozier. 2010. Conventional and conservation tillage: Influence on seasonal runoff, sediment, and nutrient losses in the Canadian prairies. J. Environ. Qual. 39: 964-980.

Tuppad, P., K.R. Douglas-Mankin, T. Lee, R. Srinivasan, and J.G. Arnold. 2011. Soil and Water Assessment Tool (SWAT) hydrologic/water quality model: Extended capability and wider adoption. Trans. ASABE 54: 1677-1684.

United States Census Bureau. 2012. 2010 census urban and rural classification and urban area criteria. United States Census Bureau. http://www.census.gov/geo/www/ua/2010urbanruralclass.html (accessed on Oct 10, 2012).

USDA. 2013. National Soil Survey Handbook, Title 430-VI, United States Department of Agriculture, Natural Resources Conservation Service http://soils.usda.gov/technical/handbook/ (accessed on March 13, 2013).

USDA NRCS (Natural Resources Conservation Service). 2013. Conservation Effects Assessment Project (CEAP). USDA Natural Resources Conservation Service. http://www.nrcs.usda.gov/wps/portal/nrcs/main/national/technical/nra/ceap/

USEPA. 2002. Onsite wastewater treatment systems manual. Office of Research and Development, Office of Water. EPA/625/R-00/008. United States Environmental Protection Agency, Cincinnati, OH.

Uttormark, P.D., J.D. Chapin, and K.M. Green. 1974. Estimating nutrient loading of lakes from non-point sources. Report No. 660/13-74-020. Ecological Research Series. USEPA, Corvallis, OR.

Vadas, P.A., and M.J. White. 2010. Validating soil phosphorus routines in the SWAT model. Trans. ASABE 53: 1469-1476.

Vogel, T., and M. Cislerova. 1988. On the reliability of unsaturated hydraulic conductivity calculated from the moisture retention curve. Transp. Porous Media. 3(1): 1-15.

Vohla, C., M. Koiv, H.J. Bavor, F. Chazarenc, and U. Mander. 2011. Filter materials for phosphorus removal from wastewater in treatment wetlands – a review. Ecol. Eng. 37: 70-89.

Weintraub, L., C.W. Chen, W. Tsai, J. Herr, R.A. Goldstein, and R.L. Siegrist. 2002. Modifications of WARMF to assess the efficacy of onsite wastewater systems on public health. In: WEFTEC Conference Proceedings, Chicago, IL. Oct. 2002. Water Environment Federation, Alexandria, VA.

Whitehead, P.G., L. Jin, H.M. Baulch, D.A. Butterfield, S.K. Oni, P.J. Dillon, M. Futter, A.J. Wade, R. North, E.M. O'Connor, and H.P. Jarvie. 2011. Modelling phosphorus dynamics in multi-branch river systems: A study of the Black River, Lake Simcoe, Ontario, Canada. Sci. Total Environ. 412-413: 315-323.

Wilhelm, S.R., S.L. Schiff, and W.D. Robertson. 1994. Chemical fate and transport in a domestic septic system: Unsaturated and saturated zone geochemistry. Environ. Toxicol. Chem. 13(2): 193-203.

Wilson, J., L. Boutilier, R. Jamieson, P. Havard, and C. Lake. 2011. Effects of hydraulic loading rate and filter length on the performance of lateral flow sand filters for on-site wastewater treatment. J. Hydrologic Eng. 16(8): 639-649.

Withers, P.J.A., H.P. Jarvie, R.A. Hodgkinson, E.J. Palmer-Felgate, A. Bates, M. Neal, R. Howells, C.M. Withers, and H.D. Wickham. 2009. Characterization of phosphorus sources in rural watersheds. J. Environ. Qual. 38: 1998-2011.

Withers, P.J.A., H.P. Jarvie, and C. Stoate. 2011. Quantifying the impact of septic tank systems on eutrophication risk in rural headwaters. Environ. Int. 37: 644-653.

Withers, P.J.A., L. May, H.P. Jarvie, P. Jordan, D. Doody, R.H. Foy, M. Bechmann, S. Cooksley, R. Dils, and N. Deal. 2012. Nutrient emissions to water from septic tank systems in rural catchments: Uncertainties and implications for policy. Environ. Sci. and Policy 24: 71-82.

Yang, Q., G.A. Benoy, T.L. Chow, J.-L. Daigle, C.P-A. Bourque, and F.-R. Meng. 2012. Using the soil and water assessment tool to estimate achievable water quality targets through implementation of beneficial management practices in an agricultural watershed. J. Environ. Qual. 41: 64-72.

Yang, Q., F.-R. Meng, Z. Zhao, T.L. Chow, G. Benoy, H.W. Rees, and C.P.-A. Bourque. 2009. Assessing the impacts of flow diversion terraces on stream water and sediment yields at a watershed level using SWAT model. Agric., Ecosyst. Environ. 132: 23-31.

Zanini, L., W.D. Robertson, C.J. Ptacek, S.L. Schiff, and T. Mayer. 1998. Phosphorus characterization in sediments impacted by septic effluent at four sites in central Canada. J. Contam. Hydrol. 33: 405-429.

Zurawsky, M.A., W.D. Robertson, C.J. Ptacek, and S.L. Schiff. 2004. Geochemical stability of phosphorus solids below septic system infiltration beds. J. Contam. Hydrol. 73: 129-143.

APPENDIX A COPYRIGHT PERMISSION LETTER

September 18, 2013
Journal of Environmental Engineering
American Society of Civil Engineers
1801 Alexander Bell Drive
Reston, VA USA
20191-4400
I am preparing my Ph.D. thesis for submission to the Faculty of Graduate Studies at Dalhousie University, Halifax, Nova Scotia, Canada. I am seeking your permission to include a manuscript version of the following paper(s) as a chapter in the thesis:
Modeling Phosphorus Treatment, Capacities of On-Site Wastewater Lateral Flow Sand Filters; Andrew Sinclair, Rob Jamieson, Robert J. Gordon, Ali Madani, and William Hart; Journal of Environmental Engineering; Ref.: Ms. No. EEENG-2185
Canadian graduate theses are reproduced by the Library and Archives of Canada (formerly National Library of Canada) through a non-exclusive, world-wide license to reproduce, loan, distribute, or sell theses. I am also seeking your permission for the material described above to be reproduced and distributed by the LAC(NLC). Further details about the LAC(NLC) thesis program are available on the LAC(NLC) website (www.nlc-bnc.ca).
Full publication details and a copy of this permission letter will be included in the thesis.
Yours sincerely,
Andrew Sinclair
Permission is granted for:
a) the inclusion of the material described above in your thesis.

b) for the material described above to be included in the copy of your thesis that is sent to the Library and Archives of Canada (formerly National Library of Canada) for reproduction and distribution.

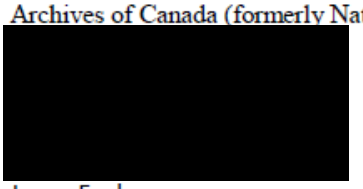

Joann Fogleson
American Society of Civil Engineers
1801 Alexander Bell Drive
Reston, VA 20191
(703) 295-6278-FAX
PERMISSIONS@asce.org
Permission is granted, under the condition that the paper makes up less than 25% of your new work. A full credit line must be added to the material being reprinted. For reuse in non-ASCE publications, add the words "With permission from ASCE" to your source citation. For Intranet posting, add the following additional notice: "This material may be downloaded for personal use only. Any other use requires prior permission of the American Society of Civil Engineers."

Each license is unique, covering only the terms and conditions specified in it. Even if you have obtained a license for certain ASCE copyrighted content, you will need to obtain another license if you plan to reuse that content outside the terms of the existing license. For example: If you already have a license to reuse a figure in a journal, you still need a new license to use the same figure in a magazine. You need separate license for each edition. For more information please view Terms and Conditions at: http://www.asce.org/Books-and-Journals/Permissions/Permission-Requests/Terms-and-Conditions/